

Coupling ORCHESTRA to Python

A modelling framework for simulating waste degradation in a
bioreactor

By
G. de Zeeuw

in partial fulfillment of the requirements for the degree of

Master of Science
in Applied Earth Sciences

at the Delft University of Technology
to be defended publicly on Monday August 29, 2022 at 15:30 AM.

supervisor

Prof. dr. ir. T. J. Heimovaara

thesis committee

Dr. ir. J. C. L. Meeussen

Dr. ir. D. V. Voskov

C. F. Andrade Corona MSc



Acknowledgement

After 7 years of studying, the fulfilment of finalising this thesis, the final manuscript, is tremendous. However, completing this study was not possible without the help of the people around me.

First and foremost, I want to express my deepest gratitude to my supervisor Prof. dr. ir. T. J. Heimovaara for giving me the opportunity to do this study. His expertise and supervision have allowed me to develop both my academic and coding skills. I would also like to thank C. F. Andrade Corona MSc for being part of the committee, providing me with daily valuable comments and suggestions. His enthusiasm for the project motivated me even more than I already did. My gratitude goes to Dr. ir. J. C. L. Meeussen, for his guidance in understanding ORCHESTRA and getting me introduced to C++. Thanks also to Dr. ir. D. V. Voskov, for being part of the committee and reading the thesis.

Special thanks to Dr. B. Meulenbroek, for his presence during the weekly meetings with Dr. ir. J. C. L. Meeussen and for his interest in the project. I would like to extend my special gratitude to Dr. J. Gebert for overseeing the CURE project, scheduling the CURE meetings and allowing me to present my work on various occasions. This thanks also goes to all the members of the CURE organization, for the joyful talks and discussions and for making me feel truly part of the project.

I want to thank the people that are closest around me. My mother and father, who supported me at all times, providing me with cups of tea during the late-night studies. My brother, who forced me to go out and exercise at times I locked myself up in my room to study. My dearest friend, Jesse Blom MSc MA, for the great laughs and support, even when he moved across the globe to study Chinese. And to Marckque Heemskerk, for the nice discussions during our get-togethers.

Lastly, of course, my greatest thanks to my girlfriend Madelief van de Beek, for all her love and support.

Abstract

Over the years, modelling frameworks have been proposed to describe and predict the degradation of municipal solid waste in landfills. These frameworks, however, fail to couple the kinetic solutions to the real-time equilibrium state of the system. Because of this, fundamental processes such as pH changes, NH_4^+ adsorption to the waste surface and changes to the fluid composition are often not (or inadequate) taken into account. In this study, we propose a degradation model that couples a kinetic solver to the chemical equilibrium software, ORCHESTRA. For this, a tool is developed that allows seamless operability between ORCHESTRA and the Python environment. The modelling framework is used to simulate the degradation of solid organic matter in a batch reactor following a simplified, but comprehensive, reaction network. Reaction rates are based on Monod kinetics that includes a wide variety of inhibition functions. The Freundlich equation is used to capture NH_4^+ adsorption to the waste surface. Results from various case studies show that the modelling framework is suitable for coupling real-time landfill chemistry to degradation kinetics. We found that NH_4^+ concentrations play a dominant role in the presented model. While low NH_4^+ concentrations limit biomass growth by substrate inhibition, high concentrations ($>0.002\ mol/L$) affect the hydrolysis rate by toxicity inhibition. This translates to a model that is sensitive to a variety of input parameters such as the initial C/N ratio, the K_d (degree of adsorption) value and the initial organic fraction. A comparison with literature studies, however, implies that the model lacks fundamental processes such as gas and fluid transport or changes in volume and temperature. In addition to this, we discuss that the Freundlich isotherms may be inappropriate to capture adsorption in a coupled framework as no ion exchange is taken into account. Models that do so, such as the NICA-Donnan model, could improve the model results significantly.

Keywords: Municipal Solid Waste treatment; Biogeochemical model; ORCHESTRA; NH_4^+ adsorption

Contents

1	Introduction	4
1.1	General Background	4
1.2	Landfill Aftercare	4
1.3	CURE: modelling landfill dynamics	5
1.3.1	Previous Studies	5
1.3.2	Research Question and Outline	6
2	Theoretical Framework	8
2.1	Biodegradation of Municipal Solid Waste	8
2.2	Biodegradation rates	9
2.3	Nitrogen in a landfill	10
2.3.1	Ammonification	10
2.3.2	Nitrification	11
2.3.3	Denitrification	11
2.3.4	Adsorption	12
2.4	Metabolism	12
3	Model Description	14
3.1	System description for modelling landfill chemistry	14
3.1.1	Kinetic vs equilibrium reactions	15
3.2	Reaction network	15
3.2.1	Metabolic reactions	16
3.2.2	Stoichiometry matrix	17
3.3	Reaction kinetics	18
3.3.1	Michaelis-Menten and Monod kinetics	18
3.3.2	Inhibition functions	19
3.3.3	Combining reaction rates with reaction stoichiometry	20
3.4	Chemical equilibrium	20
3.4.1	Using ORCHESTRA in Python: Pybind11	21
3.4.2	Modelling landfill chemistry with ORCHESTRA	22
3.5	Porosity, saturation and organic fraction	24
3.6	Case Studies	24
3.6.1	Case study 1: Degradation of waste in a closed system with no NH_4^+ adsorption	24
3.6.2	Case study 2: Degradation of waste in an open system with no NH_4^+ adsorption	25
3.6.3	Case study 3: Degradation of waste in an open system with NH_4^+ adsorption to the mass waste	25
3.6.4	Case study 4: Degradation following kinetic rate parameters from the literature	26
4	Results & Discussion	28
4.1	Case 1: Degradation of waste in a closed system with no NH_4^+ adsorption	28
4.2	Case 2: Degradation of waste in a (partly) open system with no NH_4^+ adsorption	30
4.3	Case 3: Degradation of waste in a (partly) open system with NH_4^+ adsorption	33
4.3.1	Case 3a: Effects of waste composition	33
4.3.2	Case 3b: Effects of Kd	35
4.3.3	Case 3c: Effects of initial organic fraction	37
4.4	Case 4: Degradation following kinetic rate parameters from the literature	39

5 Additional discussion	42
5.1 Inhibitions related to NH_4^+	42
5.2 Effects of K_d value and sorption models	42
5.3 Effects of initial organic fraction and C/N ratio	43
5.4 Limitations and simplifications	44
6 Conclusion	46
A Formulation of the reaction network	47
A.1 Hydrolysis lumped with acidogenesis & acetogenesis	47
A.2 Methanogenesis of acetate	47
A.3 Oxidation of acetate	47
A.4 Nitrification	48
A.5 Denitrification	48
A.6 Biomass growth	49
A.7 Biomass decay	49
B PyORCHESTRA documentation	50

Chapter 1

Introduction

1.1 General Background

At present, the world's total urban population is estimated at 4.36 billion (of a total of 8 billion), which increases rapidly at a yearly rate of ca. 1.87% (WorldBank, 2021). Because of this, the global generated municipal solid waste (MSW) is at a record height, estimated at 2.01 billion tonnes per year (WorldBank, 2021). To deal with such amounts of waste, proper waste management is required. In the Netherlands, waste management includes recycling, incineration and landfill storage. In the past (<1990), the Netherlands relied heavily on the use of landfills, accounting for approximately 35% of the total waste generated (Lieten, 2018). Over the years, however, this fraction has decreased significantly because of regulations that stimulate recycling and waste recovery. As a result, there are currently only 19 landfills in operation within the Netherlands, storing ca. 2% of the total waste generated. This fraction represents waste unsuitable for recycling or incineration (Scharff, 2014). While this paradigm shift has led to a vast reduction of landfilled waste in the Netherlands, landfills are still heavily exploited in most parts of the world. In the United States of America, for example, 1812 individual landfill sites are used to store 80% of the MSW that is produced (Gerba et al., 2011).

The use of landfills tends to be discouraged because of their environmental impact, both during and after operation. Two main emission pathways of landfill waste are distinguished: landfill gas and leachate. (1) Landfill gas (or LFG) is a direct product of the microbial degradation of solid organic matter (Vaverková, 2020). The main components of LFG are CH₄, CO₂ and N₂ (the former two accounting for >90 vol% Majdinasab et al., 2017). (2) Landfill leachate consists of rainwater and other liquids that reside in the landfill that percolates through the waste body and, by that, remove dissolved particles from the landfill (Wiszniewski et al., 2006). Leachate contains toxic organic compounds, heavy metals and nitrogen compounds such as ammonia-nitrogen, nitrate and nitrite that may pollute soils and groundwater (Wiszniewski et al., 2006; Renou et al., 2008).

1.2 Landfill Aftercare

To mitigate landfill emissions, landfill aftercare has been mandatory since 1996 in the Netherlands (Scharff, 2014; Lieten, 2018). The traditional aftercare of landfills includes sealing the landfill completely with liners, a thin high-density polyethylene (HDPE) layer that prevents water from entering (and leaving) the landfill (Brand et al., 2016). This strategy, although adequate in terms of immediate environmental protection, has several major disadvantages. By sealing the landfill, the biochemical degradation process is very slow, presenting a long-term threat to the environment (Brand et al., 2016; Dijkstra et al., 2018). Apart from its everlasting emission potential, this also has economic consequences as extensive monitoring and maintenance of the liner is required; depending on the conditions, the lifetime of an HDPE liner may be less than a decade (Rowe and Sangam, 2002).

As a result, Dutch researchers have studied methods to enhance biodegradation in landfills (e.g. Kattenberg and Heimovaara, 2011; Turnhout et al., 2018; Turnhout et al., 2020). With enhanced biodegradation, as well as stimulating immobilization of (e.g.) heavy metals, the emission potential of the landfill decreases rapidly (Kattenberg and Heimovaara, 2011). It aims to - controllably - deplete a landfill from polluting compounds such, that further maintenance of the landfill is no more needed. In other words: 'terminating' eternal aftercare.

Two methods of enhanced landfill waste degradation are (1) recirculation and treatment of leachate and (2) aeration. Leachate recirculation increases the water flow within a landfill which, in turn, stimulates the mixing of solutes and bacteria (Turnhout et al., 2018). This, in combination with the increased moisture content, enhances microbial degradation. However, leachate recirculation stimulates the ammonification rate, resulting in higher, undesired, levels of NH₄⁺ (Li et al., 2019). Leachate circulation can therefore be combined with

aeration (Ritzkowski and Stegmann, 2012). The presence of oxygen (O_2) induces aerobic degradation of solid organic matter, which is significantly faster than anaerobic degradation (Erses et al., 2008). Aeration allows for nitrification (followed by denitrification) of ammonium (NH_4^+ ; Turnhout et al., 2018). By allowing nitrification (and denitrification) to occur, part of the produced NH_4^+ is removed by converting it to nitrogen gas (N_2). Apart from this, a shift in gas composition can also be found as aerobic degradation produces CO_2 rather than CH_4 ; oxygen is toxic for methanogens. This has the benefit of CO_2 being a greenhouse gas that is 21 times less harmful to the climate (Amodeo et al., 2019).

1.3 CURE: modelling landfill dynamics

In 2020, a project was launched to identify, describe, and predict the heavily coupled processes that occur within a landfill with the aim to reduce landfill emissions (CURE, ‘Coupled multi-process research for reducing landfill emissions’). This is done by extensively monitoring sanitary landfills at three locations (at Braambergen, Kragge and Wieringermeer) at which the waste mass is stabilized by leachate recirculation or aeration. In combination with results from laboratory studies, the monitoring data is used to predict long-term emissions by developing and calibrating a modelling framework that couples reactive transport, biochemical reactions and residence time functions.

Within this framework, a transport model was developed that predicts chloride concentrations within the leachate, based on a travel time distribution curve (Correspondence with Timo Heimovaara, February 9th, 2022). The model predicts chloride depletion over time, a trend that is in agreement with the existing landfill data. Chloride is used here as it has a very low adsorption affinity and bonding strength (Hendry et al., 2000). This makes chloride ideal for tracer studies as no to a simple reaction network has to be taken into account (Blume et al., 2016). However, to be able to capture full-scale landfill dynamics, the transport model should also include other important chemical compounds, which are often part of a more complex reaction network. An example of such a complex reaction network is that of the nitrogen species. NH_4^+ , for example, is a highly relevant compound because of its toxicity (Chanem et al., 2020; Deng et al., 2022); while $<50 \frac{\mu mol}{L}$ resides naturally in a persons blood, levels exceeding $>100 \frac{\mu mol}{L}$ are damaging to the human body, ranging from feeling nauseated up to reaching states of unconsciousness.

NH_4^+ is released during the hydrolysis and further natural degradation of solid organic matter (SOM). In the literature, waste degradation is often described as a three-step process (e.g. Reichel et al., 2007; Vavilin et al., 2008; Meima et al., 2008; Turnhout et al., 2018). The first step, hydrolysis, is the enzymatic breakdown of SOM in the presence of bacteria (Morgenroth et al., 2002). Hydrolysis is succeeded by acetogenesis, during which acetate is produced using glucose and other volatile fatty acids (VFA’s) as carbon sources (Reichel et al., 2007). The final step of waste degradation includes methanogenesis, which breaks down the acetate leading to the production of CO_2 and CH_4 gas (Batstone et al., 2002).

1.3.1 Previous Studies

The degradation pathway described above is often regarded as the foundation for modelling biodegradation. Studies show that using this reaction network, or those adapted from it, can be used to model landfill dynamics. Reichel et al. (2007), for example, propose a model that couples biodegradation of waste to biomass production. This framework allowed the authors to simulate gas production from a bioreactor that fitted well against experimental data. However, the pH and temperatures obtained from the laboratory experiments were used as input functions, rather than allowing the model to calculate those by itself. This limits the model in predicting gas production for a time series that succeeds the experimental data. In addition to this, the chemical reactions are defined such, that the authors did not need to take the complexity of redox reactions into account. As a result, the authors imply that hydrolysis increases the pH (Reichel et al., 2007, table 1, R1). This is in contrast to the literature, where the hydrolysis of waste is related to a pH reduction (He et al., 2007).

A different study by van Turnhout et al. (2018) presents a model that couples biochemistry to fluid transport. The model predicts the chemical composition of landfill leachate, including the nitrogen species, and gas production under anaerobic and aerobic conditions. By incorporating a large chemical reaction network defined by stoichiometry and reaction kinetics, they predicted the development of concentrations of important components (e.g. pH, $NH_4^+ - N$, $NO_x^- - N$ and SO_4^{2-}) with progressive degradation. The model simulations suggest that $NH_4^+ - N$ and Cl^- concentrations decrease over time. Instinctively, this behaviour is as expected as $NH_4^+ - N$ and Cl^- are effectively “flushed out” of the landfill. However, landfill monitoring data suggests that while Cl^- concentrations decrease, $NH_4^+ - N$ concentrations remain constant over time. A clear increase in

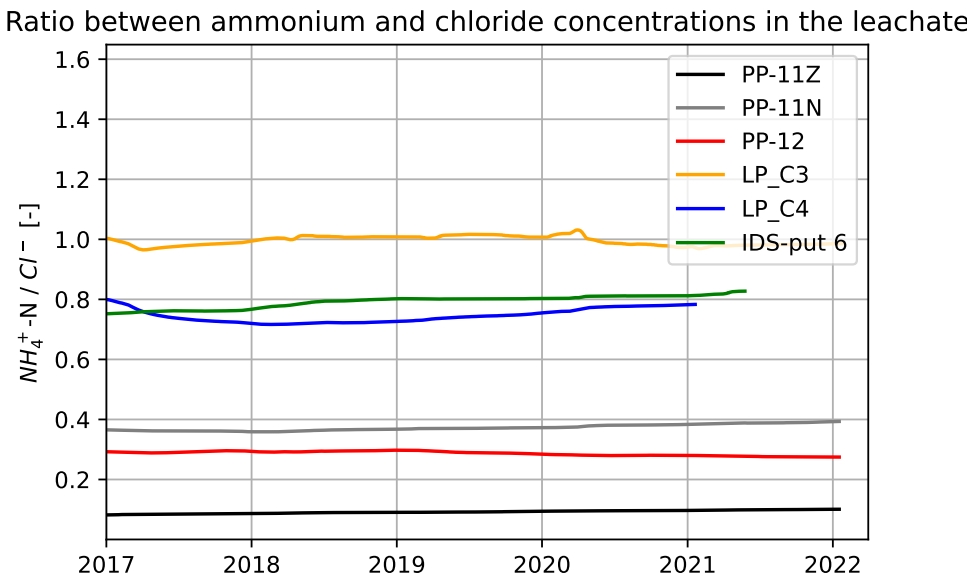


Figure 1.1: The $\frac{NH_4^+-N}{Cl^-}$ ratios in the leachate at the different sites from 2017 onward

$\frac{NH_4^+-N}{Cl^-}$ ratio (based on cumulative data) is observed at the sites PP-11N & PP-11Z (Braambergen), IDS-put 6 (Kragge) and LP_C4 (Wieringermeer) from 2017 onward (Fig. 1.1). In addition to this, recent studies within the CURE project showed that only 0.59-3.5% of the initial nitrogen was removed from the landfills through the leachate (correspondence with Nathali Meza, June 29th, 2022).

Predicting NH_4^+ -N concentrations is found to be a common problem in models simulating landfill waste degradation. Lu et al. (2021), for example, propose a multi-phase, multi-component model to predict the chemical and physical development of a landfill under anaerobic conditions. Their results agree with laboratory studies but NH_4^+ concentrations show different results. The authors ascribe this to the lack of information on the protein content of the solid waste and to the complexity of the laboratory experiments being impossible to model accurately (Lu et al., 2021).

Both the models presented by Lu et al. (2021) and van Turnhout et al. (2018) do not take solute adsorption and desorption into account. These fundamental processes, however, affect the behaviour of NH_4^+ significantly, as indicated by a study on ammonia removal from a bioreactor (Berge et al., 2006). Berge et al. (2006) showed that part (10-20%) of the ammonium could be even unrecoverable as it is fixed to the waste mass. The importance of such a fundamental process suggests that the NH_4^+ behaviour is described by a complex coupled system. The complexity of the nitrogen species is further emphasized by the literature, considering many processes including (de)nitrification, anaerobic ammonium oxidation and nitrate reduction (Berge et al., 2005).

1.3.2 Research Question and Outline

Most available studies present models where the reaction network is fully described by kinetic rate equations. A kinetic solver by itself, however, is not suitable for keeping track of the pH, molar activities and NH_4^+ adsorption to the waste body. Separate equilibrium software is required to include such factors. Recent developments within the CURE organization have suggested ORCHESTRA, a chemical equilibrium software package, as a useful tool to calculate chemical equilibrium conditions in the landfill. ORCHESTRA (Object Representing CHEmical Speciation and TRAnsport) is a chemical equilibrium model developed in the early 2000's to be a valid replacement of other available software (Meeussen and C., 2003). Van Turnhout et al. (2018) showed that this tool can be correctly coupled to a kinetic solver. However, their solver is written in Matlab, whereas the modelling environment for CURE took a shift towards the open source coding language "Python". In addition to this, their study does not conclude on how ORCHESTRA can be used to include the adsorption of NH_4^+ .

To close the bridge between the Matlab solver developed by van Turnhout et al. (2018) and the modelling framework within CURE, this study aimed to develop a tool that binds ORCHESTRA to Python. By coupling the tool to a kinetic solver that simulates waste degradation in a bioreactor, the study examines the importance of such a tool for modelling landfill dynamics. For this, the following research questions are answered:

1. "How can we use ORCHESTRA in Python?"
2. "How is ORCHESTRA coupled to a kinetic solver environment that simulates landfill waste degradation?"
3. "How does NH_4^+ adsorption to the mass waste affect waste degradation in a bioreactor?"

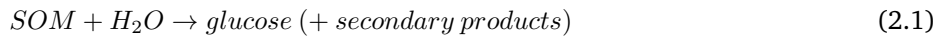
In the next chapter (Chapter 2: *Theoretical Framework*), a literature study is presented that describes the chemical system within a landfill. This includes a brief description of the general degradation pathway of waste and the chemical behaviour of the NH_4^+ -species within a landfill. Chapter 3 (*Model Description*) describes the modelling framework that is used to model landfill dynamics. Here, a distinction is made between the reaction kinetics and the calculation of chemical equilibrium. Following the model description, the model results are presented and discussed in Chapter 4 (*Results and Discussion*). An additional discussion is included in Chapter 5 (*Additional Discussion*). This chapter also contains a brief elaboration on the limitations of the model. Lastly, the study results are summarized in Chapter 6 (*Conclusion*).

Chapter 2

Theoretical Framework

2.1 Biodegradation of Municipal Solid Waste

Microbial decomposition of municipal solid waste (MSW) is the breakdown of solid organic matter (*SOM*). Under anaerobic conditions, waste degradation is a sequential process containing four stages: hydrolysis, acidogenesis, acetogenesis and methanogenesis (Aldin et al., 2011). *Hydrolysis* is the enzymatic breakdown of solid organic waste (*SOM*) under the presence of hydrolytic microorganisms (Veeken et al., 2000; Sekhohola-Dlamini and Memory, 2019):



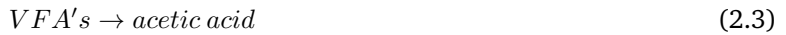
Its primary product is glucose but, depending on the parent material, monosaccharides (from hemicellulose) and fatty acids (from lipids) may be formed (O'Flaherty et al., 2010). Under aerobic conditions, hydrolysis may also lead to secondary products such as nitrates and sulphates due to the subsequent oxidation of sulphur and nitrogen (Khalil et al., 2014).

The next step in waste degradation is *acidogenesis*, a fermentation process that breaks down the glucose to form volatile fatty acids (VFA's) (Lin and Chang, 1999; Munawar, 2014):



Common VFA's are (1) acetate, (2) propionate and (3) butyrate (Zhang et al., 2022). Acetate is the main byproduct in the presence of H_2 utilizing bacteria (Munawar, 2014).

The third step is *acetogenesis*, during which the VFA's other than acetate are converted to acetic acid:



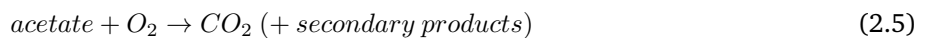
Under anaerobic conditions, acetogenesis is a process induced by acetogenic bacteria (Munawar, 2014). Acetogens can be found in most anaerobic environments, under both normal and extreme conditions (Drake, 2012). The most widespread acetogens include *Synthrophobacter* and *Synthrophomona* (Staszewska and Pawlowska, 2011). Most acidogens and acetogens only thrive under fully anaerobic conditions. However, facultative anaerobes - organisms that may switch from fermentation to aerobic respiration under the presence of oxygen - may produce acetate even when the system is fully aerated (e.g. Farmer and Liao, 1997).

The last stage in the anaerobic waste degradation sequence is *methanogenesis*, during which methanogenic organisms use available substrates to produce methane (Lyu et al., 2018):



While methanogenesis includes the consumption of a wide variety of carbon sources (CO_2 , alcohol, acetate), the largest fraction of CH_4 production (ca. 70%) is related to the consumption of acetate (Staszewska and Pawlowska, 2011). Interestingly, while most CH_4 production is related to the consumption of acetate, there are only a few methanogens that use acetate as a carbon source.

Methanogens are fully inhibited under aerobic conditions. Under aerobic conditions, other organisms play a major role in the degradation of acetate. These organisms include heterotrophic bacteria that use O_2 as an electron acceptor for acetate oxidation (Corsino et al., 2016):



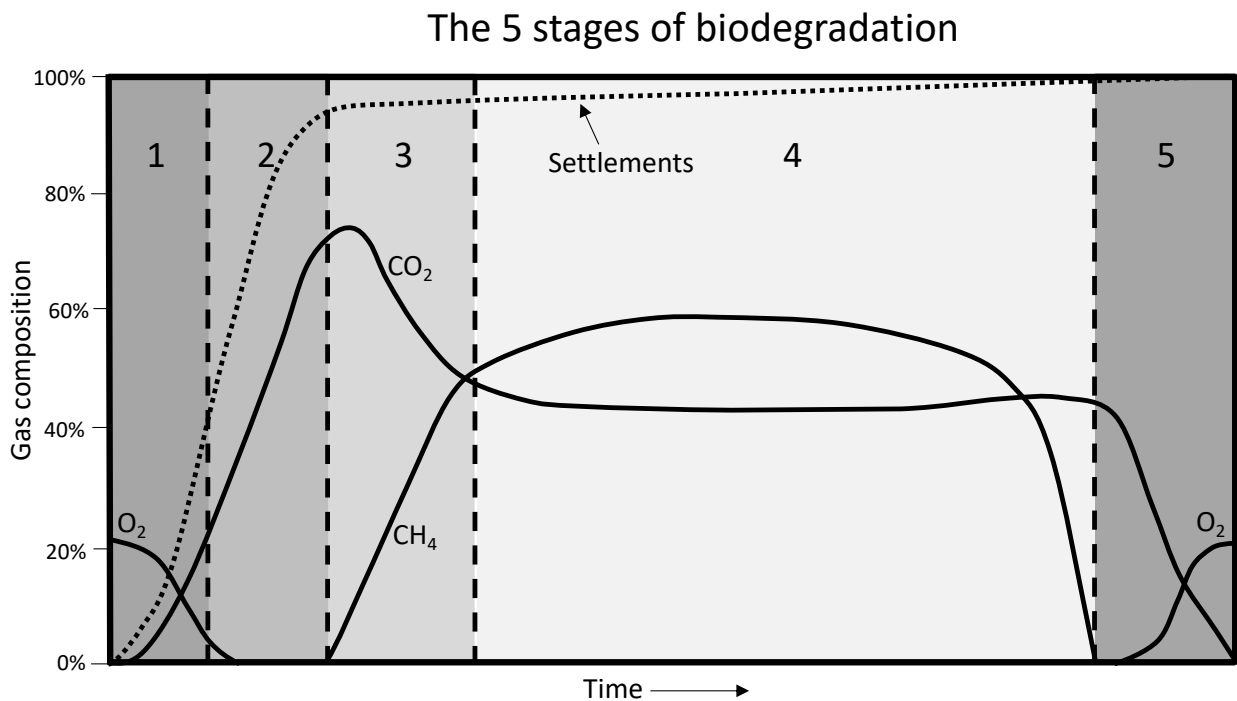


Figure 2.1: The five stages of biodegradation. See text for elaboration. Adapted from Sanci and Panarello, 2012

Note, that acetate oxidation solely leads to the production of CO₂.

This interplay between aerobic and anaerobic activity presents a dynamic process where the biodegradation pathway may alternate between both states. Figure 2.1 illustrates the five stages of biodegradation in a landfill (Sanci and Panarello, 2012). At the initial stage, the presence of O₂ inhibits anaerobic processes and, therefore, allows aerobic processes to dominate the system. During this stage, gas production fully consists of CO₂. Stage 2-3 represent the intermediate stages during which the system gets depleted in O₂, allowing methanogens to slowly take over biodegradation. This shift leads to a change in gas composition where both CO₂ and CH₄ are produced. A steady state of methanogenic activity is reached in the 4th stage, leading to a peak methane gas production (ca. 70%). The final stage is reached when most substrate is decomposed, causing the system to equilibrate back to its original atmospheric conditions. Figure 2.1 also presents the relative settlements related to biodegradation for the different stages. Most settlements are reached during the first two stages, after which settlement rates decline drastically under fully anaerobic conditions.

2.2 Biodegradation rates

Hydrolysis is often considered the rate-limiting step in solid waste degradation (Vavilin et al., 2007; Ghasemzadeh et al., 2017; Alvarado et al., 2021). Because of this, hydrolysis, acidogenesis and acetogenesis are often lumped together:



As hydrolysis is rate limiting, it is no surprise that the parameters affecting its rate are well described in the literature (e.g. Sanders et al., 2000; Dimock and Morgenroth, 2006; Vavilin et al., 2007; He et al., 2007; Alvarado et al., 2021). Firstly, the hydrolysis rate is dependent on the type of substrate. For example, Vavilin et al. (2007) state that the hydrolysis rate of carbohydrates is ca. 5-100 times faster than that of lipids; the wide range relates to differences in experimental conditions. When modelling biodegradation, it is therefore common to subdivide the mass of substrate in hardly- and easily degradable waste, each described by a different degradation rate.

Secondly, the particle size of the substrate may affect the hydrolysis rate significantly (Hills and Nakano, 1984; Dimock and Morgenroth, 2006). Hills & Nakano (1984) performed a study on the effects of particle size on the anaerobic digestion of tomato slices. The results showed an inverse linear relationship between particle size and methane production. However, other studies present an exponential relationship (Valentini et al., 1997):

$$k = k_0 e^{-\frac{d}{K_d}} \quad (2.7)$$

where k_0 is the hydrolysis kinetic constant when approaching a particle diameter of 0, d is the particle diameter and K_d is a constant.

When the enzyme concentration is not rate-limiting, the temperature effect on the hydrolysis rate, as with all kinetic reactions, can be described by the Arrhenius equation (Veeken and Hamelers, 1999; Sanders, 2001):

$$k = Ae^{-\frac{\Delta G^*}{RT}} \quad (2.8)$$

where A is the Arrhenius constant, G^* is the standard free energy of activation, T is the absolute temperature and R is the gas constant. The Arrhenius equation implies that the hydrolysis rate is highest at $T \rightarrow \infty$. However, it has been repeatedly reported that enzymatic activity decreases when a certain temperature is reached as a result of enzyme denaturation (Aguiar et al., 2019; Zamri et al., 2021). This suggests that the hydrolysis rate relates to an optimal temperature, illustrated in Figure 2.2. Note that as microbial activity results in the release of heat

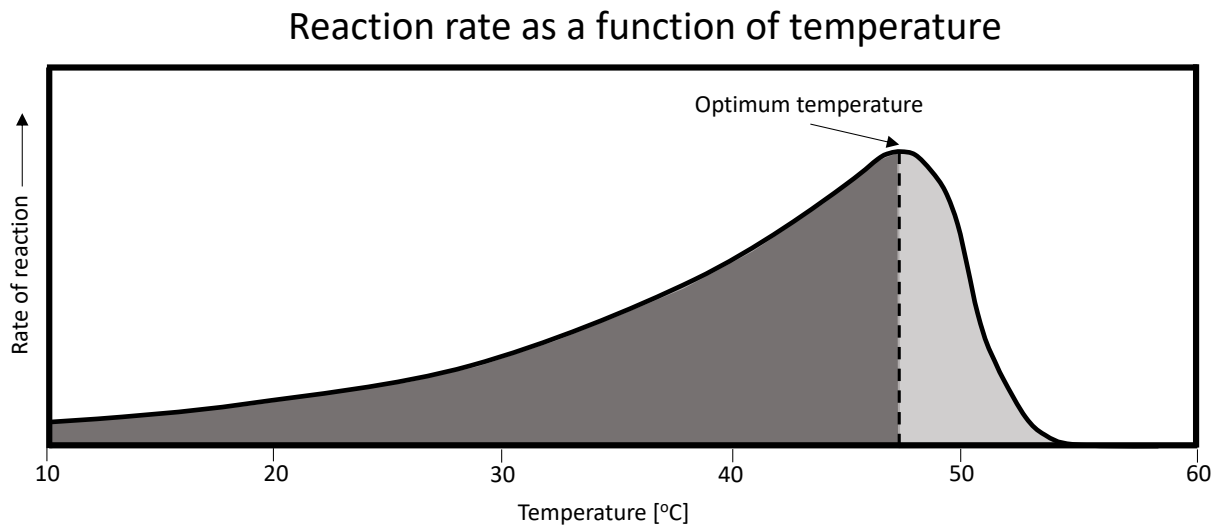


Figure 2.2: Illustration of the effects of temperature on the rate of an enzyme driven reaction. Based on Daniel et al., 2008.

(Xiao et al., 2021), this relation describes a self-enhancing system in the low-temperature range ($T < T_{opt}$).

As with temperature, the pH relates to the enzymatic activity by having an optimal pH level at which enzymatic activity is the highest (Henze et al., 1995). At low pH ranges, the toxicity of undissociated forms of VFAs inhibits the activity (Mormile et al., 1996). Other studies describe this relationship as a symmetric bell-shaped curve with a single optimum, while implying that this is most likely a simplified shape (Sanders, 2001); in a landfill, there are multiple enzymes present, each with a different pH optimum.

Lastly, the hydrolysis rate is affected by the general composition of the landfill solute. As hydrolysis is microbially induced, a loss in biomass would negatively affect the hydrolysis rate. Besides that, it has been reported that hydrolysis of biowaste is possibly affected by the presence of volatile fatty acids (VFAs) (Veeken et al., 2000). It was found that at VFA levels of 40-50 g/L anaerobic hydrolysis was fully inhibited. Veeken et al. (2000) note, however, that these concentrations were accompanied by high acidity levels (pH 5-5.5) stating that this relation should be treated with care.

2.3 Nitrogen in a landfill

Municipal solid waste can be denoted as a chemical compound containing carbon, hydrogen, oxygen and nitrogen, often in the form of $C_wH_xO_yN_z$. Upon degradation, the organic nitrogen is released in the form of ammonium, NH_4^+ . The following sections describe the general pathways of NH_4^+ in a bioreactor landfill.

2.3.1 Ammonification

The release of NH_4^+ in the landfill leachate is a result of the ammonification of proteins containing nitrogen. Ammonification is a two-step process where the hydrolysis of proteins release amino acids followed by deamination (*aerobic*) or fermentation (*anaerobic*) (Staszewska and Pawlowska, 2011). By doing so, bacteria derive metabolic energy where part of the released ammonium is incorporated in newly formed biomass. Ammonium that is in

excess of the metabolic requirements, however, is released to the leachate (Strock, 2008). The ammonification reaction can be schematically generalized to:



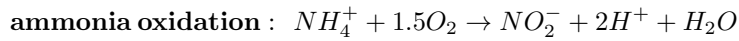
Note, that, ammonification leads to acidification of the system following the chemical equilibrium reaction:



The degree of acidification by this process is dependent on the concurrent conditions (pH and T) in the landfill.

2.3.2 Nitrification

Under aerobic conditions, NH_4^+ is used by nitrifying bacteria to produce nitrate (NO_3^-). First, the ammonium is oxidized to nitrite (NO_2^-) by *Nitrosomonas* (Berge et al., 2005):



Subsequently, *Nitrobacter* oxidize the formed NO_2^- to nitrate (NO_3^-), following:



Nitrification is a pH-lowering process, as H^+ is released into the system during the oxidation of ammonia.

In the literature, oxidation of NH_4^+ is described as the rate-limiting step. This is because the growth rate of *Nitrosomonas* bacteria is slower than that of *Nitrobacter* (Grady et al., 1999). Nitrification is considered to occur only via autotroph bacteria, although some heterotrophic organisms can nitrify (Berge et al., 2005). The reason for this is that the rate at which heterotrophic bacteria initiate nitrification is multiple orders of magnitudes lower than that for autotrophic bacteria (Gupta, 1997).

Nitrification has the benefit of removing NH_4^+ from the landfill leachate. However, nitrification is an aerobic process, whereas landfills are predominantly anaerobic. To allow nitrification to occur in landfills, an aeration system can be installed to supply the nitrifying bacteria with a constant source of O_2 . However, the growth of *Nitrobacter* is inhibited at high O_2 concentrations (Schmidt et al., 2003). Therefore, the oxygen levels within the landfill must be maintained carefully to avoid nitrite accumulation in the leachate.

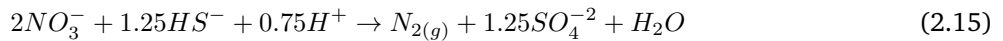
2.3.3 Denitrification

Denitrification is an anaerobic process that reduces nitrate (NO_3^-) in several steps to nitrogen gas (Heinen, 2006). The process is induced by heterotrophic bacteria that use the nitrite as the electron acceptor under the absence of O_2 (Berge et al., 2005). Denitrification can be summarized by the following reactions:



Here, denitrification follows the reduction path of nitrate to nitrite, nitric oxide, nitrous oxide and nitrogen gas. The processes involving the reduction of nitrate are energetically favoured over methanogenic and sulfate reduction processes (Berge et al., 2005). Reactor studies even show that methanogenesis may be fully inhibited when nitrate is present (Price et al., 2003).

Autotrophic microbial species may use an inorganic sulfur source to reduce NO_3^- to N_2 (Onay and Pohland, 2001), where:



Berge et al. (2005) state that this pathway is favoured over heterotrophic reduction when the carbon to nitrogen ratio (C/N) is very low.

2.3.4 Adsorption

Adsorption is the process where a sorbate (e.g. NH_4^+) adheres to a sorbent (e.g. solid organic matter). For landfill studies, this is an important process as the amount of NH_4^+ sorbed to the waste body may be significant (Berge et al., 2005). A study on the adsorption of NH_4^+ on organic material showed that the amount sorbed to the sorbate could even exceed the concentrations in the bulk liquid (Nielsen, 1996).

Studies suggest that NH_4^+ adsorption to the waste mass can be simulated following the Langmuir and Freundlich constitutive models (Halim et al., 2010; Yao et al., 2015). The Langmuir isotherm is used to calculate the amount of adsorbate concentration in the solid phase (q_a) at equilibrium based on the adsorption capacity (q_m in mg/g), the affinity constant (K_a in L/mg) and the concentration of the sorbate in the liquid phase (q_c):

$$q_e = \frac{q_m K_a q_c}{1 + K_a q_c} \quad (2.16)$$

The Langmuir isotherm is based on theoretical methods, whereas the Freundlich isotherm is fully empirical:

$$\log(q_e) = \log(K_d) + n \log(q_c) \quad (2.17)$$

Where K_d is the Freundlich constant and n is a parameter that determines if the curve is convex or concave. Both isotherm equations are useful for simulating adsorption behaviour at a fixed pH, while pH-dependent adsorption effects cannot be fully captured (Jeppu and Clement, 2012). In addition to this, adsorption is also dependent on the ionic strength of the solution. Increasing ionic strength may lead to a decrease in adsorption as a result of competition with other ions (Petrizzelli et al., 1985). Therefore, both relationships (Langmuir and Freundlich) should be treated with care, as studies have presented data that do not fit well with one or both isotherms (Sposito, 1982).

To include the effects of pH and ionic strength of the solute, authors have proposed alternative relationships. For example, studies show that metal adsorption varies linearly with the pH (Anderson and Christensen, 1988). Based on this, Jeppu and Clement (2012) formulated an expression for K_d :

$$K_d = m \cdot pH + b \quad (2.18)$$

Where m and b are model parameters.

Another limitation of the Langmuir and Freundlich models is that they do not describe ion exchange between the adsorbed and solution phase. However, competition between ions in the solution may heavily influence the affinity of NH_4^+ adsorption to the waste surface. This was observed by measuring the NH_4^+ exchange capacity on clinoptite in tap-water and distilled water (Jorgensen et al., 1976; Hedström, 2001); the ion exchange was found to be much lower when using tap-water. To include this behaviour, the NICA-Donnan model may be a preferred approach (Droge and Goss, 2012). This approach explains cation adsorption as a combination of competition to a heterogeneous material and electrostatic interaction between ions and the sorbate (Droge and Goss, 2013). The NICA equation, accounting for the competitive binding state, is given by Eq. (Milne et al., 2003) :

$$Q_i = \frac{n_{i1}}{n_{H1}} \cdot Q_{max1,H} \cdot \frac{(K_{i1}c_i)^{n_{i1}}}{\sum(K_{i1}c_i)^{n_{i1}}} \cdot \frac{[\sum(K_{i1}c_i)^{n_{i1}}]^{p_1}}{1 + [\sum(K_{i1}c_i)^{n_{i1}}]^{p_1}} + \\ \frac{n_{i2}}{n_{H2}} \cdot Q_{max2,H} \cdot \frac{(K_{i2}c_i)^{n_{i2}}}{\sum(K_{i2}c_i)^{n_{i2}}} \cdot \frac{[\sum(K_{i2}c_i)^{n_{i2}}]^{p_2}}{2 + [\sum(K_{i2}c_i)^{n_{i2}}]^{p_2}} \quad (2.19)$$

Where Q_i and c_i are the sorbed amount and the given concentration of component i . $Q_{max1,H}$ and $Q_{max2,H}$ are the maximum proton site density of the substrate, p_1 and p_2 describe the heterogeneity of the material and K_{i1} , K_{i2} , n_{i1} and n_{i2} represent parameters that describe the affinities and non-ideality for each distribution. While the NICA model takes the specific binding to the reactive sites into account, a Donan-submodule is included for the non-specific binding related to the, normally negative, charge to the substance. For this, it is assumed that the sorbent behaves as a gel, having a homogeneous charge (Milne et al., 2003).

2.4 Metabolism

The degradation of waste leads to the generation of energy that bacteria may use for biomass growth. The subsequent consumption of substrate and production of biomass is called a *metabolic* reaction. The main components for a metabolic reaction are illustrated in Figure 2.3. *Catabolism* describes the reaction where a substrate (S) is converted to a product (P) and by that generating metabolic energy (ATP). In turn, bacteria use this energy to construct biomass under the presence of a carbon (C) and nitrogen (N) source in the *anabolic* reaction (Kleerebezem and Van Loosdrecht, 2010). Part of the generated ATP (m_{ATP}) is not used for biomass growth but rather for maintenance processes.

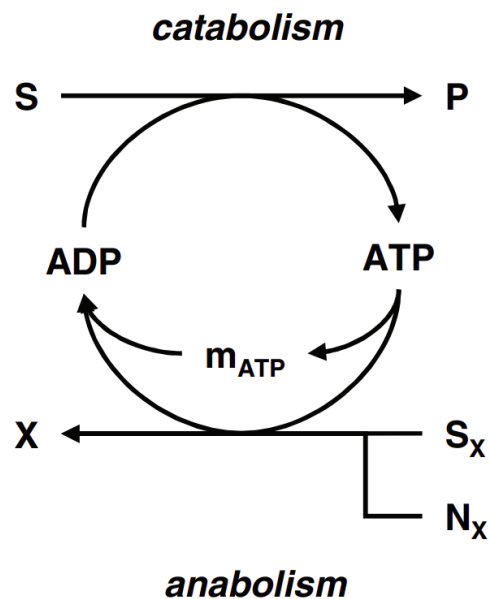


Figure 2.3: General scheme of metabolism. source: Kleerebezem and Van Loosdrecht, 2010

Chapter 3

Model Description

3.1 System description for modelling landfill chemistry

Chapter 2 describes landfill behaviour as a highly complex and coupled system where the chemical reaction rates are dependent on the concurrent conditions within the landfill. To model this behaviour, let us consider a 1 dm^3 volume element where the total volume is the sum of different volume fractions (Fig. 3.1):

$$V_{tot} = V_{inert} + V_{SOM} + V_{aq} + V_g \quad (3.1)$$

Where V_{inert} is the chemically inert waste volume, V_{SOM} is the volume of solid organic matter that is chemically active, V_{aq} is the water volume and V_g the gas volume. The volume element represents a bioreactor where the top of the element can either be opened or closed, illustrated by a hinge at the top-right corner of the waste volume.

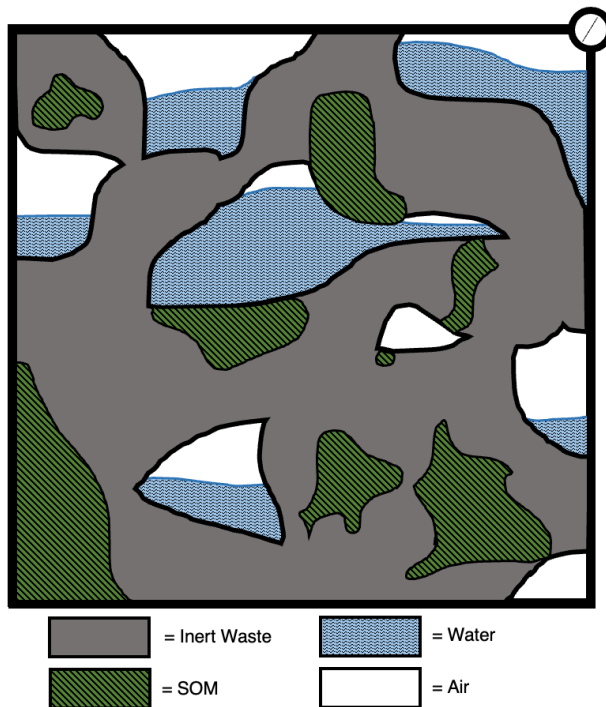


Figure 3.1: Illustration of the model system waste body. The solid fraction consists of chemically inert material and solid organic matter (SOM). The pore space is partly filled with water.

Degradation of chemically active fraction of waste occurs under the presence of bacteria, causing a relative change of the different volume fractions in Eq. 3.1. Waste degradation is modelled by formulating a reaction network that includes the processes described in Chapter 2 (see Section 3.2 for the full reaction network). The rates at which the reactions take place are calculated by considering them as a set of differential equations. These

differential equations are solved using the 'scipy.integrate.solve_ivp' ODE (ordinary differential equations) solver in Python. This package solves a set of ODE's given an initial set of input values following the governing equation:

$$\frac{dY}{dt} = f(t, Y) \quad (3.2)$$

where t represents a 1-Dimensional time vector and Y is a multi-dimensional vector listing the state parameter values at time t. In most-simple words, the solver updates the state values at time $t + i$ based on the calculated rates of change at time t using the current 'state' of the system. This allows the user to implement complex coupled systems where the rate of change of a state parameter Y_i may be dependent on other state values, e.g. Y_j , Y_k and Y_l :

$$\frac{dY_i}{dt} = f(t, [Y_j, Y_k, Y_l]) \quad (3.3)$$

`scipy.integrate.solve_ivp` comes with several available integration methods ('RK45', 'RK23', 'DOP853', 'Radau', 'BDF' and 'LSODA'), given the specific problem. For this study, the implicit BDF solver is used, as it can be used for stiff problems and may work with complex numbers. The BDF method is a multi-step and variable-order method that solves the following equation (Shampine and Reichelt, 1997):

$$\sum_{m=1}^k \frac{1}{m} \nabla^m Y_{n+1} - h f(t_{n+1}, Y_{n+1}) = 0 \quad (3.4)$$

where k is the function order and h is the step size. A simplified Newton equation is used to solve for Y_{n+1} , starting with a predicted value Y_{n+1}^0 .

The full code can be found on the gitlab repository: https://gitlab.tudelft.nl/guidozeew/orchestra_python.

3.1.1 Kinetic vs equilibrium reactions

Modelling landfill chemistry can be described as an interplay between the degradation rate and the concurrent conditions within the landfill. Chapter 2 illustrates that the pH, temperature and chemical composition of the landfill leachate affect the reaction rates significantly. For this, it is important to note that different reactions may have very different reaction rates; some reactions may take several minutes to reach equilibrium (e.g. the chemical equilibrium in water between 1. CO_3^{2-} and HCO_3^- or 2. NH_4^+ and NH_3), while others may take hours or days to complete (e.g. hydrolysis of waste or biomass growth/decay). As the model presented here will simulate landfill dynamics on a relatively large scale (days to weeks), it would be futile to include very fast reactions within the kinetic solver. However, fully excluding the fast reactions from the model calculations would be highly incorrect, as they affect the conditions within the landfill (e.g. pH, T, molar activities). Therefore, reactions that reach equilibrium relatively fast are included by treating them as instantaneous. By doing so, the concurrent landfill conditions (pH and leachate composition) can be calculated at any given time using external equilibrium software.

To relate the kinetic rates to the landfill conditions, the model is subdivided into two parts: (1) reaction kinetics and (2) equilibrium chemistry. The calculation of reaction kinetics is further subdivided into two parts where the total rate of change is dependent on the updated reaction stoichiometry and reaction rates.

3.2 Reaction network

The Python solver is used to solve a set of predefined chemical reactions that encompasses the general biochemical degradation pathway of waste. These reactions include (1) lumped hydrolysis, acidogenesis and acetogenesis with hydrolysis as the limiting step, (2) methanogenesis (anaerobic), (3) oxidation of acetate (aerobic), (4) nitrification, (5) denitrification, (6) biomass ($\text{CH}_{1.8}\text{O}_{0.5}\text{N}_{0.2}$) growth and (7) biomass decay (Table 3.1). The reactions are based on the method proposed by Kleerebezem & van Loosdrecht (2010), by formulating a set of redox half-reactions. A full derivation of the individual reactions can be found in Appendix A. Note that hydrolysis is described as a fermentation reaction where acetate, rather than O_2 , acts as the electron acceptor. In addition to this, the stoichiometry of the hydrolysis reaction is formulated such that it is dependent on the elemental composition of the waste, $\text{CH}_a\text{O}_b\text{N}_c$, where H, O and N are normalized to C.

The proposed reaction network differentiates between aerobic and anaerobic conditions. When O_2 is present, waste degradation will follow the aerobic degradation pathway following reactions 1, 3 and 4. Under anaerobic conditions, waste degradation follows the pathway of reactions 1 & 2. Note, that biomass production (reaction 5) is related to reaction 2-4 (a detailed description is given in Section 3.2.1). Biomass decay (reaction 6) is non-related to the aerobic state of the system.

Table 3.1: Used reaction network for this study. Reactions are based on method proposed by Kleerebezem & van Loosdrecht (2010). Notation is based on electron balance. The hydrolysis reaction is generalized for any chemical composition of solid organic matter ($CH_aO_bN_c$).

1. Hydrolysis lumped with acidogenesis & acetogenesis
$-CH_aO_bN_c - (\frac{2-a+3c}{2})H_2O - (\frac{a+2b+3c}{4})HCO_3^- + (\frac{4+a+2b+3c}{8})CH_3COO^- + cNH_4^+ + (\frac{4+1a+2b+5c}{8})H^+ = 0$
2. Methanogenesis of acetate (anaerobic)
$-CH_3COO^- - H^+ + CO_2 + CH_4 = 0$
3. Oxidation of Acetate (aerobic)
$-CH_3COO^- - 2O_2 - H^+ + 2CO_2 + 2H_2O = 0$
4. Nitrification (aerobic)
$-NH_4^+ - 2O_2 + NO_3^- + 2H^+ + H_2O = 0$
5. Denitrification (anaerobic)
$-0.625CH_3COO^- - NO_3^- - 0.375H^+ + 0.5N_2 + 1.25HCO_3^- + 0.5H_2O = 0$
6. Biomass growth
$-0.525CH_3COO^- - 0.2NH_4^+ - 0.275H^+ + CH_{1.8}O_{0.5}N_{0.2} + 0.05HCO_3^- + 0.4H_2O = 0$
7. Biomass decay
$-CH_{1.8}O_{0.5}N_{0.2} - 0.4H_2O - 0.05HCO_3^- + 0.525CH_3COO^- + 0.2NH_4^+ + 0.275H^+ = 0$

3.2.1 Metabolic reactions

The reactions listed in Table 3.1 present a set of metabolic systems between the *catabolic* (reaction 2-5) and *anabolic* (reaction 6) reactions. The overall stoichiometry of the *metabolic* reactions are established following the method proposed by Kleerebezem & van Loosdrecht (2010), with the governing equation:

$$Y_{met} = \lambda_{cat}Y_{cat} + \lambda_{an}Y_{an} \quad (3.5)$$

Where Y_{met} , Y_{cat} and Y_{an} represent the stoichiometry coefficients of the metabolic, catabolic and anabolic reaction. λ_{cat} and λ_{an} are multiplication factors for the respective catabolic and anabolic reactions. If we define λ_{an} as 1, λ_{cat} represents the yield factor. This factor describes the number of times the catabolic reaction needs to take place to generate sufficient energy to form 1 mole of biomass (Roels, 1980). To calculate the yield factor, the following equation is used:

$$\lambda_{cat} = \frac{\Delta G_{an}^1 + \Delta G_{Dis}}{-\Delta G_{cat}^1} \quad (3.6)$$

Where ΔG_{cat}^1 and ΔG_{an}^1 are the change in Gibb's energy of the catabolic and anabolic reaction in Joules. ΔG_{Dis} accounts for the energy that dissipates as a result of bioenergetic inefficiencies.

The calculation of ΔG_R^1 (where R denotes either the catabolic or anabolic reaction) is illustrated for the following reaction where the reactants A and B lead to the products C and D:



Y_n is the stoichiometry coefficient for component n . The change in Gibb's energy for this reaction is given by Eq. 3.8 (Leupold, 2018):

$$\Delta G_R^1 = \Delta G_R^0 + R \cdot T \cdot \ln \frac{a_C^{Y_C} \cdot a_D^{Y_D}}{a_A^{Y_A} \cdot a_B^{Y_B}} \quad (3.8)$$

Here, ΔG_R^0 is the change in standard Gibb's free energy (in $\frac{J}{mol}$), R is the gas constant (8.314 $\frac{J}{K \cdot mol}$), T is the temperature (in K) and $a_n^{Y_n}$ is the molar activity of the given reactant/product in the solution (in $\frac{mol}{L}$). For any given reaction with n chemical species, Eq. 3.8 can be rewritten to a more generic form:

$$\Delta G_R^1 = \Delta G_R^0 + R \cdot T \cdot \sum_{i=1}^n Y_i \cdot \ln(a_i) \quad (3.9)$$

Note, that the second term in Eq. 3.8 and 3.9 accounts for the non-ideality of the system. ΔG_R^0 is the change in Gibb's free energy under ideal conditions, and is given by the following equation:

$$\Delta G_R^0 = \sum_{i=1}^n Y_i \cdot \Delta G_f^0 \quad (3.10)$$

Table 3.2: (left) Gibb's formation energy for species part of the metabolic reactions; (right) the change of Gibb's energy for the individual reactions listed in Table 3.1.

Name	Structure	ΔG_f (kJ/moles)	Reaction	ΔG_R^0 (kJ/moles)
acetate	CH_3COO^-	-369.4	2	-75.7
biomass	$CH_{1.8}O_{0.5}N_{0.2}$	-67.0	3	-893.8
ammonium	NH_4^+	-79.4	4	-269.1
nitrate	NO_3^-	-111.3	5	-510.04
carbon dioxide	CO_2	-394.4	6	18.39
methane	CH_4	-50.7		
bicarbonate	HCO_3^-	-586.9		
proton	H^+	0.0		
water	H_2O	-237.2		
oxygen	O_2	0.0		
nitrogen gas	N_2	0.0		

ΔG_f^0 is the Gibb's formation energy for chemical species i , which describes the change in energy that is used or generated during the formation of 1 mole of substance i (usually defined at $25^\circ C$). Table 3.2 lists the values for ΔG_f^0 of the different species. In addition to this, the ΔG_R^0 values are listed for the individual reactions in Table 3.1. Note, that by convention a reaction with a negative ΔG_R^1 releases energy and a reaction with a positive ΔG_R^1 takes up energy.

Kleerebezem & van Loosdrecht (2010) state that ΔG_{Dis} is only dependent on the carbon source used for growth. Here a distinction is made between ΔG_{Dis} for heterotrophic (bacteria that utilize an organic carbon source for growth) and autotrophic (bacteria that utilize a non-organic carbon source, e.g. CO_2 for growth). For heterotrophic growth, ΔG_{Dis} is calculated following Eq. 3.11 is used (Kleerebezem and Van Loosdrecht, 2010):

$$\Delta G_{Dis}^X = 200 + 18(6 - NoC)^{1.8} + e^{((-0.2 - \gamma)^2)^{0.16}} \cdot (3.6 + 0.4 \cdot NoC) \quad (3.11)$$

Here, NoC is the carbon chain length of the carbon source (e.g. =6 for glucose; =2 for acetate) and γ is the oxidation state of the carbon source. For γ , the elemental carbon of the carbon source is used as a reference for the oxidation state, being 0 for glucose and +0.5 for acetate. Adopting these values leads to $\Delta G_{Dis}^X = 250.7\text{ kJ/mol}_X$ for using acetate as a carbon source.

For autotrophic growth using CO_2 as a carbon source, ΔG_{Dis}^X depends on the electron donor utilized in the anabolic reaction (Kleerebezem and Van Loosdrecht, 2010). Weak electron donors provide electrons that have not sufficient energy to reduce CO_2 to biomass (Heijnen and Kleerebezem, 1999). To account for this, microorganisms increase the energy level of these electrons by investing Gibb's energy. This process is called reverse electron transfer (RET; Sieber et al., 2012). In general, the following relation can be used:

$$\Delta G_{Dis}^X = \begin{cases} 986 \text{ kJ/mol}_X & \text{No RET, strong electron donors } (H_2/H^-, HS^{-1}/SO_4^{2-}) \\ 3500 \text{ kJ/mol}_X & \text{RET, weak electron donors } (Fe^{+2}/Fe^{+3}, NH_4^+/NO_3^-) \end{cases} \quad (3.12)$$

Note, that for this study, all metabolic systems use acetate as the carbon source for biomass growth (Table 3.2, the same anabolic reaction is coupled to all catabolic reactions). Therefore, all reactions use the same value for the dissipation energy, calculated at 250.7 kJ/mol_X (for acetate).

3.2.2 Stoichiometry matrix

The set of reactions listed in Table 3.1 is used to formulate a single stoichiometry matrix that will be used as input for the model, listing the reactions and their stoichiometry coefficients for the individual species (Table 3.3). The reactions are either named 'C' (for the catabolic reactions) or 'A' (for the anabolic reactions) followed by an index number. This number is used to correspond the catabolic reaction to the correct anabolic reaction; for example, reactions C3 and A3 are linked to form the metabolic reaction M3. When no anabolic counterpart is provided for a given catabolic reaction, the reaction is treated as final. Note that stoichiometry coefficients for the hydrolysis reaction of waste (C1) are included for illustrative purposes; the true stoichiometry is dependent on the specific elemental composition of waste.

Table 3.3: Stoichiometry input for model.

Reaction	SOM	acetate	biomass	NH ₄ ⁺	NO ₃ ⁻	O ₂	N ₂	CO ₂	CH ₄	HCO ₃ ⁻	H ⁺	H ₂ O
C1 ¹	-1	0.5783		0.03125						-0.1566	0.3904	-0.1869
C2	-1						1	1			-1	
A2 ²	-0.525	1		-0.2						0.05	-0.275	0.4
C3	-1					-2		2			-1	2
A3 ²	-0.525	1		-0.2						0.05	-0.275	0.4
C4				-1	1	-2					2	1
A4 ²	-0.525	1		-0.2						0.05	-0.275	0.4
C5	-0.625				-1			0.5		1.25	-0.375	0.5
A5 ²	-0.525	1		-0.2						0.05	-0.275	0.4
C6 ³	0.525	-1		0.2						-0.05	0.275	-0.4

The stoichiometry matrix is used to obtain two matrices, $\mathbf{M}_{C(m \times n)}$ and $\mathbf{M}_{A(m \times n)}$. $\mathbf{M}_{C(m \times n)}$ contains the stoichiometry coefficients of all catabolic reactions, where m is the number of catabolic reactions ($=6$) and n is the number of chemical species ($=12$). The anabolic stoichiometry coefficients are represented by matrix $\mathbf{M}_{A(m \times n)}$, having the same shape ($m \times n$). The row position of the anabolic reaction in $\mathbf{M}_{A(m \times n)}$ is the same as its catabolic counterpart. In case no anabolic reaction is provided (here, at the 1st and 6th position) the row is filled with 0's. $\mathbf{M}_{C(m \times n)}$ and $\mathbf{M}_{A(m \times n)}$ for the stoichiometry matrix in Table 3.3 are given below:

$$\mathbf{M}_{C(5 \times 13)} = \begin{bmatrix} -1 & 0.5783 & \dots & 0.3904 & -0.1869 \\ 0 & -1 & \dots & -1 & 0 \\ 0 & -1 & \dots & -1 & 2 \\ 0 & 0 & \dots & 2 & 1 \\ 0 & -0.625 & \dots & -0.375 & 0.5 \\ 0 & 0.525 & \dots & 0.275 & -0.4 \end{bmatrix} \quad \mathbf{M}_{A(5 \times 13)} = \begin{bmatrix} 0 & 0 & \dots & 0 & 0 \\ 0 & -0.525 & \dots & -0.275 & 0.4 \\ 0 & -0.525 & \dots & -0.275 & 0.4 \\ 0 & -0.525 & \dots & -0.275 & 0.4 \\ 0 & -0.525 & \dots & -0.275 & 0.4 \\ 0 & 0 & \dots & 0 & 0 \end{bmatrix}$$

Using $\mathbf{M}_{C(m \times n)}$ and $\mathbf{M}_{A(m \times n)}$ with Eq. 3.6 and 3.9 and the values from table 3.2 results in a vector containing the yield factor for each reaction, λ_{cat} . The final stoichiometry matrix ($\mathbf{M}_{M(M \times n)}$) is then obtained using Eq. 3.5. A vector $\beta_{1 \times n}$ is introduced (a vector where all elements are set to 1) to allow for elementwise multiplication between λ_{cat} and $\mathbf{M}_{C(m \times n)}$, leading to:

$$\mathbf{M}_{M(m \times n)} = (\lambda_{cat} \times \beta_{1 \times n}) * \mathbf{M}_{C(m \times n)} + \mathbf{M}_{A(m \times n)} \quad (3.13)$$

Where $*$ is an operator that indicates elementwise multiplication.

3.3 Reaction kinetics

3.3.1 Michaelis-Menten and Monod kinetics

The rates at which the different reactions (Table 3.2) occur are calculated in Python, following Michaelis-Menten and Monod kinetics. The enzyme-driven reaction (C1, reaction 1 in Table 3.1) - the hydrolysis of waste-producing acetate - is described by the Michaelis-Menten equation (Haarstrick et al., 2001):

$$v = V_{max} \frac{|S|}{|S| + K_M} \quad (3.14)$$

Where V_{max} is the maximum reaction rate (in d^{-1}), $|S|$ is the concentration of the limiting substrate and K_M is the Michaelis constant. From Eq. 3.14 follows that $v \rightarrow 0$ when $|S| \rightarrow 0$.

The same mathematical approach is taken for the biomass growth (C2-C4), where the growth rate (μ) is based on Monod kinetics (Walsh, 2018):

$$\mu = \mu_{max} \frac{|S|}{K_s + |S|} \quad (3.15)$$

In this equation, μ_{max} is the maximum growth rate (in d^{-1}) and K_s is the half-velocity constant. Note, that Eq. 3.14 and 3.15 share the same mathematical structure. Biomass decay (C5, reaction 6 in Table 3.1) is calculated

¹For an elemental composition $CH_{1.72}O_{0.5}N_{0.0313}$

²Anabolic reaction that forms biomass

³Biomass decay

adopting a negative value for μ . The rate equations are used to formulate a single vector, \vec{R} , listing the reaction rates for reactions C1-C6:

$$\vec{R} = \begin{pmatrix} v \\ \mu_1 \\ \mu_2 \\ \mu_3 \\ \mu_4 \\ -\mu_5 \end{pmatrix} \quad (3.16)$$

3.3.2 Inhibition functions

Michaelis-Menten and Monod kinetics have been proven to be highly effective for modelling landfill dynamics (e.g. Reichel et al., 2007; Majdinasab et al., 2017; Lu and Feng, 2020). This effectiveness is ascribed to the option of adding multiple inhibition terms (f_i) to the rate equation. An inhibition function is a dimensionless factor which ranges from 0 to 1 and accounts for system conditions that may limit a specific reaction (Luong, 1987). The first example is already presented in Eq. 3.14 and 3.15 where the reaction and growth rate are inhibited by the substrate concentration, called *substrate inhibition* (f_s , Fig. 3.2, top-left). Here, only one limiting substrate is shown, while in fact, multiple substrates could play an inhibiting role. For example, aerobic reactions (reaction 3 and 4 in Table 3.1) are dependent on the oxygen concentrations ($|O_2|$) and nitrifying bacteria (reaction C4, Table 3.2) require NH_4^+ to be present. Other inhibition functions include those for pH (Fig. 3.2, top-right) and temperature (Fig. 3.2, bottom-left) (Reichel et al., 2007). This leads to the following set of inhibition functions:

$$f_{NH_4^+} = \frac{|NH_4^+|}{|NH_4^+| + K_{NH_4^+}} \quad f_{O_2} = \frac{|O_2|}{|O_2| + K_{O_2}} \quad (3.17)$$

$$f_{pH} = \frac{K_{pH}}{K_{pH} + \frac{10^{pH}}{10^{pH_{opt.1}}} + \frac{10^{pH_{opt.2}}}{10^{pH}} - 2} \quad f_T = e^{-(\kappa \cdot (T - T_{opt}))^2}$$

Where $pH_{opt.1}$ and $pH_{opt.2}$ are the respective upper and lower bound of the optimal pH range for the reaction to occur. κ is a temperature constant and T_{opt} is the optimal temperature (in K) for a given reaction.

Different types of inhibition functions

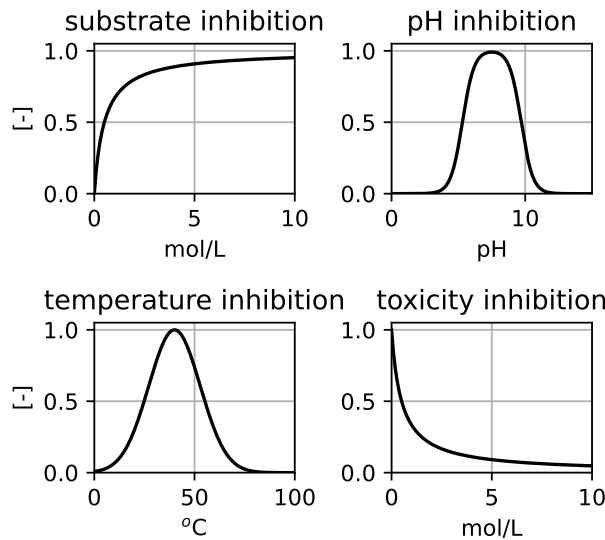


Figure 3.2: Examples of the various inhibitions described by the mathematical expressions in Eq. 3.17, 3.18 and 3.19.

Three special cases of inhibition are further introduced. The first accounts for inhibition by toxicity (Fig. 3.2, bottom-right):

$$f_{tox} = 1 - \frac{|C|}{|C| + K_{tox}^C} \quad (3.18)$$

Where $|C|$ is the concentration of the toxic component. An example of *toxicity inhibition* is the presence of O_2 inhibiting the activity of anaerobic bacteria (e.g. Lu and Imlay, 2021), affecting reactions C2 and C5 (Table 3.2). For these reactions, Eq. 3.18 implies that $f_{tox} \rightarrow 0$ when high oxygen levels are reached. In a similar matter, it is documented that high NH_4^+ concentrations tend to inhibit the hydrolysis rate of waste (Valencia et al., 2011). A toxicity inhibition for is therefore also applied to reaction C1 (Table 3.2), related to the NH_4^+ concentrations.

Secondly, the model should be able to distinguish waste that is hardly, moderately, and easily degradable. Previous studies incorporate this by introducing three types of waste, each characterized by different kinetic parameters ($\mu_{max,hardl.} < \mu_{max,model.} < \mu_{max,easy}$) (e.g. Reichel et al., 2007; Lu et al., 2019). In this study, we propose a different approach, where the biodegradability of solid organic matter is based on the fraction of waste that has been degraded:

$$f_{degr} = \frac{SOM}{K_{degr} + SOM} \quad (3.19)$$

Lastly, an inhibition function for the hydrolysis of waste is introduced that accounts for the presence of biomass. Hydrolysis is microbially induced and a reduction in biomass would result in a reduction in the hydrolysis rate. For this study, this term follows the same structure as substrate limitation, being dependent on the biomass concentration, $|X|$, and a half-constant, K_X :

$$f_X = \frac{|X|}{|X| + K_X} \quad (3.20)$$

3.3.3 Combining reaction rates with reaction stoichiometry

The maximum rates (V_{max} and μ_{max}) and the inhibition functions are combined with the stoichiometry matrix, $\mathbf{M}_{M(m \times n)}$, to obtain the rate of change for the individual chemical species for the different reactions, following:

$$\Delta\mathbf{M}_{M(m \times n)} = \vec{R} \cdot \mathbf{M}_{M(m \times n)}^{norm} \quad (3.21)$$

Here, $\mathbf{M}_{M(m \times n)}^{norm}$ is the final stoichiometry matrix ($\mathbf{M}_{M(m \times n)}$) normalized to the stoichiometry of the monitoring species of each reaction. The monitoring species is the species for which the growth rate is calculated. For example, the rate at which acetate is consumed by methanogens (reaction C2, Table 3.2). The monitoring species of the different reactions are listed in Table 3.4.

Table 3.4: Monitoring species for the reactions listed in Table 3.2.

Reaction	Monitoring species
C1	acetate
C2/A2	biomass
C3/A3	biomass
C4/A4	biomass
C5/A5	biomass
C6	biomass

Substitution of Eq. 3.16 in Eq. 3.21 with the addition of the inhibition functions leads to the final equation:

$$\Delta\mathbf{M}_{M(m \times n)} = (\vec{\mu}_{max} \cdot \prod_{i=0}^j \vec{f}_i) \cdot \mathbf{M}_{M(m \times n)}^{norm} \quad (3.22)$$

Where $\vec{\mu}_{max}$ is the vector listing the maximum rates (μ_{max} and V_{max}) for the different reactions and \vec{f}_i a vector listing the inhibition functions. j is the number of inhibition functions; By default, non-specified inhibition functions have a value of 1.

3.4 Chemical equilibrium

The kinetic rate equations presented in Chapter 3.3 introduce a coupled process where the reaction rates are dependent on the concurrent conditions within the landfill (Eq. 3.17-3.22). However, as the reaction network (3.1) describes a progressing and ever-changing system, the pH and leachate composition cannot be assumed

constant and must be known at all times to predict landfill dynamics correctly. For this, the use of chemical equilibrium software is required, which is used to calculate chemical speciation within the leachate (composition and pH). Recent developments within the CURE program have allowed the use of such chemical equilibrium software: ORCHESTRA.

It must be noted, however, that the more conventional chemical equilibrium software (e.g. MINTEQA2, PHREEQC, MINEQL and ECOSAT) are already very powerful. These programs work by selecting a set of chemical reactions and their reaction constants, followed by a correct calculation of the chemical speciation. However, the problem arises with the general structure regarding such software. While the user can select a set of chemical components, the reactions related to those components are already pre-defined within the source code. Although this allows for a user-friendly experience, it also poses little transparency and flexibility. For example, if one would desire to change or add model definitions (e.g. exclude chemical equilibrium reactions from the calculation), this would require changing and recompiling the source code. For this, the source code must available in the first place and even if this is the case, recompiling may take up a significant amount of time as the source code files may be very large.

This is the main reason why ORCHESTRA was created. With ORCHESTRA, the model definitions (e.g. chemical reactions, kinetics, general conditions) are defined in an input file. The calculation is done in a separate kernel that uses this input file. This means that the calculation kernel (or source code) does not contain any chemical information in itself and only acts as a calculator object. By structuring the software this way, changing model definitions does not require changing and recompiling the source code. This allows the user to quickly select the reactions that the solver should include for calculating chemical equilibrium. The user can thereby exclude reactions that are described kinetically from those partaking in chemical equilibrium. Separating the model definitions from the source code also means that the calculation kernel is extremely small and, because of that, very efficient.

Although the calculator in itself is less complex and more flexible compared to the other equilibrium models, the difficulty with ORCHESTRA lies in correctly defining the chemical input file. To counteract the loss of a user-friendly experience, a graphical user interface (GUI) is developed to interactively set up the input file. The GUI can be downloaded from <http://orchestra.meeussen.nl>. The user interface comes standard with the ORCHESTRA-ready database for PHREEQC and various adsorption models. If needed, the user can create its own database with user-defined reactions.

3.4.1 Using ORCHESTRA in Python: Pybind11

ORCHESTRA is available for either Java or C++, while the kinetic solver for this study runs in Python. For a smooth transition between Python and ORCHESTRA, a submodule is required that allows the full functionality of ORCHESTRA to be integrated within the Python environment. This study aimed to develop a submodule that 'wraps' ORCHESTRA to Python.

Because Python itself is written in C++ code it is possible to wrap the C++ version of ORCHESTRA to Python. For this, the lightweight Pybind11 library is used. With Pybind11, C++ classes and functions can be easily embedded within the Python interface by integrating the C++ objects within a Python submodule. The ORCHESTRA submodule can then be used in Python similar to other modules, e.g.:

```
import numpy as np
from math import *
import PyORCHESTRA #here the ORCHESTRA module is imported
```

Subsequently, the user creates an ORCHESTRA object:

```
p = PyORCHESTRA.ORCHESTRA() #get the C++ object
```

This 'p'-object includes everything that is required to use ORCHESTRA from within Python, containing 4 different functions:

- `p.initialise`: a function with the chemistry file containing model definitions as input. This function initializes the ORCHESTRA calculator object.
- `p.updatevalues`: a function that updates the user-defined input chemistry for which chemical equilibrium will be calculated.
- `p.calculate`: a function that calculates chemical equilibrium. The output is an array with values for user-defined variables.

- `p.set_and_calculate`: combines `updatevalues` and `calculate` to directly set new input parameters and calculate chemical equilibrium.

By storing all chemical information within the '`p`'-object, no information on the chemical solver is lost when going back and forth between Python and ORCHESTRA. This makes the solver highly efficient as `p.initialise` has to only be called once at the start of the simulation.

For this study, it was decided to make the Python wrapper for ORCHESTRA as general as possible. This allows the developed tool to be used by others that wish to use ORCHESTRA within a Python environment. For this reason, a detailed documentation of the ORCHESTRA wrapper is not presented here but made available as a separate document (Appendix B). However, the documentation should be seen as an integral part of this thesis. The source code to install the wrapper can be found on the gitlab repository: https://gitlab.tudelft.nl/guidozeeuw/orchestra_python.

3.4.2 Modelling landfill chemistry with ORCHESTRA

ORCHESTRA is used to calculate a set of parameters that are needed to solve the kinetic equations presented in section 3.2.1 and 3.3. In summary, Table 3.5 relates the different ORCHESTRA **output** parameters to the different equations. To calculate chemical equilibrium, ORCHESTRA requires information on the bulk composition of the system, for example: the total amount of nitrogen (*N*), carbon (*C*), oxygen (*O*) and hydrogen (*H*) available. However, keeping track of the elemental composition can be a complicated task in a kinetic solver environment where many different species are considered. Therefore, rather than using the elemental composition, we define a set of *primary entities* (or 'building blocks') to describe the bulk composition of the system. For this study, these include: (1) *SOM*, (2) acetate, (3) biomass, (4) NH_4^+ , (5) NO_3^- , (6) N_2 , (7), SO_4^{2-} , (8) Ca^{+2} , (9) CO_3^{2-} , (10) O_2 and (11) H . By keeping track of the 'totals' of the primary entities in Python, ORCHESTRA can calculate chemical equilibrium for any given composition. This is illustrated in Figure 3.3 where at every timestep ($t = i$), the Python solver 'sends' a list with the composition of the primary entities to ORCHESTRA which, in turn, returns a list with the output parameters that follow from chemical equilibrium (listed in Table 3.5).

When coupling the Python kinetic solver to ORCHESTRA, the user must distinguish between reactions that are solved kinetically and those that are captured by the chemical equilibrium calculation in ORCHESTRA. The reactions listed in table 3.1 are all captured by the kinetic solver and are therefore not included in the ORCHESTRA solver. This is because (1) they describe relatively slow reactions that require a kinetic solution and (2) they are microbially induced and therefore treated as irreversible. Equilibrium reactions, on the other hand, must be included in the ORCHESTRA solver. Examples of such reactions are: (1) $\text{NH}_4^+ \leftrightarrow \text{NH}_3 + \text{H}^+$, (2) $\text{CO}_3^{2-} + \text{H}^+ \leftrightarrow \text{HCO}_3^-$ and (3) $\text{CaCO}_3 \leftrightarrow \text{Ca}^{+2} + \text{SO}_4^{2-}$. Note, that when a reaction is included in the ORCHESTRA solver, it is treated as instant (no rates are taken into account). An example of this is the relation between nitrification and the chemical equilibrium between NH_4^+ and NH_3 . Nitrification is described kinetically where a calculated rate determines how much NH_4^+ is converted to NO_3^- . However, a change in NH_4^+ as a result of nitrification leads to a direct change in NH_3 concentrations following the equilibrium reaction.

The question may arise why *SOM*, acetate and biomass are part of primary entities in ORCHESTRA, as they

Table 3.5: ORCHESTRA output parameters and their relation to the different equations

Output parameter description	ORCHESTRA syntax	Related Equations
Molar activities (in $\frac{\text{mol}}{\text{L}}$) of the reactants and products part of the reactions presented in Table 3.1.	[X].logact	3.8
Molar activities (in $\frac{\text{mol}}{\text{L}}$) of species that affect inhibition functions.	[X].logact	3.14, 3.15, 3.17-3.21
pH	pH	3.17

do not partake in any chemical equilibrium reaction; their change is described kinetically. They are, however, used by ORCHESTRA to determine the share of totals on which equilibrium is based. For further information on this, the reader is referred to the documentation, example 2 (Appendix B). Similar to `calcite_mineral.tot` in this example, primary entities are created for *SOM*, acetate and biomass where:

```
@composition(SOM, 1, CO3-2, 1.595, H, -2.5, 0)1,2
@composition(acetate, 2, CO3-2, 3, H, -4, 0)1
@composition(biomass, 1, CO3-2, 1, H, -2.5, 0)1
```

Note that *N* is not included in the composition of *SOM* and biomass. This is because the totals of NH_4^+ are already monitored by the kinetic solver.

¹Compositions rewritten to the primary entities CO_3^{2-} , NH_4^+ , *O* and *H*. As NH_4^+ is monitored kinetically, NH_4^+ is extracted from the used composition in ORCHESTRA.

²For composition $\text{CH}_{1.72}\text{O}_{0.5}\text{N}_{0.0313}$.

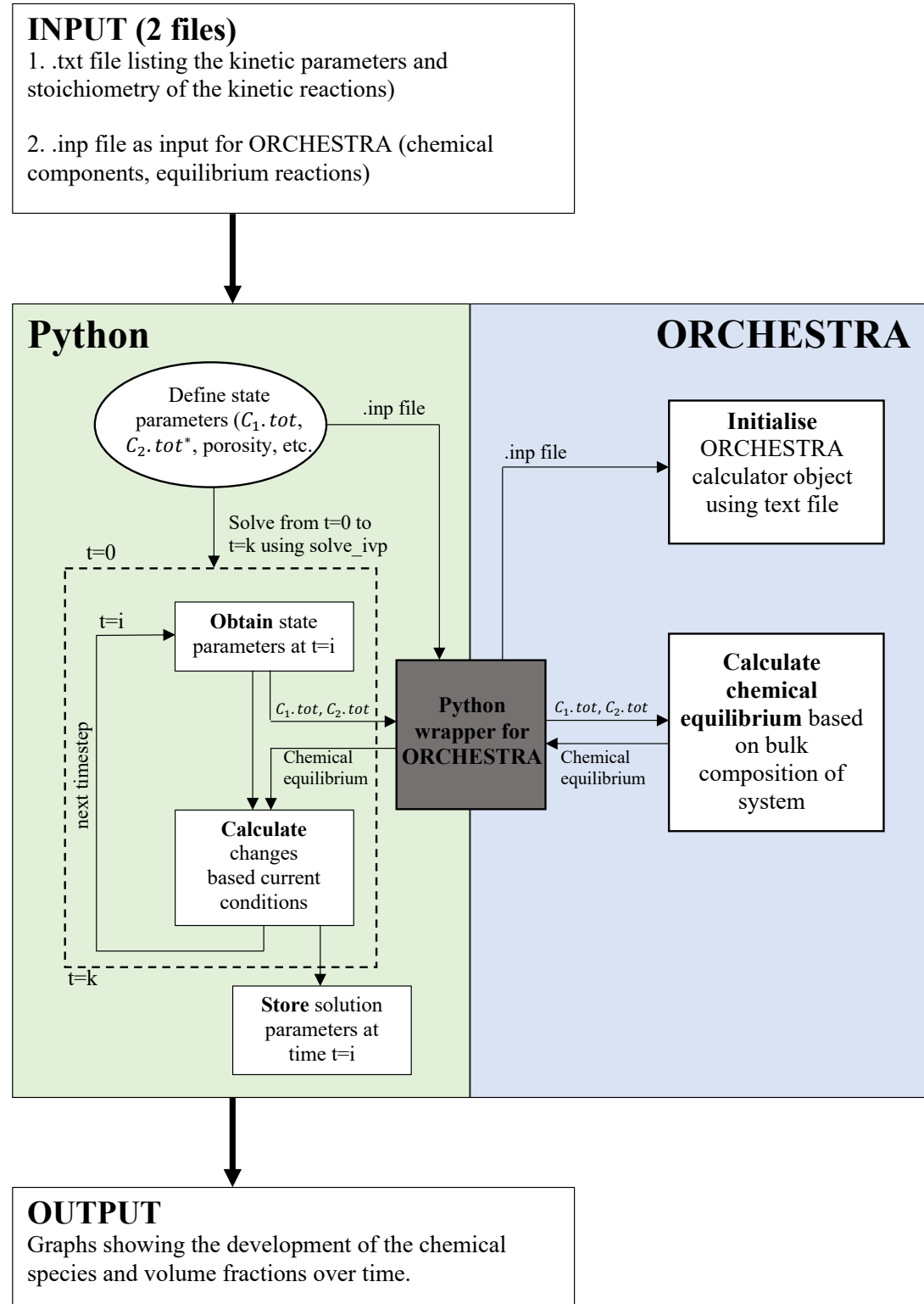


Figure 3.3: Pseudocode of the model. The figure illustrates how ORCHESTRA is used to calculate equilibrium conditions for a system with given bulk composition.

3.5 Porosity, saturation and organic fraction

Degradation of waste in a 0-D volume element will lead to changes in the different volume fractions. The change of the total volume (Eq. 3.1) is then given by:

$$\Delta V_{tot} = \Delta V_{inert} + \Delta V_{SOM} + \Delta V_{aq} + \Delta V_g \quad (3.23)$$

V_{inert} and V_{aq} are assumed to be constant over time; the chemically inert waste is not degradable and no water transport is considered. If no loss in volume is assumed ($\Delta V_{tot} = 0$), then the change in the waste volume is fully accounted for by a change in the air volume:

$$-\Delta V_{SOM} = \Delta V_{air} \quad (3.24)$$

Because constant volume is assumed, the change in porosity is calculated directly from a change in V_{SOM} , where:

$$\Delta n = -\frac{\Delta V_{SOM}}{V_{tot}} = -\frac{\Delta Mole_{SOM}}{Mole_{SOM}} \cdot \frac{V_{SOM}}{V_{tot}} \quad (3.25)$$

Here, $Mole_{SOM}$ and $\Delta Mole_{SOM}$ are the respective total amount and change in the total amount of mole waste at time t . The change in porosity is used to calculate the change in saturation, which is based on finite differences:

$$\Delta S = S^{t+\Delta t} - S^t \quad (3.26)$$

Where S^t is the known saturation at time t and $S^{t+\Delta t}$ is related to the change in porosity, following:

$$S^{t+\Delta t} = \frac{n^t \cdot S^t}{n^{t+\Delta t}} \quad (3.27)$$

Where:

$$n^{t+\Delta t} = n^t + \Delta n \quad (3.28)$$

3.6 Case Studies

The model system described in the previous sections is used to examine the effects of NH_4^+ adsorption on the waste body. For this, four case studies are presented:

1. Degradation in a **closed** system **without** NH_4^+ adsorption
2. Degradation in a **partly open** system **without** NH_4^+ adsorption
3. Degradation in a **partly open** system **with** NH_4^+ adsorption
4. Degradation in a **partly open** system **with** NH_4^+ adsorption following kinetic parameters from the literature.

Note, that case studies 1 & 2 mainly function as a verification of the model implementation. Their results are used to examine whether the model is capable of simulating waste degradation in a bioreactor. With this, the implications of using ORCHESTRA with the kinetic solver are discussed as well. Case study 3 is then used to examine the effects of NH_4^+ adsorption to the waste surface. Lastly, a case study is presented where the model includes kinetic parameters based on literature data. In the following chapters, the model boundary conditions for the individual cases are further elaborated.

3.6.1 Case study 1: Degradation of waste in a closed system with no NH_4^+ adsorption

The first case study simulates waste degradation as depicted in Figure 3.1, where the top of the volume element is closed at the start of the model calculation. This represents a bioreaction experiment without aeration as no O_2 is added to the system at $t > 0$. Table 3.6 lists the used parameter values for the kinetic solver. While these parameter values are not based on available literature data, they are chosen as such to represent landfill behaviour, where aerobic degradation occurs at a faster rate than anaerobic degradation. Note, that kinetic parameters for the temperature dependency on biomass decay are also provided. This is done, as the literature shows that biomass decay increases with increasing temperature (Reichel et al., 2007; Gholamifard et al., 2008). Note, however, that no temperature changes are included in the model, where the temperature is kept constant at 21 °C.

The initial conditions are presented in Table 3.7. Here, the chemical parameters are defined as 'totals'

Table 3.6: Model parameters used for Case 1, 2 & 3

Reaction	μ_{max} d^{-1}	K_{pH} [-]	pH_{opt}^1 [-]	pH_{opt}^2 [-]	T_{opt} $^{\circ}C$	κ_T $^{\circ}C^{-1}$	K_s $mol L^{-1}$	$K_{lim}^{NH_4^+}$ $mol L^{-1}$	$K_{tox}^{NH_4^+}$ $mol L^{-1}$	$K_{tox}^{O_2}$ $mol L^{-1}$	$K_{lim}^{O_2}$ $mol L^{-1}$	K_{degr} mol
hydrolysis	0.03	500	6.5	7.5	60	0.03	0.5	-	0.0001	-	-	2.0
methanogenesis	0.1	500	6	7	60	0.06	0.4	0.01	-	0.00001	-	-
oxidation	0.8	500	6	7	60	0.06	0.3	0.01	-	-	0.00001	-
nitrification	0.6	500	6	7	60	0.06	0.3	0.01	-	-	0.00001	-
denitrification	0.2	500	6	7	60	0.06	0.1	0.01	-	0.00001	-	-
decay ¹	0.015	-	-	-	80	0.053	0.02	-	-	-	-	-

representing the composition of the system as a whole (solid + liquid + gas). The absence of acetate, NH_4^+ and NO_3^- imply that no waste degradation took place before the simulation. Solid organic matter is described by the elemental composition $CH_{1.72}O_{0.5}N_{0.03125}$, having a C/N ratio of 32:1. This composition agrees with literature data (e.g. Puyuelo et al., 2011; Komilis et al., 2012).

Table 3.7: Initial conditions for the models presented in Case study 1, 2 & 3

Variable	$mol L^{-1}$	Variable	$mol L^{-1}$	Variable	[-]
SOM.tot	3.11	H.tot	5.11	porosity	0.25
acetate.tot	0	Ca^{+2}	0.47	saturation	0.9
methanogens.tot	0.01	NH_4^+ .tot	0	organic fraction	0.3
oxidizers.tot	0.01	NO_3^- .tot	0		
nitrifiers.tot	0.01	O_2 .tot	0.0051		
denitrifiers.tot	0.01	SO_4^{2-} .tot	0.1		
CO_3^{2-} .tot	3.22	N_2 .tot	0		

3.6.2 Case study 2: Degradation of waste in an open system with no NH_4^+ adsorption

For this case study, the initial conditions are identical to those from case study 1. The only difference here is, that the system is periodically "opened", allowing O_2 to flow into the system. This 'inflow' of oxygen is implemented kinetically, similar to the kinetics of the chemical reactions. For this, an inhibition function is applied that halts the addition of oxygen when atmospheric levels (20% oxygen) are reached. This leads to the following mathematical description of the oxygen addition:

$$\mu_{O_2 \text{ addition}} = W \cdot \mu_{max} \cdot \frac{0.2 - O_{2(g)}^{act}}{0.2} \quad (3.29)$$

Here, 0.2 is the gas activity of oxygen at atmospheric levels and $O_{2(g)}^{act}$ is the concurrent gas activity. W acts as a 'switch' (either 0 or 1) that determines whether O_2 is allowed to enter the system (open vs closed conditions). The inflow is treated as a Robin boundary condition where μ_{max} is chosen as such that the inflow of oxygen is very high. This ensures quick aeration of the system.

3.6.3 Case study 3: Degradation of waste in an open system with NH_4^+ adsorption to the mass waste

Following up on case study 2, NH_4^+ adsorption to the waste body is considered here. To include adsorption, the Freundlich approach as described in section 2.3.4 is used:

$$\log(q) = \log(K_d) + n \log(C) \quad (3.30)$$

Including adsorption in the model could allow us to consider microbial activity to occur primarily at the waste body surface, as most bacteria reside in surface attached biofilms (Muhammad et al., 2020). Microbial activity is then dependent on the NH_4^+ adsorbed to the waste surface. The model in its current state, however, introduces a serious limitation as adsorption of other components (e.g. H^+ & NO_3^-) is not considered. Simulating biomass activity in a biofilm would therefore be inconsistent following the approach described here. As a result, we propose a different approach where microbial activity is considered only in the solution phase. Now, bacteria may only use the NH_4^+ present in the leachate. Note that this requires the reader to treat the model results in the following chapter with care, as the approach poses a simplification of reality.

¹Bacterial decay is separately calculated for each species but use the same parameters.

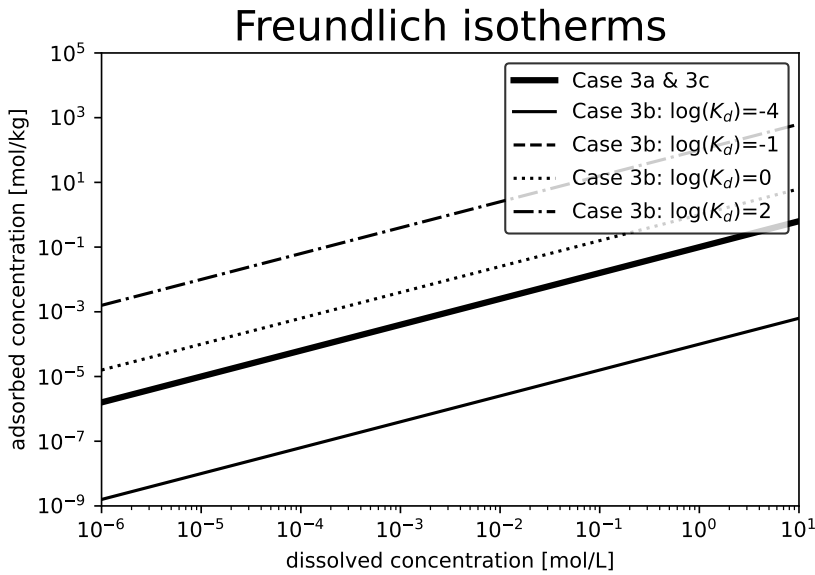


Figure 3.4: Curves for the different Freundlich isotherms used by the different cases on a log-log scale.

NH_4^+ adsorption is considered by including the Freundlich isotherm for NH_4^+ in the ORCHESTRA solver. Doing so, 3 different subcases are examined:

1. Effects of C/N ratio: The effects of the C/N ratio are examined by conducting 4 model simulations with increasing C/N ratio: 5:1, 14:1, 32:1 & 50:1.
2. Effects of K_d : Eq. 3.30 introduces a K_d value characterizing the degree of adsorption for a given component. 4 cases are presented with different $\log(K_d)$ values: -4, -1, 0 & 2.
3. Effects of initial organic fraction: 4 cases are included with a different initial organic fraction: 0.1, 0.2, 0.3, 0.4.

All cases include a n -value of 0.8. For subcase 3a and 3b, a $\log(K_d)$ value of -1 is adopted. Figure 3.4 shows the different isotherms for the different cases plotted on a log-log scale. The figure presents a direct limitation of the Freundlich model as the adsorbed concentrations are not maximized at a high dissolved concentration.

3.6.4 Case study 4: Degradation following kinetic rate parameters from the literature

A final case study is proposed that aims to close the bridge between the modelling framework and literature study. This includes the use of rate parameters obtained from literature data. There is quite extensive literature on the rate kinetics of different processes. Table 3.8 lists the kinetic parameters used for the case study. Parameters that are not included are taken from Table 3.6.

Table 3.8: Kinetic parameters from the literature

Process/Parameter	Unit	Literature Values	Reference	Used Values
Fermentation of solid organic matter				
v_{max}	[d ⁻¹]	0.09 – 0.26	^a	0.08
$pH_{opt,1}$	[–]	6.5	^b	6.5
$pH_{opt,2}$	[–]	7.5	^b	7.5
K_{pH}	[–]	500	^b	500
T_{opt}	[°C]	60	^b	60
κ_T	[°C ⁻¹]	0.03 – 0.08	^b	0.05
K_S	[mol L ⁻¹]	0.045	^c	0.05
Methanogenesis of acetate				
μ_{max}	[d ⁻¹]	0.35 – 0.8	^{a,d}	0.5
$pH_{opt,1}$	[–]	6	^b	6
$pH_{opt,2}$	[–]	8	^b	8
K_{pH}	[–]	500	^b	500
T_{opt}	[°C]	60 – 65	^b	65
κ_T	[°C ⁻¹]	0.045	^b	0.055
K_S	[mol L ⁻¹]	0.03 – 420	^{a,b}	0.4
Oxidation of acetate				
μ_{max}	[d ⁻¹]	6.72 – 11.52	^{e,f}	10
$pH_{opt,1}$	[–]	-	-	6
$pH_{opt,2}$	[–]	-	-	7.5
K_{pH}	[–]	-	-	500
T_{opt}	[°C]	-	-	60
κ_T	[°C ⁻¹]	-	-	0.05
K_S	[mol L ⁻¹]	0.0123	^e	0.03
Nitrification				
μ_{max}	[d ⁻¹]	1.15 – 1.4	^{a,g}	1.4
$pH_{opt,1}$	[–]	7	^h	7
$pH_{opt,2}$	[–]	8	^h	8
K_{pH}	[–]	-	-	500
T_{opt}	[°C]	32	ⁱ	32
κ_T	[°C ⁻¹]	-	-	0.055
K_S	[mol L ⁻¹]	0.003 – 0.2856	^j	0.3
Denitrification				
μ_{max}	[d ⁻¹]	0.2 – 0.8	^{g,k}	1
$pH_{opt,1}$	[–]	7	^g	7
$pH_{opt,2}$	[–]	8	^g	8
K_{pH}	[–]	-	-	500
T_{opt}	[°C]	35	^l	35
κ_T	[°C ⁻¹]	-	-	0.055
K_S	[mol L ⁻¹]	-	-	0.3
Biomass decay				
μ_{max}	[d ⁻¹]	0.002 – 3.84	^{b,c,d,m}	0.015
T_{opt}	[°C]	80	^b	80
κ_T	[°C ⁻¹]	0.4	^b	0.048

^aTurnhout et al., 2018; ^bReichel et al., 2007; ^cFytanidis and Voudrias, 2014;^dGholamifard et al., 2008; ^eTang et al., 2007;^fVogelaar et al., 2003; ^gDincer and Kargi, 2000; ^hAWWA, 2002; ⁱCho et al., 2014;^jBerge et al., 2006; ^kMetcalf et al., 1991; ^lFeng et al., 2015;^mNeill and Gignoux, 2006

Chapter 4

Results & Discussion

4.1 Case 1: Degradation of waste in a closed system with no NH_4^+ adsorption

The model results for degradation in a closed system are shown in Figure 4.1. The figure depicts the 60-year development of the most important chemical species. All results are plotted on a gradient background representing the aerobic state (O_2^{aq} in mol/L) of the system. A distinction is made between the growth of four biomass species (methanogens, oxidizers, nitrifiers and denitrifiers), related to reactions 2, 3, 4 and 5 (in Table 3.1), respectively. Figure 4.2 presents the inhibition functions related to the acetate production by hydrolysis and the growth of the different biomass species.

The results show that the system is characterized by two different phases: aerobic (year 0-1.5) and anaerobic (>1.5 years). In the first phase, aerobic bacteria (oxidizers and nitrifiers) consume O_2 to form biomass. This is characterized by a small increase in X_{ox} and X_{nitr} while O_2^{aq} concentrations quickly decrease. During this phase, no growth of methanogens and denitrifiers is observed. This is related to the inhibition by O_2 toxicity, as shown in Figure 4.2 where $f_{tox}^{O_2}$ is almost 0 in the first 1.5 years for methanogens and denitrifiers growth. As the system gets depleted in O_2 (around 1.5 years), opposite relations are found: methanogens and denitrifiers populations increase while the growth of oxidizers and nitrifiers is inhibited as O_2 is no longer present. Interestingly, methanogens dominate the system during this stage, while the growth of denitrifiers falls behind after $t=4$ years. Figure 4.2 shows that this is related to NO_3^- substrate inhibition; denitrifiers consume NO_3^- leading to a system depletion of NO_3^- and limiting further growth. In the model proposed here, this implies a dependency for denitrifiers on the activity of nitrifiers: nitrification no longer takes place for $t>1.5$ years, halting the production of NO_3^- , leading to the inhibition of denitrification when NO_3^- concentrations reach 0 mol/L.

The system is characterized by the growth of methanogens until ca. 10 years. Figure 4.1 and 4.2 indicate that at $t>10$ years, further growth of methanogens is stopped. This is a result of acetate substrate inhibition as acetate concentrations reach 0 mol/L. This decrease in acetate is related to the inhibition of hydrolysis by the presence of NH_4^+ (toxicity inhibition). In turn, the NH_4^+ concentration increases as nitrifiers are inhibited under anaerobic conditions. This presents a heavily coupled system being dependent on the aerobic/anaerobic conditions.

Under aerobic conditions: (1) The presence of O_2 allows oxidizers and nitrifiers to grow while methanogens and denitrifiers are fully inhibited. (2) Acetate oxidation and nitrification lead to a decrease in NH_4^+ and increase in NO_3^- concentrations. (3) The high consumption of NH_4^+ results in low NH_4^+ concentrations, causing hydrolysis not being inhibited by NH_4^+ toxicity (=faster hydrolysis rate). (4) A high hydrolysis rate leads to a higher production of acetate.

Under anaerobic conditions: (1) Oxidizers and nitrifiers growth is inhibited while methanogens and denitrifiers are allowed to grow. (2) Denitrification leads to consumption of NO_3^- . As the system gets depleted in NO_3^- , denitrification stops (*substrate inhibition*). (3) The inhibition of nitrification leads to an increase in NH_4^+ concentration inhibiting the hydrolysis (*toxicity inhibition*). (4) Limited hydrolysis leads to less production of acetate. As acetate is consumed by methanogens and denitrifiers, the system gets depleted in acetate, leading to the inhibition of biomass growth (*substrate inhibition*).

Model results for a closed system with no adsorption

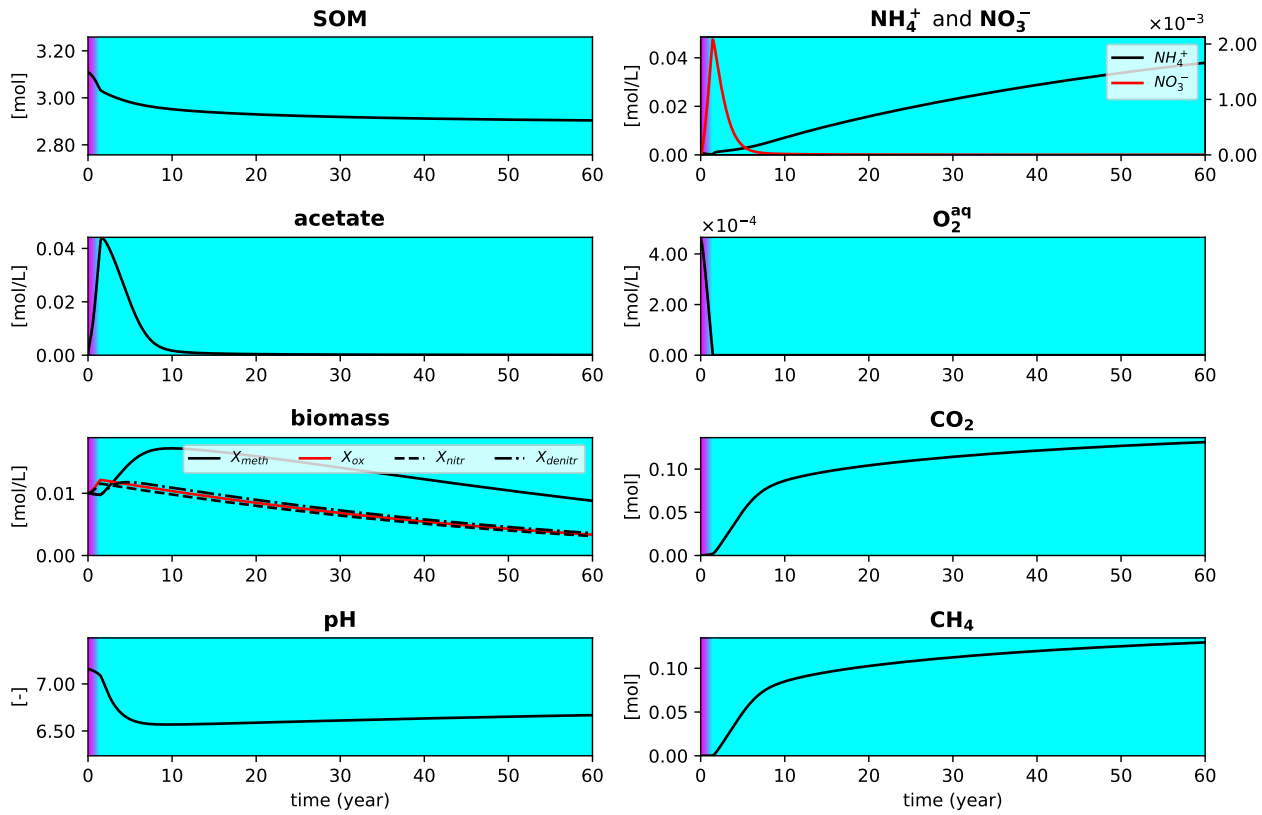


Figure 4.1: Model results for a closed system without adsorption of NH_4^+ to the waste body. The results are plotted on top of a gradient representing the aerobic state (O_2^{aq} in mol/L) of the system.

Inhibitions for the different reactions

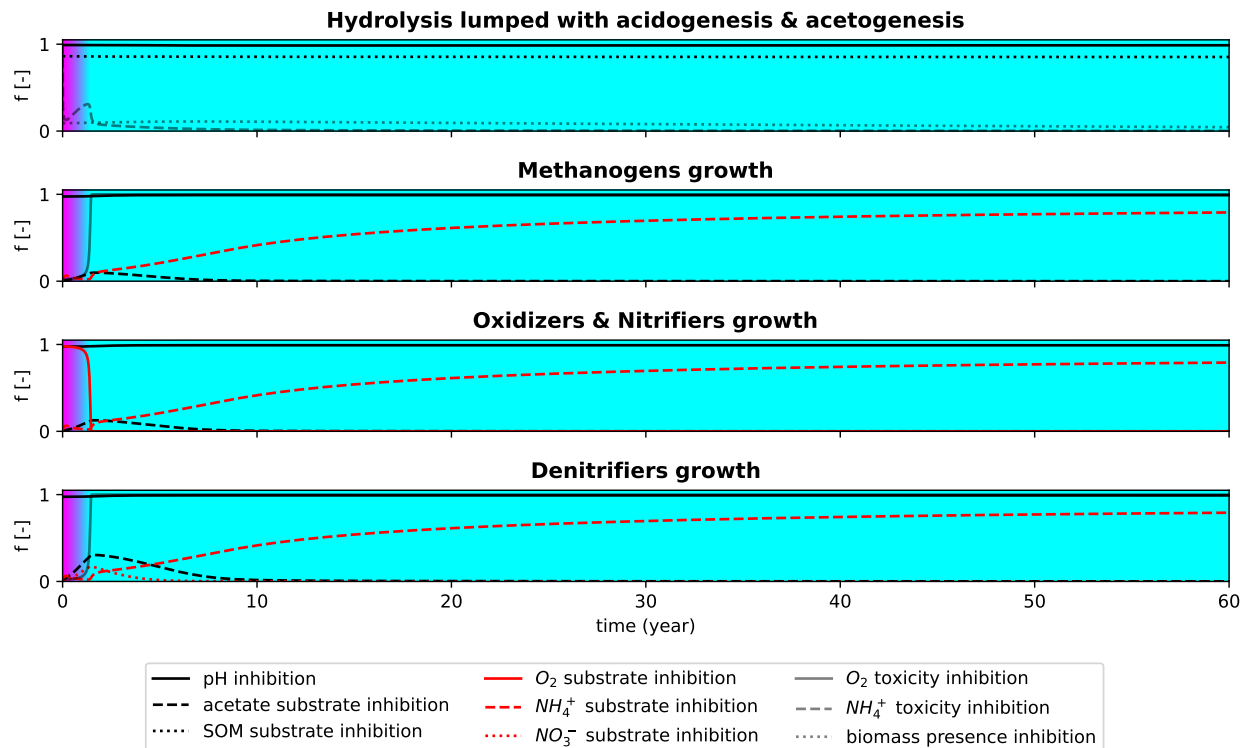


Figure 4.2: The inhibition functions for acetate production by hydrolysis and biomass growth. The results are plotted on top of a gradient representing the aerobic state (O_2^{aq} in mol/L) of the system.

4.2 Case 2: Degradation of waste in a (partly) open system with no NH_4^+ adsorption

Figure 4.3 presents the results of a bioreactor model where the system is periodically aerated. The moments of aeration are shown in the O_2^{aq} -figure where oxygen levels are increased to their initial level (20% air composition) for short amounts of time. After each period of aeration, the system is closed again, marked by a decline in O_2^{aq} concentrations. This leads to a distinctive seesaw pattern throughout the model simulation. Note, that apart from the addition of O_2 , the system is identical to the one presented in section 4.1.

The model results show a repeating pattern of the results found in case study 1. In anaerobic conditions, biodegradation follows the anaerobic pathway, showing an increase in methanogens and denitrifiers, whereas nitrification and acetate oxidation is inhibited. As a result, NH_4^+ concentrations increase. In aerobic conditions, aerobic processes dominate biodegradation. Here, the opposite trend is found where the methanogenic and denitrifying populations decrease while the nitrifiers and oxidizers concentrations increase. This translates to a reduction in NH_4^+ concentrations (consumption by nitrifiers). This development of NH_4^+ concentrations in anaerobic versus aerobic conditions is in agreement with the literature (e.g. Erses et al., 2008).

While most model results can be ascribed to similar processes as for the first case study, several interesting developments are found. The system acidity shows an alternating pattern where the pH decreases under aerobic conditions but increases during an anaerobic state. This behaviour is explained by the individual reaction processes and their effects on pH (Table 4.1). While fermentation of waste is a pH-lowering process, the reaction rate is very slow under anaerobic conditions (inhibited by NH_4^+ toxicity). Because of this, methanogenesis, denitrification and biomass decay (all pH-increasing processes) result in an overall increase in the pH. During aerobic conditions, however, waste hydrolysis is significantly faster. This, in combination with nitrification, causes a reduction in pH. Note that this decrease is moderated, as pH-increasing processes (biomass decay and acetate oxidation) also take place.

Process	Effect on pH	Source
Fermentation of waste	↓	Roychowdhury et al., 1988
Methanogenesis of acetate	↑	Lozecznik et al., 2012
Oxidation of acetate	↑	This study
Nitrification	↓	Isaka et al., 2007
Denitrification	↑	Šimek and Cooper, 2002
Biomass decay	↑	Prommer et al., 2002

Table 4.1: Process effects on the pH.

Although anaerobic conditions relate to an increase in alkalinity, this relation is not found for the first anaerobic phase ($t=1.5\text{-}8$ years); a pH reduction of 7.1 to 6.55 is found. This may be related to denitrifiers being inhibited as a result of low NO_3^- and acetate concentrations (*substrate inhibition*; Figure 4.3).

Another observation is that the hydrolysis rate increases with every subsequent aeration cycle. During the second cycle (8-18 years), only 9% of the initial amount of SOM is hydrolysed. In the final cycle (48-58 years), however, this percentage is much higher, estimated at 22.5%. This increase may be ascribed to a combination of factors. Firstly, the biomass population is highest during the final cycle, leading to less inhibition by biomass absence (f_X , Eq. 3.20). In addition to this, NH_4^+ concentrations are very low during the final cycle, resulting in less toxicity inhibition by NH_4^+ . Low NH_4^+ concentrations may be ascribed to an increase in biomass growth which is no longer inhibited by acetate substrate inhibition; Figure 4.4 shows that acetate substrate inhibition is low (<0.2) during the earlier aeration cycles but high (>0.5) during the later cycles. This introduces a distinction between the early ($t < 20$ years) and late ($t > 40$ years) stages of the model.

$t < 20$ years: (1) Hydrolysis is inhibited by low biomass concentrations. (2) Biomass growth is inhibited by low acetate and NH_4^+ concentrations (*substrate inhibition*). Inhibition by low acetate concentrations exceeds inhibition by low NH_4^+ concentrations. Because of this, NH_4^+ concentrations are relatively high (no more NH_4^+ is consumed as acetate depletion inflicts full inhibition), affecting the hydrolysis rate by NH_4^+ toxicity inhibition.

$t > 40$ years: (1) Hydrolysis becomes less inhibited by biomass concentrations as the population increases. (2) With increasing cycles, acetate concentrations accumulate. (3) Inhibition by low NH_4^+ concentrations exceeds inhibition by low acetate concentrations. As a result, NH_4^+ concentrations are relatively low, less affecting the hydrolysis rate by NH_4^+ toxicity inhibition.

Model results for a (partly) open system with no adsorption

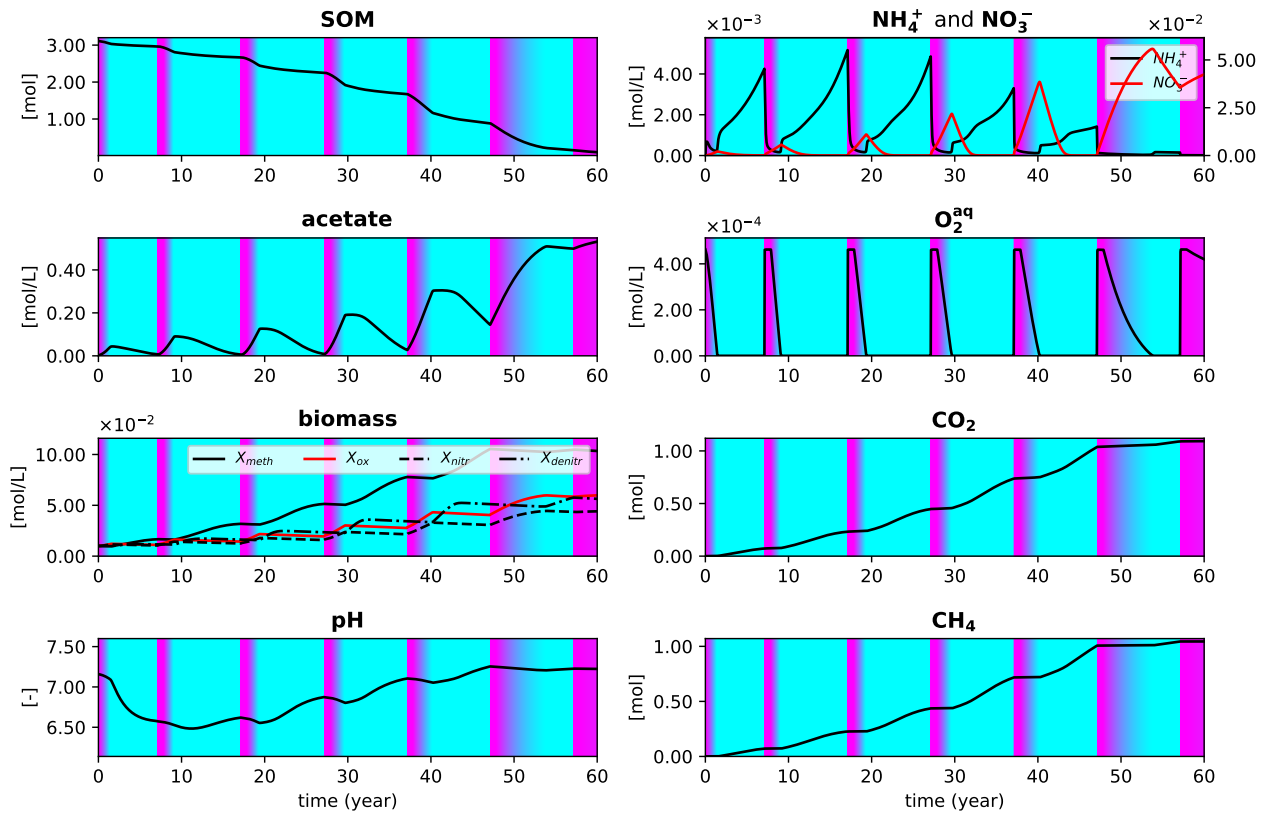


Figure 4.3: Model results for a (partly) open system without adsorption of NH_4^+ to the waste body. The results are plotted on top of a gradient representing the aerobic state (O_2^{aq} in mol/L) of the system.

Inhibitions for the different reactions

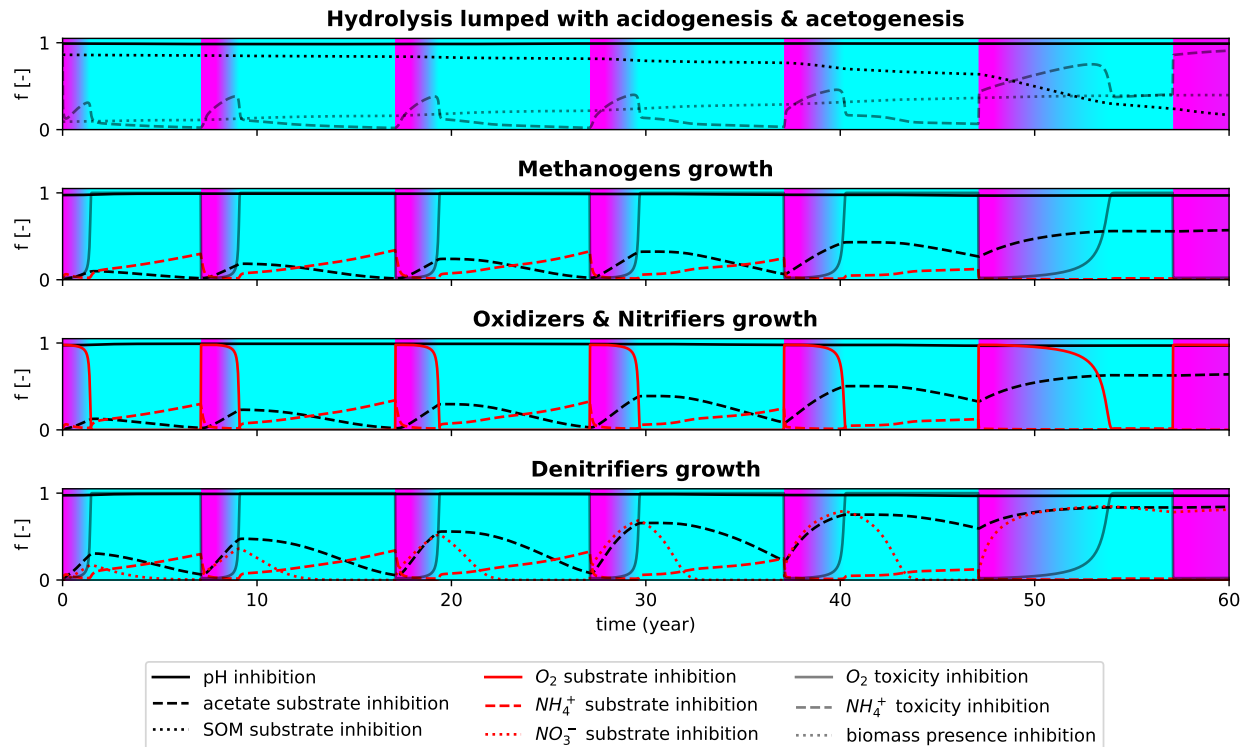


Figure 4.4: The inhibition functions for the different biomass species. The results are plotted on top of a gradient representing the aerobic state (O_2^{aq} in mol/L) of the system.

This distinction shows that the different processes are affected by different inhibitions at different times, but also on different time scales. On the small time scale (<10 years), system differences are mainly related to the aerobic state of the system (aerobic vs anaerobic degradation pathway, discussed in section 4.1), resulting in quick changes in the leachate composition. On larger time scales (>30 years), however, processes are heavily influenced by the gradual progression of the system (e.g. pH, biomass growth and acetate accumulation).

Concluding remarks involve the results on CH₄ and CO₂ production. The total CO₂ production after 60 years is only 5.2 % higher than the total CH₄ production. This result is surprising, given the fact that (1) aerobic conditions are found for ca. 33% of the simulation, (2) that CH₄ is only produced under anaerobic conditions and (3) that oxidation of acetate is significantly faster than methanogenesis (see kinetic parameters, 3.6). In addition to this, the results show that the production rate of CO₂ under aerobic conditions is lower than during anaerobic conditions. At the same time, the population of oxidizers increases significantly. This presents an apparent contradiction, as the growth of X_{ox} is directly related to the oxidation of acetate, producing CO₂. However, λ_{cat} is found to be very low for the metabolic system between acetate oxidation and biomass production from acetate (between 0.3-0.45). This implies that bacteria generate a significant amount of energy from the oxidation of biomass, reflecting on a limited CO₂ production by oxidizing bacteria. In contrast, λ_{cat} for the metabolic system methanogens is much higher (between 8-9), leading to high production of CH₄ and CO₂ under aerobic conditions.

4.3 Case 3: Degradation of waste in a (partly) open system with NH_4^+ adsorption

In the previous case studies, the results were obtained for a system where no NH_4^+ adsorption to the waste surface is taken into account. For this, it was assumed that the bacteria had full access to all NH_4^+ . For the case studies presented below, however, part of the NH_4^+ is adsorbed to the waste surface. As a result, bacteria have only access to NH_4^+ present in the aqueous phase ($=\text{NH}_4^+_{\text{aq}}$).

4.3.1 Case 3a: Effects of waste composition

Figure 4.5 presents the effects of the C/N ratio on the system. For this, it must be noted that the initial *SOM* in kg is equal for all cases, resulting in a difference in the initial amount of moles *SOM* between each case. The development of the individual biomass species is shown in Figure 4.6.

The C/N ratio has a significant effect on the system. Firstly, the hydrolysis rate of *SOM* increases with increasing the C/N ratio. Almost no *SOM* is hydrolyzed for a C/N ratio of 5 : 1 and 14 : 1 within 60 years of calculation. On the other hand, almost all organic matter is hydrolyzed after 40 years when a C/N ratio of 50 : 1 is taken. The C/N ratio determines how much nitrogen, N, is present in the system; a higher C/N ratio implies that waste contains less nitrogen. The breakdown of waste with a high C/N ratio will then lead to the release of less NH_4^+ . This is shown in both the $\text{NH}_4^+_{\text{aq}}$ and $\text{NH}_4^+_{\text{ad}}$ figures, where the concentrations decrease with increasing C/N ratio. Naturally, as NH_4^+ concentrations are lower, hydrolysis is less affected by NH_4^+ toxicity, leading to a higher hydrolysis rate.

Interesting results are found for the biomass growth, where both the highest (50 : 1) and lowest (5 : 1) C/N ratio does not lead to the highest biomass population in the system. This implies an interplay between different inhibiting factors affecting the different systems. For a very low C/N ratio (5 : 1), biomass growth is not inhibited by the absence of NH_4^+ . However, as discussed above, it leads to low hydrolysis rates and, thus, low acetate concentrations. As a result, biomass growth is inhibited by acetate substrate inhibition. On the other hand, low NH_4^+ concentrations are found when the C/N ratio is very high (50 : 1). While this leads to high acetate concentrations, biomass growth is now inhibited by NH_4^+ substrate inhibition. These findings are in agreement with the literature (e.g. Chiu et al., 2007; Yen and Brune, 2007; Mannina et al., 2017). Chiu et al. (2007) showed that nitrogen removal in a batch reactor is low for low C/N ratios as a result of a carbon deficit. For high C/N ratios, however, low concentrations of NH_4^+ were found to be a limiting factor (Yen and Brune, 2007). Yen & Brune (2007) showed that growth was limited for a C/N ratio of 36.4 : 1 with measured NH_4^+ concentrations of 65 mg/L (or 0.0036 moles).

Effects of C/N ratio for a system with NH_4^+ adsorption

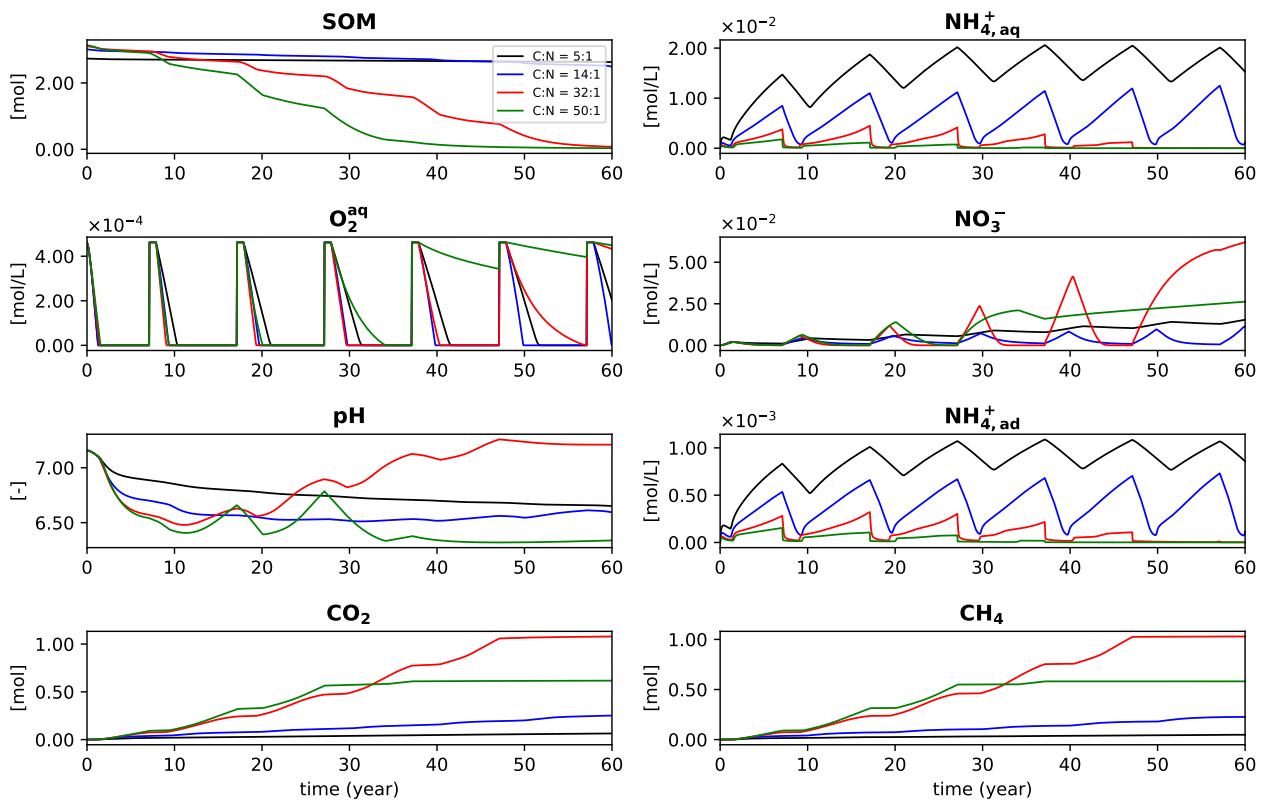


Figure 4.5: Model results for a (partly) open system with adsorption of NH_4^+ to the waste body. Different lines represent a difference in C/N ratio of the waste composition.

Effects of C/N ratio for a system with NH_4^+ adsorption

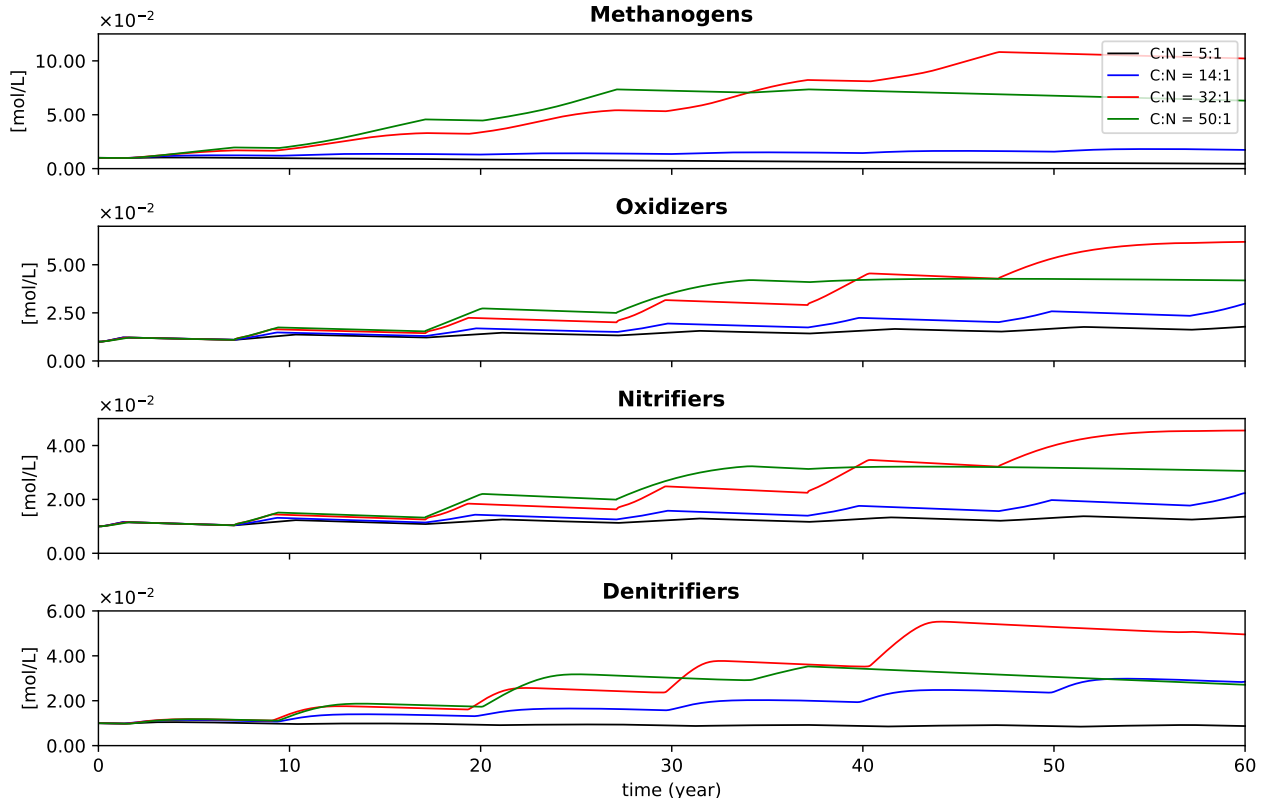


Figure 4.6: Model results for the biomass species for a (partly) open system with adsorption of NH_4^+ to the waste body. Different lines represent a difference in C/N ratio.

4.3.2 Case 3b: Effects of Kd

The effects of the K_d value on the system are shown in Figure 4.7, 4.8 and 4.9. The Figures indicate that the system is highly dependent on the K_d value for NH_4^+ adsorption, where a high K_d value leads to less NH_4^+ concentrations in the leachate (Fig. 4.8, $\text{NH}_4^+_{\text{aq}}$). This is as expected the K_d constant can be seen as the degree of adsorption, where a high K_d constant increases the amount of NH_4^+ adsorbed to the waste surface, thus leading to lower concentrations in the leachate (Buchter et al., 1989).

In the modelling framework proposed here, microbial activity is related to the NH_4^+ in the leachate. As a result, the hydrolysis of *SOM* is less affected by NH_4^+ toxicity inhibition for a high K_d constant. This is shown in Figure 4.8 where hydrolysis rates are highest for $\log(K_d) = 2$ (for $t < 20$ years) while a $\log(K_d) = -4$ (leading to high $\text{NH}_4^+_{\text{aq}}$ concentrations) leads to the slowest breakdown of *SOM*. Because hydrolysis of *SOM* is slow for $K_d = -4$ biomass growth is inhibited related to low acetate concentrations. For higher K_d constants, on the other hand, higher acetate concentrations are found leading to more biomass production; biomass growth increases as $\log(K_d)$ increases from -4 to 1 (Fig. 4.8). The biomass growth for methanogens and denitrifiers, however, is lowest for $\log(K_d) = 2$. This may be ascribed to low NH_4^+ concentrations in the leachate as most of the NH_4^+ is adsorbed to the waste surface (Fig. 4.8). As a result, biomass growth is affected by NH_4^+ substrate inhibition.

While the initial hydrolysis rate is highest for $\log(K_d) = 2$, the model results for this case show that the breakdown of *SOM* is fully stopped at ca. $t = 19$ years. In turn, as hydrolysis rates approach 0 d^{-1} , biomass growth and gas production are also halted. These observations coincide with quick acidification of the system (to $\text{pH} < 3$). An additional figure (4.7) presents the change (for $\log(K_2) = 2$) in acetate concentrations and inhibition by pH for the hydrolysis and biomass growth rate; the same pH kinetic input parameters are used for the different biomass species (Table 3.6). The figure indicates that the pH has a significant inhibitory effect on the hydrolysis rate and biomass growth around $t = 19$ years. This inhibiting effect coincides with very high acetate concentrations reaching $0.8-0.95 \text{ mol/L}$. This behaviour of system acidification accompanied by high acetate concentrations has been reported in previous studies (Ariunbaatar et al., 2015). Ariunbaatar et al. (2015) showed that VFA accumulation may lead to system failure (read: inhibition of all processes) by acidification under anaerobic conditions. The authors found that re-circulation of the leachate was necessary to maintain the correct alkalinity in the system. High acidity levels ($\text{pH } 5-5.5$) were also related to high acetate concentrations in a different study on the effects of pH and VFA's on hydrolysis (Veeken et al., 2000). Here, the hydrolysis of biowaste was fully inhibited when VFA concentrations reached $0.68-0.85 \text{ mol/L}$. These concentrations are lower than those found in this study. However, it must be noted that the model results are heavily dependent on the kinetic input parameters which are arbitrarily chosen for the case study presented here.

Additional results for $\log(K_d)=2$

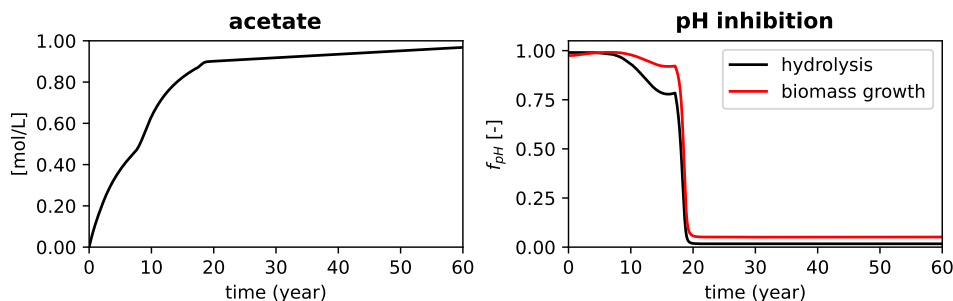


Figure 4.7: Additional results for the system where $\log(K_d) = 2$. **top:** acetate production; **bottom:** pH inhibitions affecting hydrolysis and biomass production. Note that the input parameters describing the pH inhibition are identical for all biomass species.

Effects of Kd for a system with NH_4^+ adsorption

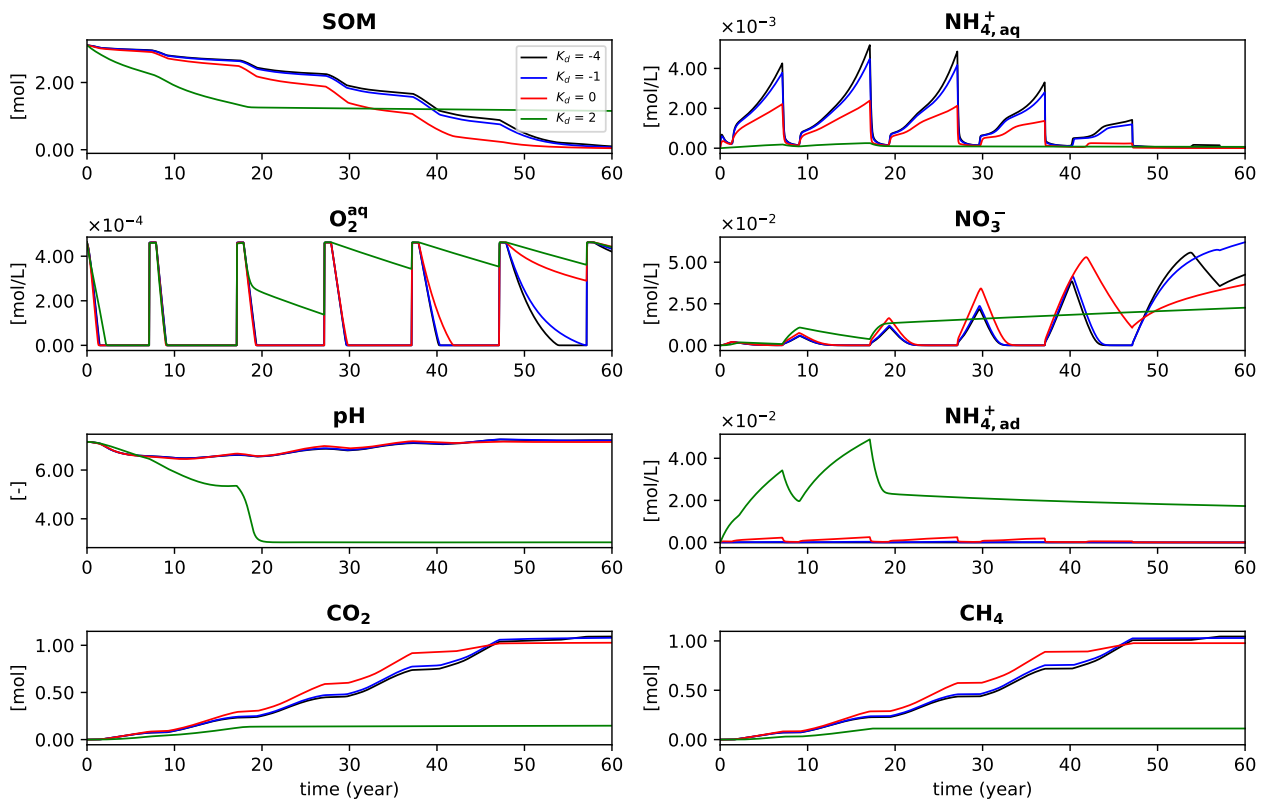


Figure 4.8: Model results for a (partly) open system with adsorption of NH_4^+ to the waste body. Different lines represent a difference in K_d values used for the Freundlich isotherm.

Effects of Kd for a system with NH_4^+ adsorption

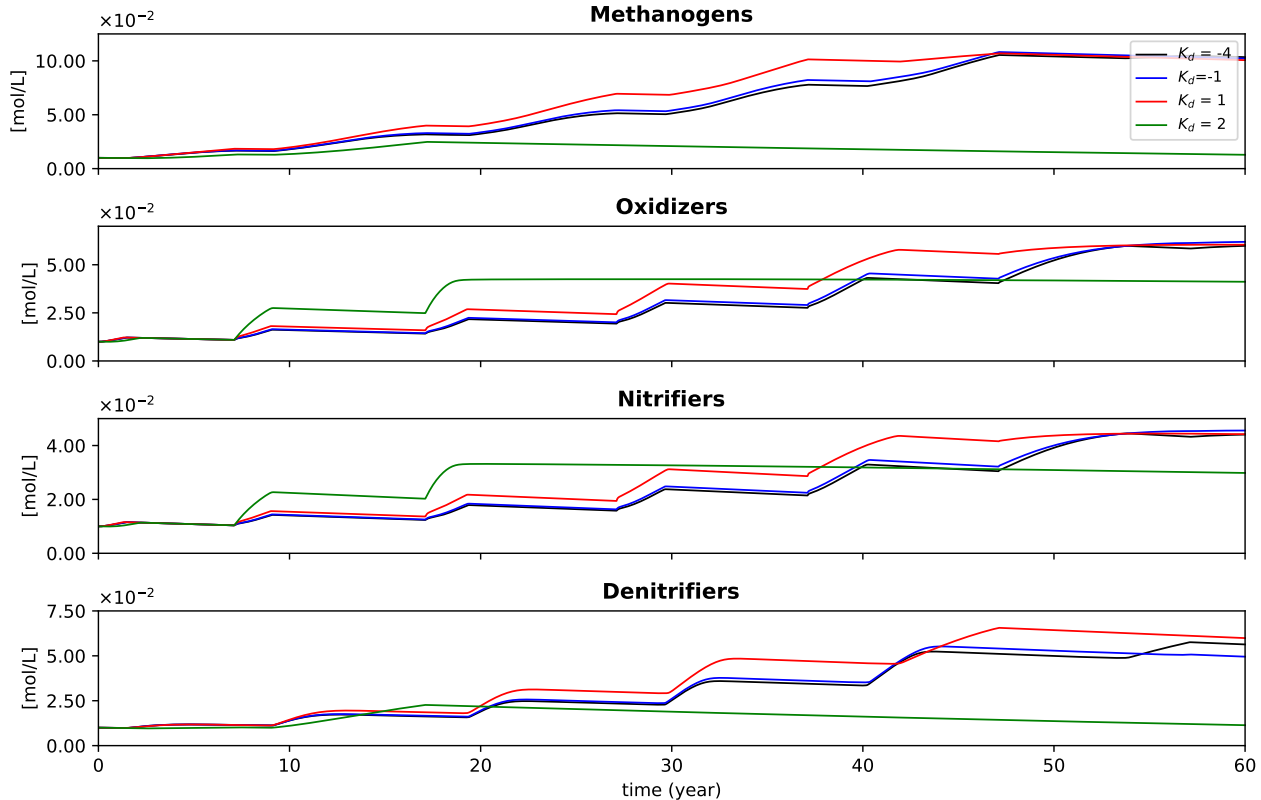


Figure 4.9: Model results for the biomass species for a (partly) open system with adsorption of NH_4^+ to the waste body. Different lines represent a difference in K_d values used for the Freundlich isotherm.

4.3.3 Case 3c: Effects of initial organic fraction

Figure 4.10 presents the effects of the initial organic fraction (0.1, 0.2, 0.3 and 0.4). In general, the results show that a higher initial organic fraction leads to more gas production, higher NH_4^+ concentrations (both in the leachate and adsorbed to the waste surface) and more biomass growth. While the results are not very surprising, they stress the importance of hydrolysis in the presented modelling framework. In the used reaction network (Table 3.1), hydrolysis of solid organic matter is the first step in biodegradation, releasing substrate (acetate) that is used for biomass growth. When the hydrolysis rate is limited, the subsequent processes (biomass growth/decay) are indirectly also inhibited. At lower initial organic fractions, the hydrolysis rate is affected by the inhibition functions posed in Eq. 3.17 (*substrate inhibition*) and 3.19 (where the degradability of *SOM* becomes harder as more waste is degraded). For the latter, it is important to note that for all cases, the same K_{degr} value is adopted (Table 3.6). This presents a complication where a lower initial fraction does not only result in less *SOM* present, but also that the initial *SOM* available is harder to degrade. The results should therefore be treated with care as they show a combined effect of (1) less organic matter present and (2) the maturity of the waste.

The results also show the effect of hydrolysis on the pH compared to the subsequent processes (methanogenesis, oxidation, nitrification, denitrification). When an initial fraction of 0.1 is adopted, almost no biomass is formed (Fig. 4.11). Because biomass growth is inhibited, pH increasing processes (table 4.1) do occur less. This results in a fixed pH staying around ca. 6.5 for $t > 10$ years, while the other simulations show an increase in pH (here, pH-increasing processes occur at a faster rate).

Effects of initial organic fraction for a system with NH_4^+ adsorption

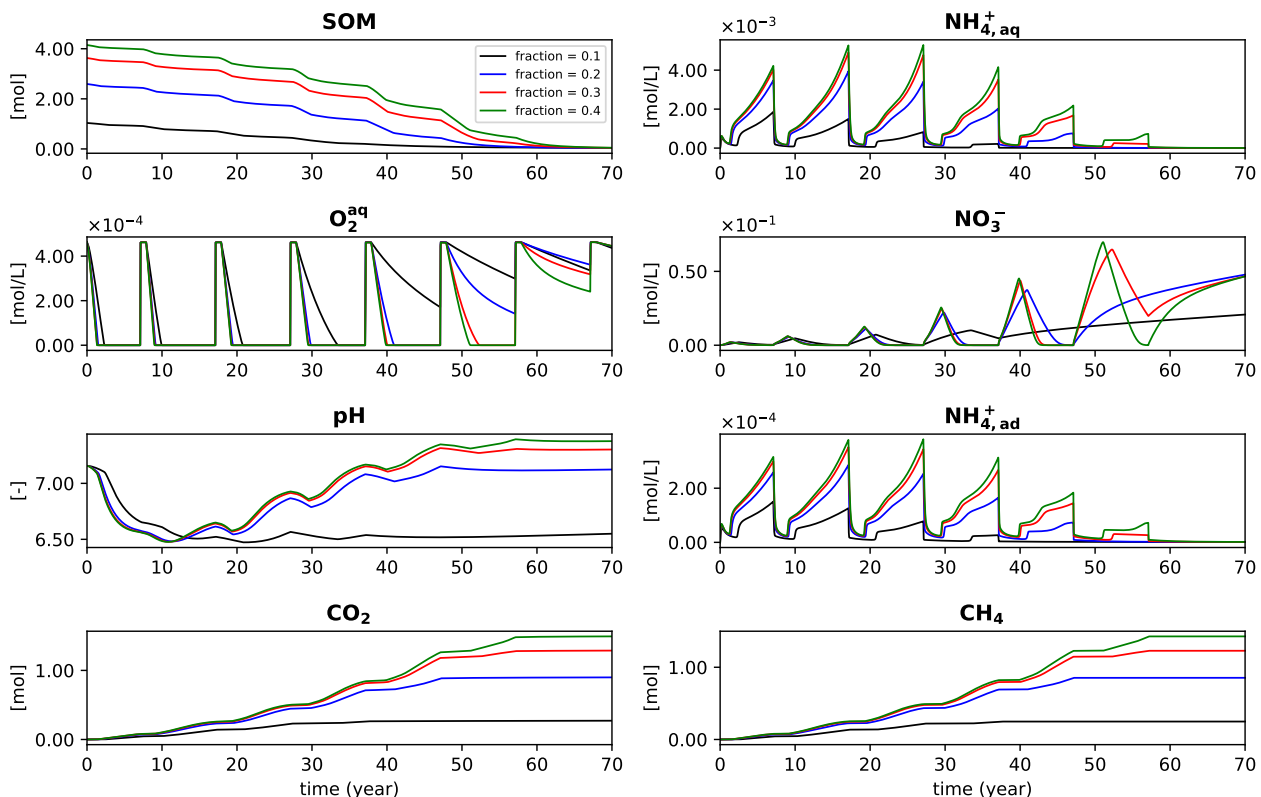


Figure 4.10: Model results for a (partly) open system with adsorption of NH_4^+ to the waste body. Different lines represent a difference in initial organic fraction of waste.

Effects of initial organic fraction for a system with NH_4^+ adsorption

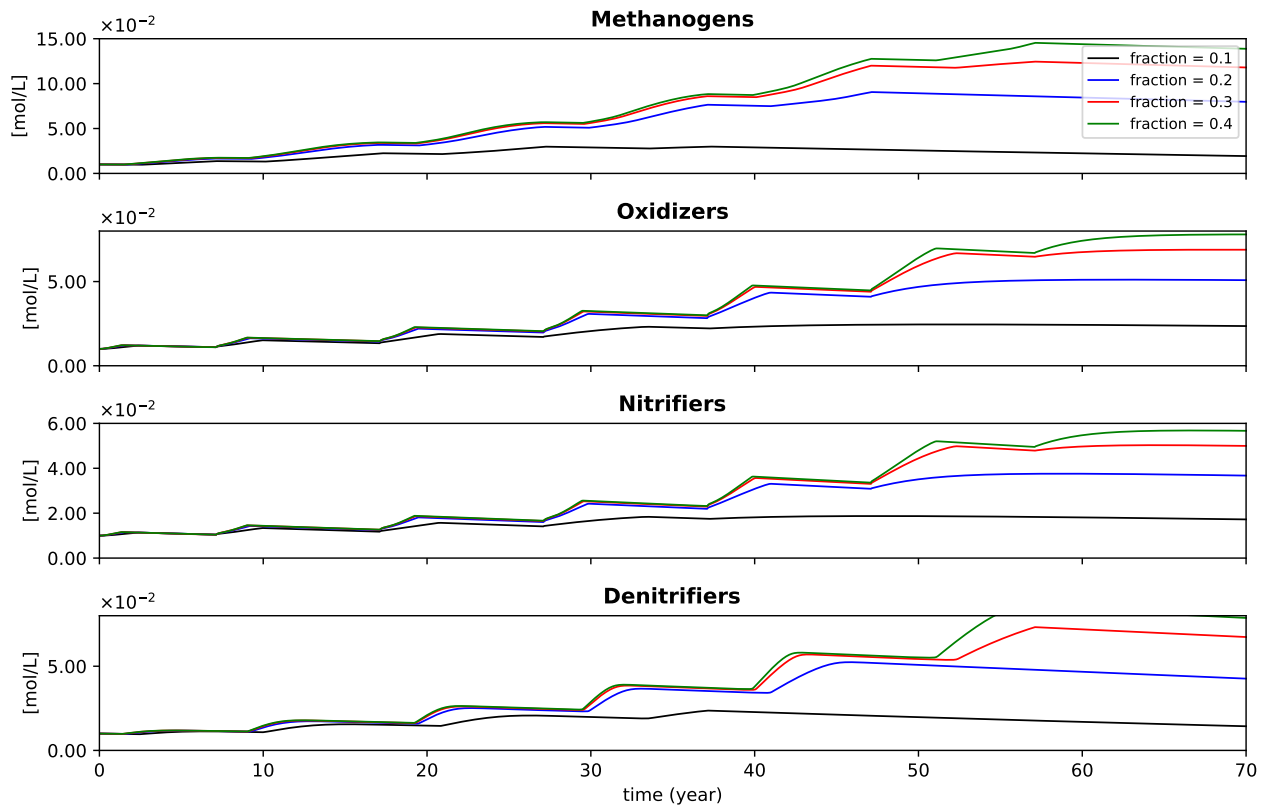


Figure 4.11: Model results for a (partly) open system with adsorption of NH_4^+ to the waste body. Different lines represent a difference in initial organic fraction of waste.

4.4 Case 4: Degradation following kinetic rate parameters from the literature

Using the kinetic parameters found in the literature, results are obtained following Figure 4.13 and 4.14. Note that the aeration frequency is doubled compared to the previous cases where the first aeration interval starts at ca. $t = 4.5$ years. This is done to ensure that the system is not predominantly dominated by anaerobic conditions as the chosen kinetic rate parameters lead to faster consumption of O_2 as opposed to the previous cases. At the start of the simulation, the results show a quick depletion of O_2 where the system is depleted in O_2 after ca. 0.5 years. These rates are significantly lower than those found in the literature, where it is documented that takes only several days to weeks for full oxygen depletion (Youcai et al., 2001). Figure 4.14 implies, however, that the initial growth rate of oxidizers and nitrifiers is inhibited following substrate inhibition by both acetate and NH_4^+ .

Interestingly, the O_2 depletion rate decreases with every aeration cycle. Figure 4.14 shows that this is an interplay between the different inhibitions. Between $t = 10$ and $t = 18$ years, aerobic growth (nitrifiers and oxidizers) is mainly inhibited by acetate substrate inhibition. Acetate concentrations are low (Fig. 4.14) because hydrolysis is fully inhibited by high NH_4^+ concentrations ($> 0.002 \text{ mol/L}$; NH_4^+ toxicity). On the other hand, for $t > 20$ years, aerobic growth is inhibited by NH_4^+ (substrate inhibition) as $NH_4^{+}_{aq}$ concentrations do not exceed 0.0005 mol/L (Fig. 4.14). Note that during this interval, acetate substrate inhibition is not dominant as acetate concentrations increase.

Similar to the aerobic bacteria, methanogens and denitrifiers are also affected by the different inhibitions. Figure 4.12 presents an enlarged presentation of the development of methanogens and denitrifiers. Their development can be subdivided into 4 different phases. During phase 1, the biomass population decreases slightly. Figure 4.14 implies that this is related to the initial low concentrations of acetate and NH_4^+ (substrate inhibition). However, acetate concentrations are still maintained as hydrolysis is allowed to take place. Therefore, the population decrease is only minimal. However, during phase 2, high NH_4^+ concentrations inhibit further release of acetate via hydrolysis, leading to a depletion in acetate. In turn, biomass growth is heavily inhibited leading to a steeper decrease in the second phase. The third phase is characterized by a slow increase in the biomass population, as the acetate concentration increase (Fig. 4.13). However, as substrate inhibition by acetate no longer takes place, the biomass growth rate is limited by the absence of NH_4^+ (substrate inhibition). This leads to low NH_4^+ concentrations while acetate concentrations are allowed to go up. Phase 4 marks the final stage of the system, during which inhibition for anaerobic growth is mainly inhibited by the presence of O_2 (toxicity inhibition) and low NH_4^+ concentrations. Depletion of O_2 is halted because the aerobic species are also inhibited by the absence of NH_4^+ in the system.

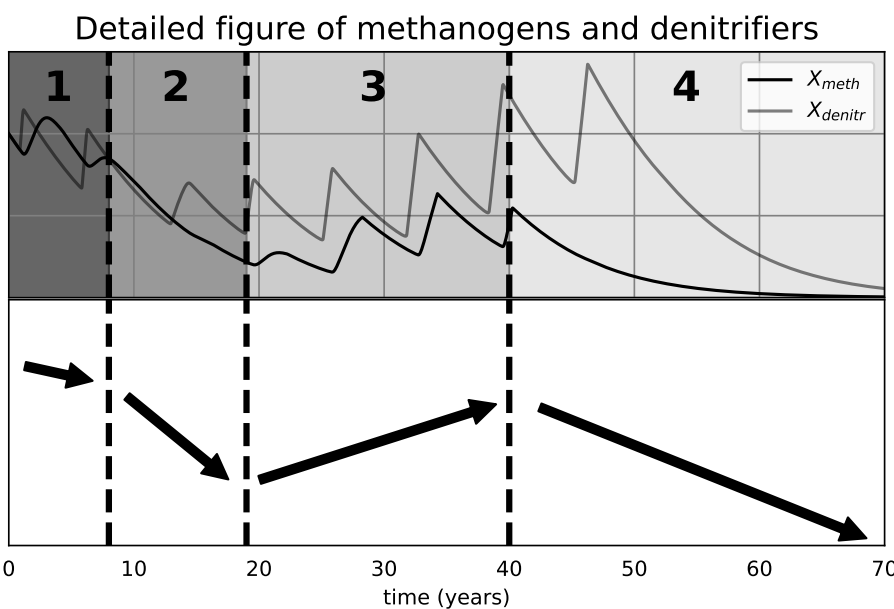


Figure 4.12: Enlarged view of the development of the anaerobic species. The bottom graph pictures the general trend of both species.

Model results for the final case study

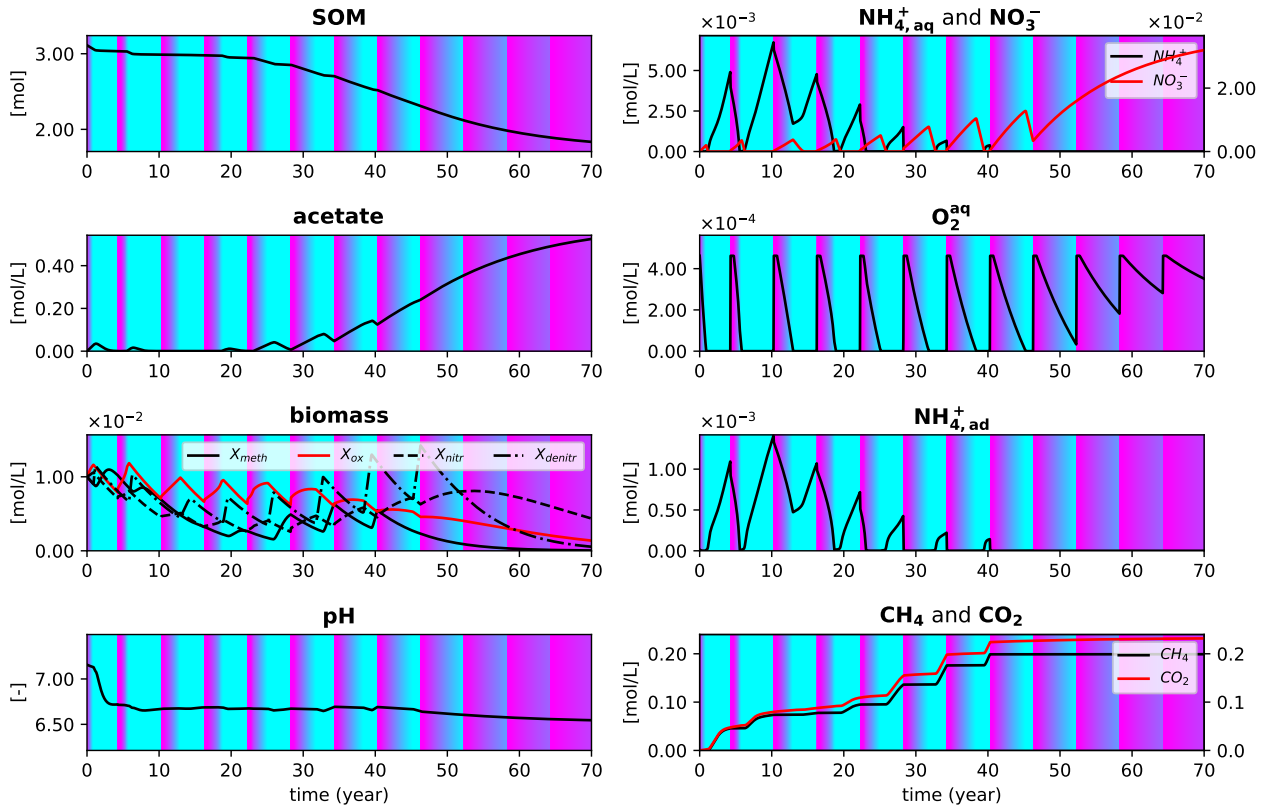


Figure 4.13: Model results for the biomass species for the final case study. The results are plotted on top of a gradient representing the aerobic state (O_2^{aq} in mol/L) of the system.

Inhibitions for the different reactions

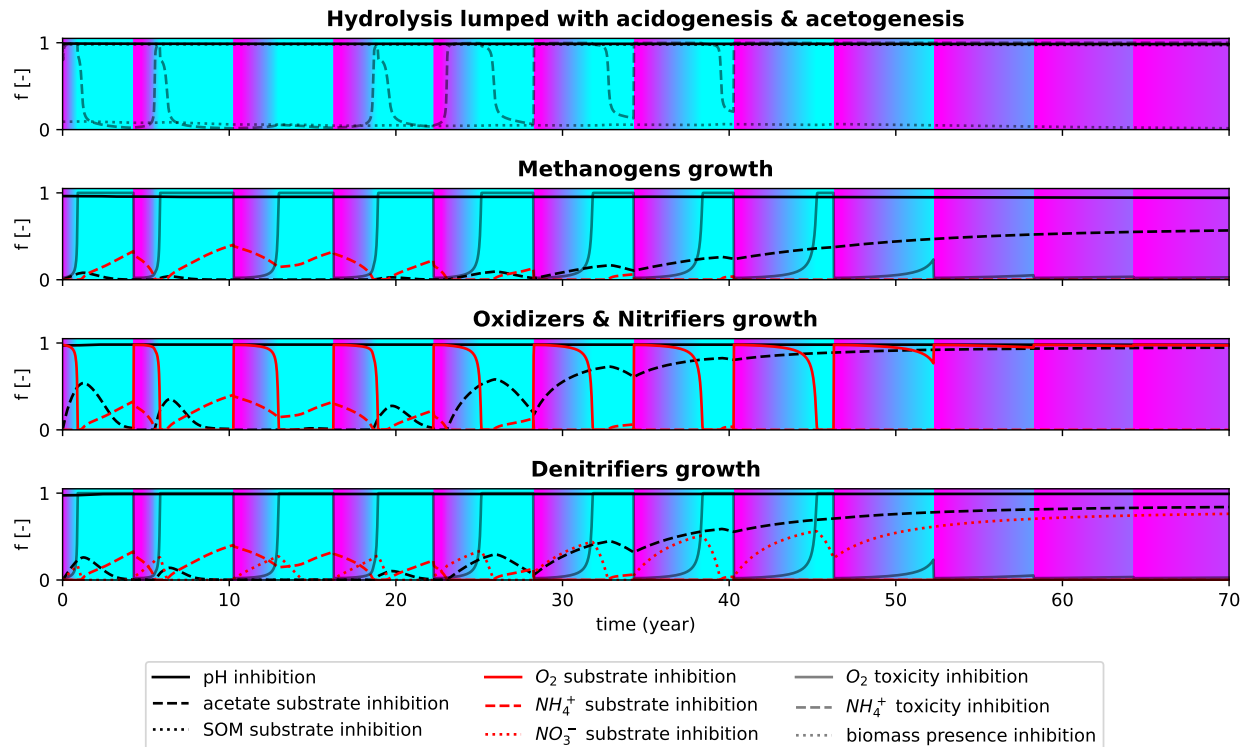


Figure 4.14: The inhibitions affecting the hydrolysis rate and biomass growth the final case study. The results are plotted on top of a gradient representing the aerobic state (O_2^{aq} in mol/L) of the system.

A final figure presents the development of the different fractions (porosity, saturation & chemically active waste fraction; Fig. 4.15). The figure shows that the hydrolysis of the chemically active fraction of waste leads to a reduction of the bulk density. At the end of the simulation (at $t = 70$ years), the bulk density has been reduced by ca. 6.2% and the chemically active waste fraction was reduced by ca. 33%. The porosity increased by 36% and the saturation decreased by ca. 28%. Note, a fixed volume is maintained and no compaction is taken into account.

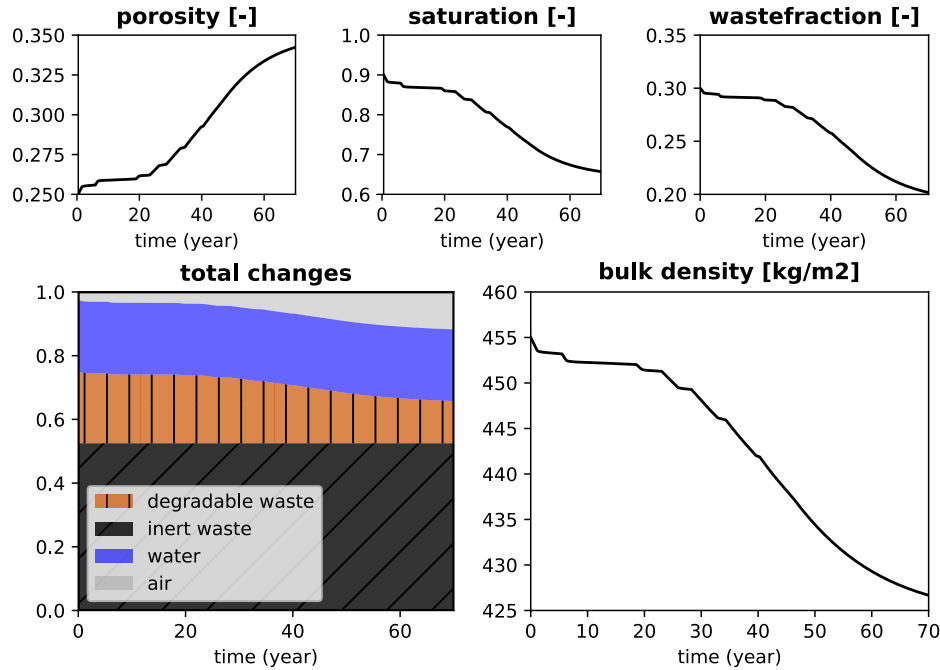


Figure 4.15: Change of the individual fractions and bulk density over time.

Chapter 5

Additional discussion

Chapter 4 present the results of a coupled model that simulates waste degradation in a bioreactor. The different cases studies were conducted as such to examine the functionality and applicability of the developed modelling framework described in Chapter 3. The results indicate that the model is capable of simulating a comprehensive, but simplified, reaction network by calculating the kinetic change of the most important species (*SOM*, acetate, biomass, NH_4^+ and NO_3^-). The model differentiates between the different reaction pathways of waste degradation related to the aerobic or anaerobic condition of the system. By doing so, model results are presented for the different biomass populations (methanogens, oxidizers, nitrifiers & denitrifiers). The most important feature of the modelling framework is the incorporation of ORCHESTRA that couples chemical equilibrium to the reaction kinetics. The developed wrapper (Chapter 3.4.1) is shown to be a highly useful tool to monitor pH and molar activities. In turn, these parameters are used to calculate the kinetic rates (affecting λ_{cat} , f_{pH} , $f_{\text{NH}_4^+}$, etc.). In addition to this, the coupling between Python and ORCHESTRA allows the model to include the effects of NH_4^+ adsorption to the mass waste.

5.1 Inhibitions related to NH_4^+

The results for the different case studies suggest that, in the presented modelling framework, NH_4^+ plays a major role in the development of the system. When NH_4^+ concentrations are low, biomass growth is limited by substrate inhibition. On the other hands, very high NH_4^+ concentrations ($>0.002 \text{ mol/L}$) inhibit the hydrolysis rate by toxicity inhibition, leading to lower production of acetate which, in turn, limits biomass growth (*substrate inhibition*). Akindele & Sartaj (2018) showed that toxicity inhibition by NH_4^+ takes place for concentrations exceeding 5000 mg/L (or 0.27 mol/L). These concentrations are much higher than those found in this study (Case study 4: $>0.002 \text{ mol/L}$). This implies that the kinetic rate parameters for NH_4^+ toxicity inhibition ($K_{tox}^{\text{NH}_4^+}$) chosen for this study may be too low. However, this also may suggest that the current definition for toxicity inhibition (Eq. 3.18, left) is not sufficient. This equation suggests that the inhibition is highly sensitive at low concentrations (Fig. 5.1). However, toxicity inhibition does not always occur for low NH_4^+ concentrations (Akindele and Sartaj, 2018). For future studies, it is therefore suggested to model toxicity inhibition following a logistic equation, e.g.:

$$-\frac{1}{\pi} \cdot \tan^{-1}(|C| \cdot K_1 - K_2) + 0.5 \quad (5.1)$$

Where $|C|$ is the concentration of the toxic compound and $|K_1|$ and $|K_2|$ are constants. This equation leads to a shape where the curve is 'flattened out' at both low and high concentrations (Fig. 5.1, right). The approach, however, introduces additional input parameters.

In addition to this, NH_4^+ toxicity inhibition is chosen to only affect the hydrolysis rate in the modelling framework presented here. However, studies show that NH_4^+ toxicity inhibition may also affect other processes (hydrolysis: Akindele and Sartaj, 2018; nitrification: Carrera et al., 2004; methanogenesis: Oosterhuis et al., 2014 & Akindele and Sartaj, 2018).

5.2 Effects of K_d value and sorption models

Case study 3b shows that the K_d value has a significant effect on the model results. The K_d value can be seen as the degree of adsorption, where a higher K_d value leads to a higher concentration of NH_4^+ adsorbed to the waste surface (Buchter et al., 1989). As biomass activity for this study is dependent on the NH_4^+ present in the liquid,

Toxicity inhibition functions

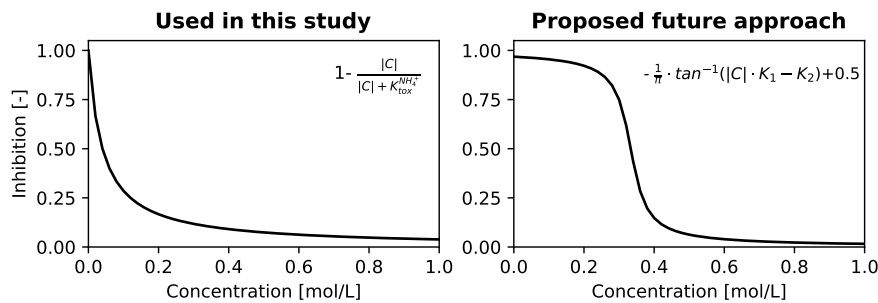


Figure 5.1: *left:* toxicity inhibition function used in this study. *right:* shape of toxicity inhibition function proposed for further studies.

almost no activity can be expected for $\log(K_d) \gg 0$. This is the case for the simulation where $\log(K_d) = 2$, where all the NH_4^+ is shown to be present at the waste surface. Because of this, metabolic reactions cannot occur which leads to a decrease in biomass. This is mainly observed for the anaerobic species.

At lower K_d values, the system is dependent on the interplay between microbial activity, NH_4^+ in the liquid and oxic conditions, where the K_d value affects biomass growth and gas production. However, apart from a very high $\log(K_d)$, the effects on the pH are limited. This is in contrast to the literature where studies indicate that ion adsorption to a reactive surface does affect pH, and vice versa (Barrow et al., 1993; Barrow et al., 2022; Fidel et al., 2018). Barrow et al. (2022) showed that the adsorption of phosphate on soils acts as a buffer; at low pH, phosphate adsorption increased the pH while a pH reduction was found at high pH. However, as discussed in section 2.3.4, the Freundlich isotherm is not capable of taking the effects of pH and ion exchange into account. It is therefore suggested that, in future studies, the mentioned NICA-Donnan approach (section 2.3.4) is used rather than the Freundlich model. Luckily, ORCHESTRA can be used along with the NICA-Donnan model, as is shown in previous studies on metal speciation in soil solution (e.g. Groenenberg et al., 2010). However, Eq. 2.19 indicates that this requires a wide set of parameters to be determined.

5.3 Effects of initial organic fraction and C/N ratio

Results on the effects of the C/N ratio and initial waste fraction meet the general expectation. A lower initial organic fraction implies there is less waste to degrade, thus leading to less gas production and NH_4^+ released in the liquid. Similarly, a higher C/N ratio indicates there is less nitrogen available, thus leading to lower NH_4^+ concentrations and less biomass production. It must be noted, however, that for each simulation a constant elemental composition was adopted and the C/N ratio does not vary with progressive degradation. In a study on the effects of the initial C/N ratio on organic matter degradation, the authors measured the C/N ratio of different mixtures at the initial and final state of the experiment (Ekinci et al., 2019). Their results are shown in Figure 5.2, indicating that the C/N ratio decreases as degradation progresses. This decrease is related to the maturity of OM (Chefetz et al., 1996). Chefetz et al. (1996) state that stable and decomposed organic matter is characterized by a C/N ratio of 10 to 12. Also, it must be noted that the used elemental composition for this study represents an average of all the different organic fractions in the waste body. However, different materials may have significant differences in the C/N ratio (Komilis et al., 2012). This, in combination with different materials having significant differences in the hydrolysis rate (Vavilin et al., 2008), questions whether the organic fraction can be considered an average of all materials.

Similarly to the C/N ratio, the organic fraction may differ significantly for different waste mixtures. Studies show that the organic share of waste is highly variable for different countries, ranging from <20% to >75% (Chen et al., 2020a). In addition to this, information on the organic fraction of waste is not always available. For the three landfill sites part of the CURE program (Wieringermeer, Kragge & Braamberg), the baseline study report only includes specific data for the organic share for the Braamberg site (29% organic share, 71% inert), while this is less clear for the other sites. However, the study presented here shows that the initial organic fraction

Table 5.1: C/N ratio for different materials.

Material	C/N
Uncooked meat	5.42
Cooked meat	5.39
Cooked pasta	28.53
Vegetables	14.73
Fruit	80.46
Raw meat fat	11.05
Grass	28.93
Leaves	46.55
Branches	159.44

may affect the model results significantly. Therefore, pre-knowledge of the organic fraction is required to optimize the model predictions.

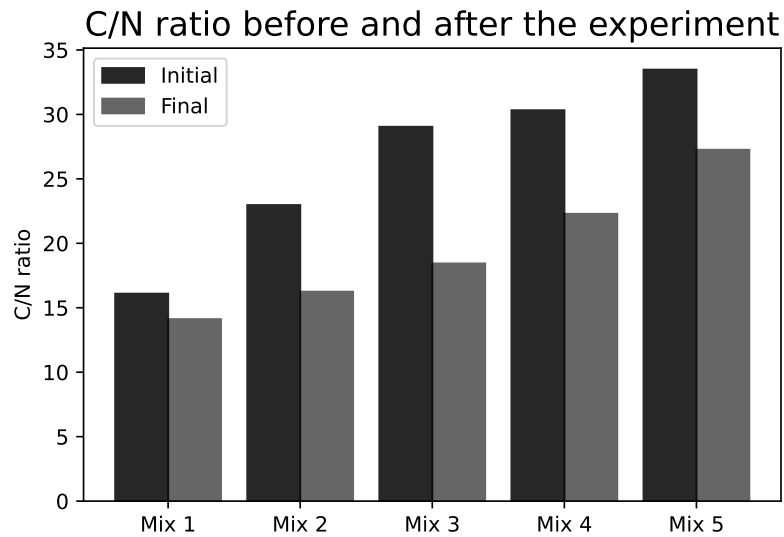


Figure 5.2: Results from a study conducted by Ekinci et al. (2019), showing the initial C/N ratio and the C/N ratio measured after degradation for 5 different mixtures. Measurements are based on the sample dry weight.

5.4 Limitations and simplifications

The model presented here may be used to simulate and predict waste degradation in a bioreactor. However, in its current state, the true behaviour of a bioreactor test cannot be fully captured. The model includes two major simplifications: (1) no volume loss and (2) no fluid and gas transport. As solid waste is degraded, void space is created (see results, section 4.4). Depending on the weight of the overlying material, this will lead to vertical compression of the volume cell. This introduces a coupled system where the bulk density of the material affects the rate of compression which, in turn, leads to a change in bulk density. By excluding this behaviour from the current model, the porosity change over time is heavily overestimated. This may affect biodegradation as the reactive surface area is influenced by porosity. This relationship is illustrated in Figure 5.3, where an initial increase in porosity increases the reactive surface. As the porosity further increases, however, pores may collide, leading to a decrease in surface area (Altrea-Williams et al., 2019). In addition to this, Chen et al. (2020) state that porosity is a very important factor in modelling the coupled behaviour in landfills, affecting permeability and hydraulic conductivities for water and gas transport.

This behaviour of changes in porosity has been examined by various authors who modeled the change in

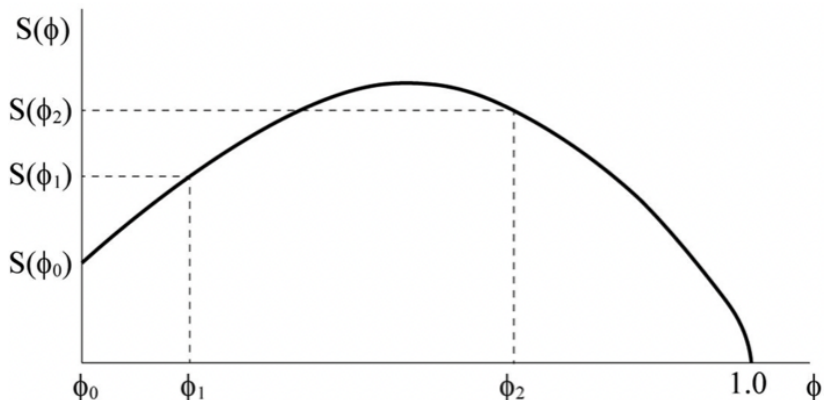


Figure 5.3: Relative reactive surface (S) as a function of porosity (ϕ), source: Altrea-Williams et al., 2019.

porosity as a function of strain (ϵ), waste mass (M) and waste density (ρ) (Chen et al., 2020b):

$$\Delta n = \Delta \epsilon - \frac{M}{\rho} \quad (5.2)$$

With this equation, the study shows that porosity decreases with progressive degradation.

Fluid and gas transport are processes that significantly influence degradation in a bioreactor. Transport is affected by degradation as this affects the hydraulic and gas conductivity. In turn, fluid and gas transport affects the chemical conditions of the landfill as chemical components are 'removed'. Note that the model presented here includes the transport of O_2 , periodically aerating the system to reach atmospheric levels. However, no transport of other gaseous species was included.

Lastly, the temperature was kept constant throughout the simulation. However, studies have shown that biological activity in a bioreactor may significantly increase the temperatures (Warith and Sharma, 1998; Warith et al., 2005). Studies suggest that temperatures up to 10 to 15 °C higher than the placement temperature may be expected as a result of aerobic degradation (Lefebvre et al., 2000). Figure 5.4 depicts the used inhibition functions for temperature for case study 4. An increase of 15 °C would imply that temperatures of 46 °C could be reached (this study adopts a constant temperature of 21°C). The figure suggests that this could affect most processes to a significant extent.

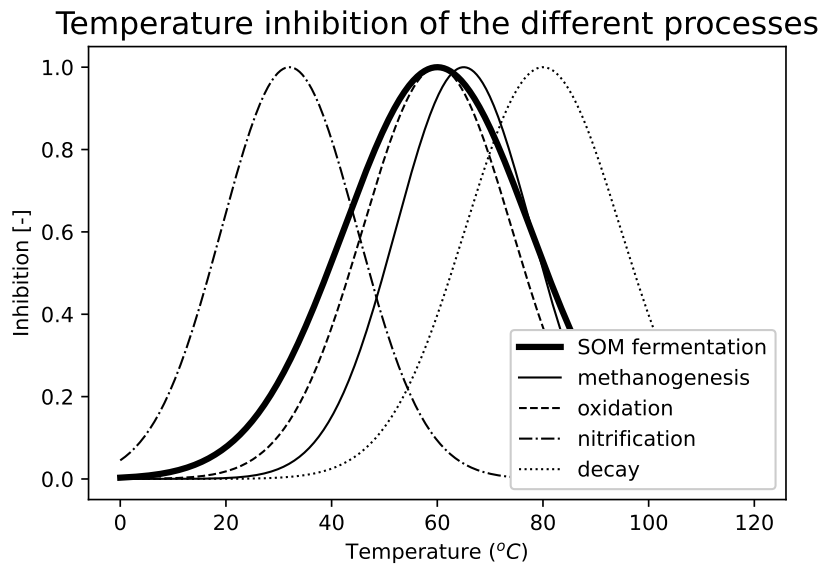


Figure 5.4: Temperature inhibition functions for the different processes in case study 4.

Temperature changes can be implemented in the model by calculating the change in enthalpy of a given reaction. The calculation of the change in enthalpy (ΔH) is similar to that of the change in Gibb's free energy, where:

$$\Delta H = \sum_{i=1}^n Y_i \cdot \Delta H f_i \quad (5.3)$$

Where n is the number of species involved in the reaction and $\Delta H f_i$ is the standard enthalpy of formulation (in kJ/mol) for species i . Following the same approach as in 3.2.1, the change in enthalpy to form 1 mole of biomass (ΔH_{met}) is then:

$$\Delta H_{met} = \lambda_{cat} \Delta H_{cat} - \Delta H_{an} \quad (5.4)$$

Where ΔH_{cat} and ΔH_{an} are the change in enthalpy for the catabolic and anabolic reactions, respectively.

Chapter 6

Conclusion

This study presents the results of a modelling framework that couples chemical equilibrium software (ORCHESTRA) to a kinetic solver that simulates waste degradation in a bioreactor landfill. Using the pybind11 Python package, a tool is developed that allows seamless operability between ORCHESTRA and the Python environment. A documentation on the tool is presented that allows the ORCHESTRA binding to be used in a wide variety of future studies. In this study, ORCHESTRA is used to formulate a modelling framework that simulates biodegradation in a 0-D batch experiment. By integrating ORCHESTRA to a kinetic solver, reaction rates are coupled to the real-time chemical conditions within the leachate, including the pH, NH_4^+ adsorption to the waste surface and the composition of the waste liquid.

Results from various case studies show that NH_4^+ has a dominant role in the presented modelling framework, inhibiting processes at both low (*substrate inhibition*) and low (*toxicity inhibition*) concentrations. This translates to a model that is sensitive to a variety of input parameters such as the C/N ratio, the degree of adsorption (K_d) and the initial organic fraction. The model results show that NH_4^+ adsorption to the waste surface is an important process for biodegradation, affecting (1) the NH_4^+ available for biomass growth and (2) the inhibition of hydrolysis by NH_4^+ toxicity. However, we discuss that the Freundlich isotherm may be inappropriate for capturing NH_4^+ adsorption in a coupled framework as it does not take the effects of pH and ion exchange into account. For future studies, it is therefore suggested to use adsorption models (e.g. NICA-Donnan) that include such behaviour. In addition to this, the literature implies that the model lacks fundamental processes such as gas and fluid transport or changes in volume and temperature. However, the modelling framework presented here can be used as a starting point for future studies that wish to implement such factors.

Appendix A

Formulation of the reaction network

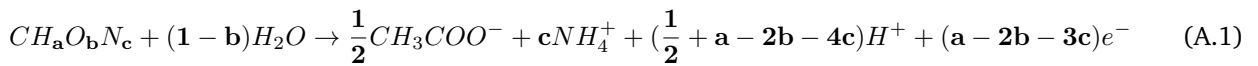
The formulation of the reactions are based on the method proposed Kleerebezem & van Loosdrecht (2010).

A.1 Hydrolysis lumped with acidogenesis & acetogenesis

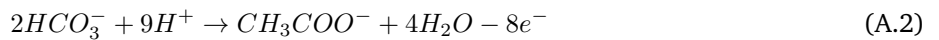
Description:

The first half-reaction describes the breakdown of solid organic matter (SOM, $CH_aO_bN_c$) to acetate (CH_3COO^-). The reaction is generalized to any given composition of SOM. For the second half-reaction, acetate is used as electron acceptor.

Half-reaction 1:

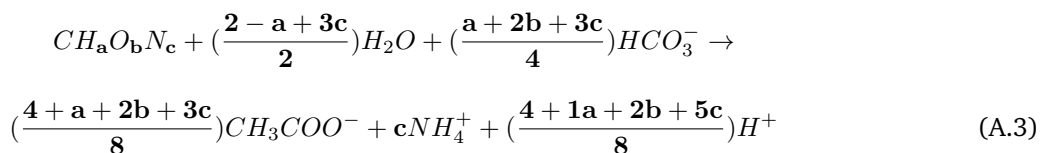


Half-reaction 2:

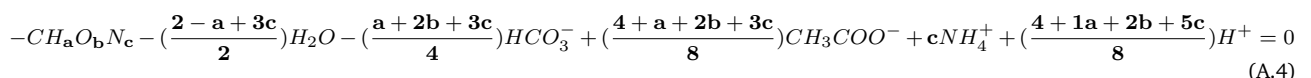


Final reaction:

The electrons balance out for Eq. (A.1) x 1 + Eq. (A.2) x $\frac{a-2b-3c}{8}$, leading to the final reaction:



Notation in electron balance:

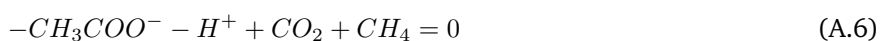


A.2 Methanogenesis of acetate

Description: Methanogenesis is an anaerobic process that produces CO_2 and CH_4 from acetate:



Notation in electron balance:



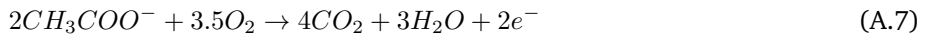
A.3 Oxidation of acetate

Description:

If O_2 is present, oxidizers use acetate generate energy, releasing CO_2 in the process. In the second half-reaction,

O_2 acts as the electron acceptor.

Half-reaction 1:



Half-reaction 2:

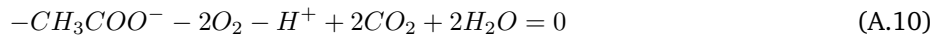


Final reaction:

The electrons balance out for Eq. (A.5) x 2 + Eq. (A.6), leading to the total reaction (after reorganizing):



Notation in electron balance:



A.4 Nitrification

Description:

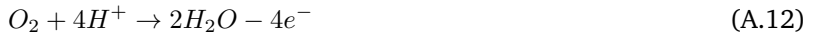
Nitrification is a two-step process of (1) oxidation of a nitrogen compound (NH_4^+ or NH_3) to nitrite (NO_2^-) and (2) oxidation of nitrite to nitrate (NO_3^-).

Oxidation of NH_4^+ to nitrite:

Half-reaction 1:

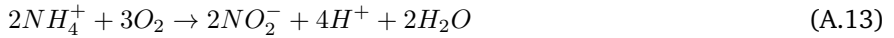


Half-reaction 2:



Final reaction:

The electrons balance out for Eq. (A.11) x 2 + Eq. (A.12), leading to the total reaction:



Oxidation of nitrite to nitrate:

Final reaction:

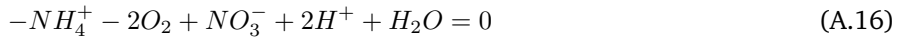


Combining reactions and reorganizing:

Final reaction nitrification:



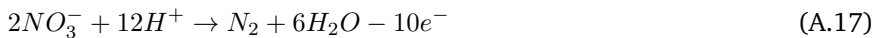
Notation in electron balance:



A.5 Denitrification

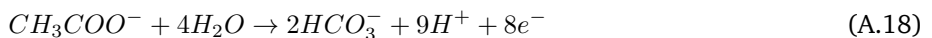
Description: Denitrification is an anaerobic process during which nitrate (NO_3^-) is oxidized to nitrogen gas (N_2).

Half-reaction 1:



Half-reaction 2:

Here, acetate is used as the electron acceptor:



Final reaction:

The electrons balance out for Eq. (A.17) x 4 + Eq. (A.18) x 5, leading to the total reaction (after reorganizing):



Notation in electron balance:

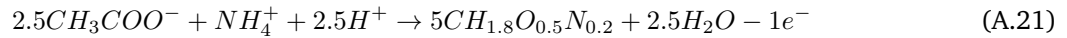


A.6 Biomass growth

Description:

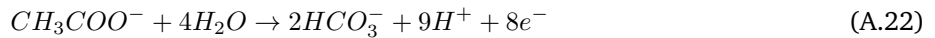
This reaction describes the formation of biomass ($\text{CH}_{1.8}\text{O}_{0.5}\text{N}_{0.2}$) using a carbon and nitrogen source. Acetate (CH_3COO^-) functions as the carbon source and ammonium (NH_4^+) functions as the nitrogen source.

Half-reaction 1:



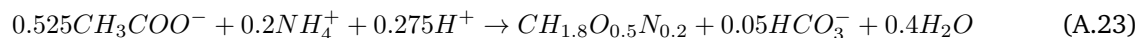
Half-reactoin 2:

Here, acetate is used as the electron acceptor:

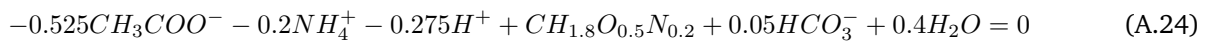


Final reaction:

The electrons balance out for Eq. (A.21) x 8 + Eq. (A.22), leading to the final reaction (after reorganizing):



Notation in electron balance:

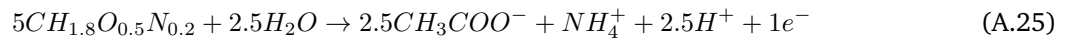


A.7 Biomass decay

Description:

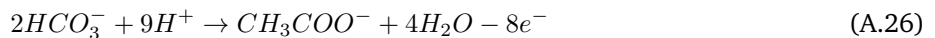
In this study, biomass decay is treated as the breakdown of biomass (lysis) leading to the release of acetate and ammonium.

Half-reaction 1:



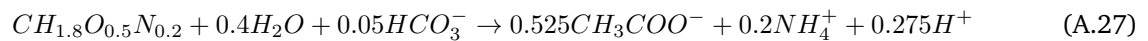
Half-reaction 2:

Here, acetate is used as electron acceptor:

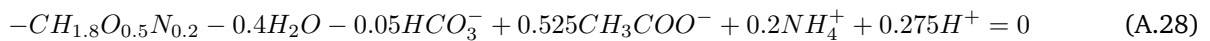


Final reaction:

The electrons balance out for Eq. (A.25) x 8 + Eq. (A.26), leading to the final reaction (after reorganizing):



Notation in electron balance:



Appendix B

PyORCHESTRA documentation

1 Introduction

Welcome to the documentation on the Python binding of ORCHESTRA! In this document, we will discuss the approach on how to use the chemical equilibrium software ORCHESTRA within Python using Pybind11. The document is part of the Master Thesis by Guido de Zeeuw for the Applied Earth Sciences master's programme at the TU Delft. The work discussed here is fully made with the collaboration of the creator of ORCHESTRA: Hans Meeussen. For information on the ORCHESTRA software, I invite you to check out the ORCHESTRA website: <http://orchestra.meeussen.nl>.

1.1 Introduction to ORCHESTRA

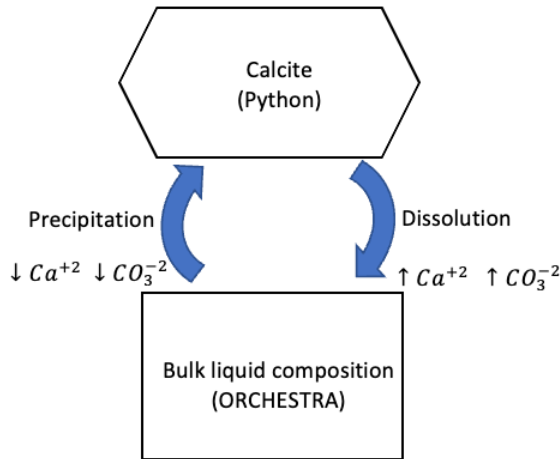
ORCHESTRA (Object Representing CHEmical Speciation and TRAnsport) is a chemical equilibrium model developed in the early 2000's to be a valid replacement for other available software (Meeussen, 2003). It must be noted, however, that the more conventional chemical equilibrium software (e.g. MINTEQA2, PHREEQC, MINEQL and ECOSAT) are already very powerful. These programs work by selecting a set of chemical reactions and their reaction constants, followed by a correct calculation of the chemical speciation. However, the problem arises with the general structure regarding such software. While the user can select a set of chemical components, the reactions related to those components are already pre-defined within the source code. Although this allows for a user-friendly experience, it also poses little transparency and flexibility. For example, if one would desire to change or add model definitions (e.g. exclude chemical equilibrium reactions from the calculation), this would require changing and recompiling the source code. For this, the source code must be available in the first place and even if this is the case, recompiling may take up a significant amount of time as the source code files may be very large.

This is the main reason why ORCHESTRA was created. With ORCHESTRA, the model definitions (e.g. chemical reactions, kinetics, general conditions) are defined in an input file. The calculation is done in a separate kernel that uses this input file. This means that the calculation kernel (or source code) does not contain any chemical information in itself and only acts as a calculator object. By structuring the software this way, changing model definitions does not require changing and recompile the source code. This allows the user to quickly select the reactions that the solver should include for calculating chemical equilibrium. The user can thereby exclude reactions that are described kinetically from those partaking in chemical equilibrium. Separating the model definitions from the source code also means that the calculation kernel is extremely small and, because of that, very efficient.

Although the calculator in itself is less complex and more flexible compared to the other equilibrium models, the difficulty with ORCHESTRA lies in correctly defining the chemical input file. To counteract the loss of a user-friendly experience, a graphical user interface (GUI) is developed to interactively set up the input file. The GUI can be downloaded from <http://orchestra.meeussen.nl>. The user interface comes standard with the ORCHESTRA-ready database for PHREEQC and various adsorption models. If needed, the user can create its own database with user-defined reactions.

1.2 Using ORCHESTRA in Python: why?

As ORCHESTRA allows the user to exclude reactions from the chemical equilibrium solver, ORCHESTRA is very useful when combined with kinetic solvers. Kinetic solvers are used to monitor the state of the system by keeping track of the reactants and products for a given reaction. A simple example is the dissolution of (e.g.) calcite, where the dissolution rate is described by a maximum rate and various inhibiting factors for different conditions (e.g. pH, liquid composition and available minerals). While the dissolution of calcite is described kinetically, other reactions (e.g. equilibrium between $H^+ + CO_3^{2-} \leftrightarrow H_2CO_3$) can be treated as instantaneous. In other words: they are not described kinetically but their relation can be calculated using ORCHESTRA. Below is an illustrative scheme on how this relation between a kinetic solver and ORCHESTRA works.



The illustration describes the effects of calcite dissolution/precipitation. Upon dissolution, the bulk composition of the liquid phase increases with CO_3^{2-} and Ca^+ . On the other hand, precipitation 'extracts' CO_3^{2-} and Ca^{+2} from the liquid system to form calcite. The kinetic solver (**in Python**) therefore monitors the *changes* in bulk composition of the liquid phase used to calculate chemical equilibrium (**in ORCHESTRA**).

This simple example directly shows the suitability of ORCHESTRA for this system. As the calcite dissolution/precipitation reaction is described kinetically, it must be excluded from the chemical equilibrium solution. As ORCHESTRA is input-based, the user only has to exclude the calcite formation from the chemical input file after which calcite dissolution/precipitation is no longer considered in the equilibrium calculation.

Note!!

Python is also a highly suitable tool for statistical analysis and managing large datasets. Apart from the option to separate reaction kinetics from equilibrium calculations, the wrapper presents additional benefits of integrating the wide variety of functions and tools presented by Python (e.g. the plotting package matplotlib or data manipulation with numpy & pandas).

2 Installing the package

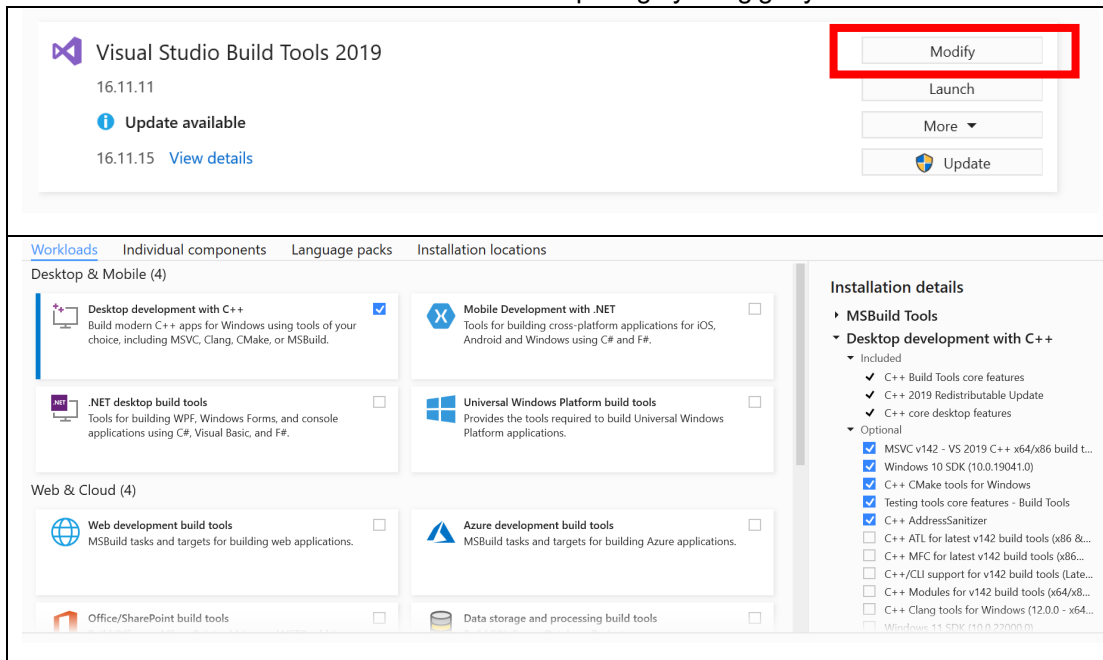
The ORCHESTRA package was written in both Java (original) and C++ (recently); the C++ version is based on Java, following the same coding structure. The binding package will be based on the C++ version, as Python is originally written in C++.

2.1 Setting up requirements

Windows:

1. Install the latest Python version (from <https://www.python.org/downloads/> or using a virtual environment, e.g. Anaconda).
2. Download and install the Build Tools for Visual Studio 2022 (to allow the computer to run C++ code): <https://visualstudio.microsoft.com/downloads/?q=build+tools> (at the bottom of the page). When the installer is finished, open the visual studio code installer. Navigate to 'modify' and check the C++ build tools box. Make sure the following boxes are checked:
 - MSVC v142 – VS 2019 C++ x64/x86 build tools (v14...)
 - Windows 10 SDK (10.0.18362.0)
 - C++ CMake tools for Windows
 - Testing tools core features – Build Tools
 - C++ AddressSanitizer (Experimental)

Press install. **To check:** the install should take up roughly 6.8 gigabytes.



3. To run the ORCHESTRA GUI, Java must be installed. To install Java, go to your preferred webbrowser and navigate to <https://www.java.com/en/download/manual.jsp>. Navigate to the offline downloader ('Windows Offline (64-bit)') and follow the instructions given by the installer.
4. Lastly, install the Pybind11 package that allows binding C++ code to Python. Open the terminal (e.g. 'command prompt') and type 'pip install pybind11'. This will install the latest version of pybind11

2.2 Cloning the gitlab repository to your local directory folder

Once the prerequisites are installed, the ORCHESTRA binding/wrapper can be copied from gitlab. To do so, open a command prompt/terminal and navigate to your local directory folder where you want the binding folder to be copied. Here, for example, we navigate to a local folder called 'gitlabs'.

```
cd Documents/Guido/gitlabs
```

When you are inside the correct directory, type:

```
git clone https://gitlab.tudelft.nl/guidozeeuw/orchestra_python.git
```

This command clones the gitlab repository to your local directory. If done correctly, a folder called 'orchestra_python' should appear. To quickly check the presence of such a folder, type 'dir' (Windows) or 'ls' (MacOS & Linux). The folder name should be listed on your command prompt/terminal window.

The 'orchestra_python' folder contains one folder 'v1.3.1' (or a different name depending on the version). In turn, the folder 'v1.3.1' contains three folders:

- Install: folder containing all files to install the PyORCHESTRA package on a local device.
- Examples: various examples from this tutorial.
- ORCHESTRA: folder containing the ORCHESTRA GUI to create chemical input files.

2.3 Installing the ORCHESTRA binding package

To install the Python binding to ORCHESTRA, open terminal ('conda prompt') and navigate to the 'setup_package' directory:

```
cd v1.0.0/multiple_nodes/setup_package
```

This folder contains the 'setup.py' file that is used to install the package. Type the following and press 'enter':

```
pip install .
```

Installing the package will take roughly 1 minute, depending on the computer specifications. the command prompt/terminal should show a print result similar to: 'successfully installed PyORCHESTRA-1.3.1'.

Congrats! The package is correctly installed to your Python environment!

3 Using PyORCHESTRA

The PyORCHESTRA submodule can be used in a Python script similar to any other Python package. First, the PyORCHESTRA submodule must be imported.

```
import numpy as np
import matplotlib.pyplot as plt
import PyORCHESTRA # here, the ORCHESTRA submodule is imported
```

To use the different functions that come with PyORCHESTRA, we assign the function class 'ORCHESTRA' to a user defined variable (here 'p').

```
p = PyORCHESTRA.ORCHESTRA() # Here, we call the function class and call it object 'p'
```

The ORCHESTRA class (now called 'p') contains 4 different functions:

- p.initialise(InputFile.inp, NoCells, InVars, OutVars)
- p.updatevalues(IN)
- p.calculate()
- p.set_and_calculate(IN)

3.1 Detailed description of functions

p.initialise(InputFile, NoCells, InVars, OutVars)

INPUT

- InputFile.inp: text file; containing chemical information, obtained with ORCHESTRA GUI.
- NoCells: int; number specifying the number of cells of the given system.
- InVars: matrix; array listing the variable names that are used as input (e.g. 'pH' or 'CO3-2.tot'). Must have the same length as defined NoCells.
- OutVars: matrix; array listing the variable names that are defined as output (e.g. 'pH' or 'CO3-2.con').

OUTPUT

None

FUNCTION DESCRIPTION

Function that takes the user defined chemical system boundaries (chemical system, number of cells) as input and constructs a so-called 'calculator'-object around this information. This information is now stored in this 'p' variable and can be used in further calculations.

p.updatevalues(IN)

INPUT

- IN: matrix; containing an array for every cell which is used to update the bulk-composition of the system for which equilibrium is calculated.

OUTPUT

None

FUNCTION DESCRIPTION

Function takes an array (or matrix for multidimensional systems) as input containing values for the variables listed in InVars (see p.initialise).

p.calculate()**INPUT**

None

OUTPUT

- Matrix containing an array for every cell with the same length as Outvars containing the output values specified in Outvars.

FUNCTION DESCRIPTION

This function calculates the equilibrium for a system with given bulk composition (initialised with p.updatevalues) and returns an array containing the results for variables specified in OutVars (see p.initialise)

p.set_and_calculate(IN)**INPUT**

- IN: matrix; array for every cell which is used to update the bulk-composition of the system for which equilibrium is calculated.

OUTPUT

- Array with the same length Outvars with output values.

FUNCTION DESCRIPTION

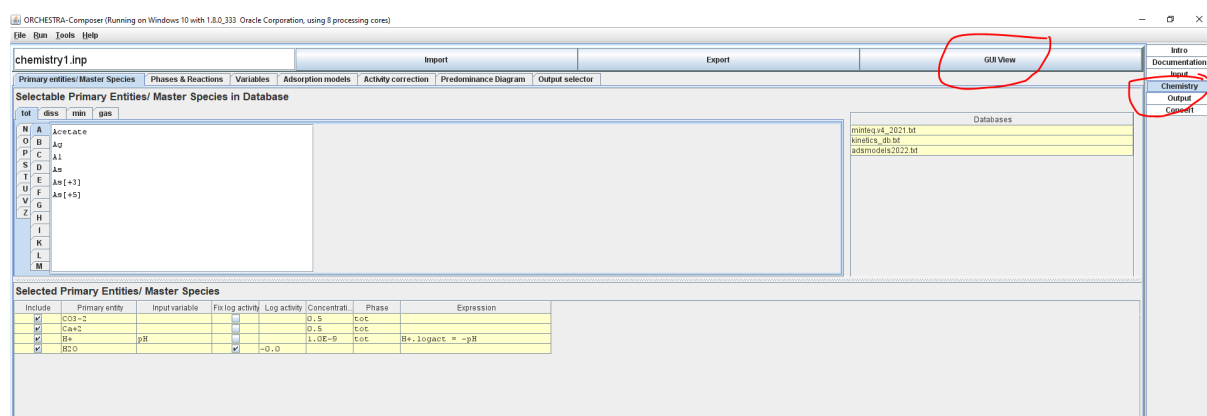
A combination of the functions p.updatevalues and p.calculate. Takes an array with values as input containing a given 'bulk composition' for the variables specified in InVars (see p.initialise). The function directly calculates the equilibrium and returns an array containing the result values for the variables specified in OutVars (see p.initialise).

4 ORCHESTRA tutorial: Chemistry input file

To calculate chemical equilibrium with ORCHESTRA, a chemical input file must be defined. This input file contains the following information:

- Variable definitions
- Phase hierarchy
- Master species
- Chemical reactions (including adsorption models)

For most cases, the chemistry file can be fully constructed with the ORCHESTRA GUI. However, in some cases, this is not the case and manually adding information to the text file is sometimes required. Therefore, a walkthrough of the input file is presented here. This walkthrough discusses the input file from top to bottom!



4.1 Setting up ORCHESTRA chemical input file with the GUI

Manually writing out the full chemistry input file can be a time-consuming task. The GUI can therefore be used to interactively create the input file. This includes:

- Specifying primary entities (section 4.6) excluding the special case discussed in section 4.9
 - Setting up variables (section 4.4)
 - Choosing the reaction network (section 4.7) excluding the special case discussed in section 4.8. The reaction network used is based on the used database.
- ORCHESTRA comes standard with the minteq database. The reader is invited to check this file and see how the individual reactions are defined.

An example of how the ORCHESTRA GUI is used is available in the example in section 5.1

4.2 Version and general commands

At the top of the chemistry input file, the user finds the version date. Here, the user may also alter some internal settings:

```
***** Version: dd/mm/yyyy hh:mm *****
@NrDigits: 12 // number of decimal places in reaction coefficients
//@rewriteReactions: //indicates that reactions are rewritten in terms of primary
entities
```

- The ‘//’ syntax is used to add comments.

4.3 Databases

In this part, the user specifies the databases that will be included in the chemistry calculation. These can either be local files or files from the internet. Here, we include the minteq database:

```
***** The database file(s) *****
//Syntax for local files:      @database: minteq.txt
//Syntax for files on internet: @database: www.meeussen.nl/orchestra/minteqv4.txt
```

```
***** end of thedatabase file(s) *****
```

Below this section, the user can specify additional parts of code by using the '@class:' command. These extra pieces of code will not be changed by the GUI.

```
***** extra text 0 *****
@class: extra_text_0(){
    @stop:
    @scan: objects2022.txt
}
@extra_text_0()
***** end of extra text 0 *****
```

Adding '@stop:' commands ORCHESTRA to create an 'iteration.dat' file when the program fails while calculating equilibrium. This file can be used as a rough results log file to examine why the calculation fails.

The '@include:' command is used to include local files. These local files may contain user-defined ORCHESTRA expressions. In this case, we include the 'objects2022.txt' file. This is a file that is standardly available in the ORCHESTRA download folder. This file contains fundamental calculation definitions used by ORCHESTRA. It is therefore advised to always include this file in the chemistry input file.

4.4 Variables

The user may specify a custom variable. A default value must be given (otherwise ORCHESTRA will raise an error). **Note:** the PyORCHESTRA wrapper allows the user to overwrite these variables from within Python! By doing so, the default value can be overwritten.

```
***** The variables *****
//general structure: @Var: [VARIABLE_NAME] [DEFAULT_VALUE]
@Var: porosity .9 //porosity of the system
@Var: saturation 1.0 //saturation of voids
@Var: totvolume 1.0 //dm3
@Var: my_own_variable_1 382.24
@Var: my_own_variable_2 -3.0
***** End of the variables *****
```

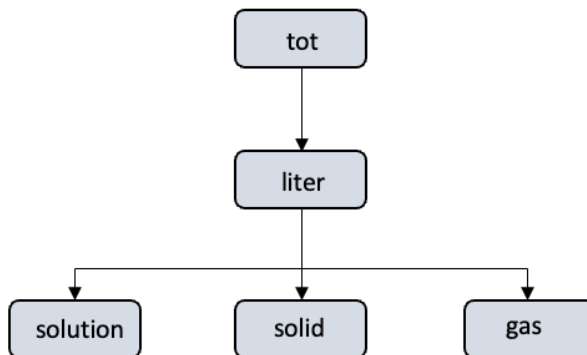
Below the variables, there is the possibility to add extra text. This extra text can be used to relate variables to each other. For example, here we give an expression for 'my_own_variable_1' and 'my_own_variable_2'. For this, use the '@Calc:' syntax.

```
***** Extra text 1 *****
@class: extra_text_1(){
    @Calc: (1, "my_own_variable_1 = porosity*totvolume*saturation") //total water volume
    @Calc: (1, "my_own_variable_2 = porosity*(1-saturation)") //total gas volume
}
@extra_text_1()
***** End of Extra text 1 *****
```

Mathematical expressions must be between the ““-syntax.

4.5 Phase Hierarchy

The standard ORCHESTRA file comes with a pre-defined phase hierarchy:



The table below indicates how the different phases relate to the given species CO_3^{2-} .

$CO_3^{2-}.tot$	The total amount of CO_3^{2-} in the system (in $\frac{mol}{L}$). Also known as the system <i>bulk composition</i> .
$CO_3^{2-}.liter$	The share of CO_3^{2-} in the <i>liter</i> phase (in $\frac{mol}{L}$).
$CO_3^{2-}.solution$	The share of CO_3^{2-} in <i>solution</i> (in $\frac{mol}{L}$).
$CO_3^{2-}.solid$	The share of CO_3^{2-} in <i>solids</i> (in $\frac{mol}{L}$).
$CO_3^{2-}.gas$	The share of CO_3^{2-} in <i>gas</i> (in $\frac{mol}{L}$).

Note, that the *liter* phase contains all of a certain species in the combined *solution*, *solid* and *gas* phase. This has no physical meaning other than to make sure that all three phases are linked together. In turn, the *solution*, *solid* and *gas* phase could be further subdivided into smaller phases. This could be useful for systems with multiple liquids (subdivide *solution* in liquid 1 and liquid 2) or with multiple solid phases (e.g. different minerals).

The hierarchy is listed in the chemical input file. For example, here we describe how the *liter* phase is linked to the *tot* phase:

1. Start by defining a *tot* phase.
2. Then define the *liter* phase
3. Link *liter* to *tot* using the @link_phase command.
 - The first argument is the phase that needs to be linked.
 - The second argument is the parent phase to which the new phase is linked.
 - The last argument determines the unit of conversion. Here the *liter* phase is the watervolume (=my_variable_1 in section 4.4). For example, let's say we have a species X with a total of 1 mol/L ($X.tot = 1 \text{ mol/L}$) of which 20% is present in the liquid. In addition to this, the porosity and saturation of the system are 0.4 and 0.9 respectively. The share of $X.tot$ in the liquid is then $1 * 20\% = 0.2 \text{ mol/L}$. But the volume of the liquid is itself $1 * 0.4 * 0.9 = 0.36 \text{ mol/L}$. Therefore the concentration in the *liter* phase ($X.liter$) is calculated as $0.2 / (0.36) = 0.556 \text{ mol/L}$.

```
@phase(tot)
@phase(liter)
@link_phase(liter, tot, "my_variable_1")
```

In a similar matter, we link the *solution* phase to the *liter* phase:

1. Define the *solution* phase. (Write also the definition of *solid* and *gas*)
2. Link *solution*, *solid*, and *gas* to *liter*. A conversion unit of 1 indicates that *solution* has the same unit. In this case, this implies that all different phases are part of the water volume phase.

```
@phase(solution)
@link_phase(solution, liter, "1")
@phase(solid)
```

```

@link_phase(solid, liter, "1")
@phase(gas)
@link_phase(gas, liter, "1")

```

4.5.1 Custom hierarchy

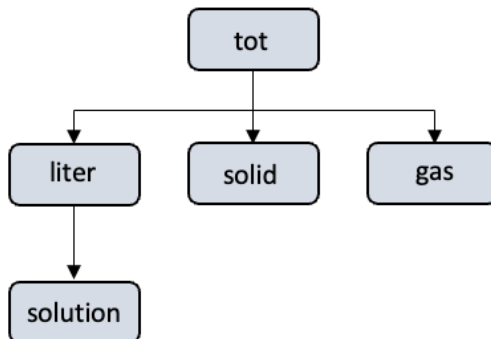
In the previous hierarchy all *gas*, *solid* and *solution* phases are part of the *liter* (or water volume) phase, indicated by the shared conversion unit “1”. However, this introduces limitations for systems where one wants to differentiate between phases not part of the *liter* phase. Luckily, the user is free to choose any type of hierarchy. For example, here we define a phase hierarchy where the *solution*, *gas* and *solid* phase do not share the same conversion unit.

```

@phase(tot)
@phase(liter)
@link_phase(liter, tot, "porosity*saturation")
@phase(solution)
@link_phase(solution, liter, "1")
@phase(solid)
@link_phase(solid, tot, "totvolume*(1-porosity)")
@phase(gas)
@link_phase(gas, tot, "porosity*(1-saturation)")

```

This notation describes the following hierarchy:



4.5.2 .con & .logact

The different phases described above list the bulk composition of a given species in the different phases. However, it is important to note that $CO_3^{2-}.solution$ is **not** the concentration of $[CO_3^{2-}]$ in the solution. It is rather the sum of CO_3^{2-} in the solution shared over all the different species (= the bulk composition):

$$CO_3^{2-}.solution = [CO_3^{2-}]_{in\ CO_3^{2-}} + [CO_3^{2-}]_{in\ H_2CO_3} + [CO_3^{2-}]_{in\ HCO_3^-} + [CO_3^{2-}]_{in\ CaCO_3} + \dots$$

Or, mathematically expressed:

$$CO_3^{2-}.solution = \sum_{i=0}^j [CO_3^{2-}]_i$$

Where j is the total amount of species and $[CO_3^{2-}]_i$ is the total amount of CO_3^{2-} in the i^{th} species.

The concentration and molar activities of a given species is obtained with by using the syntax ‘.con’ (for concentration) or ‘.logact’ (for molar activity) next to the species name. **Note:** The molar activity is given on a \log_{10} scale!

4.6 Primary entities

Now the user must specify the primary entities (or master species) that ORCHESTRA will use to calculate chemical equilibrium. The primary entities can be seen as the building blocks needed to build all the components (or ‘normal’ entities) of interest. As an example, the dissolution of calcite in water requires 4 different building blocks:

- Calcium (Ca^{+2})
- Carbonate (CO_3^{2-})
- Water (H_2O)
- Protons (H^+)

With these 4 primary entities, all the other entities are made:

- Ca^{+2}
- CO_3^{-2}
- $CaCO_3$ (calcite)
- HCO_3^-
- H_2CO_3
- H^+
- OH^-
- O_2
- CO_2
- $CaCO_3$
- $CaHCO_3^+$
- $CaOH^+$
- Aragonite
- Lime
- Portlandite

The primary entities are defined after the phase hierarchy. To include a species as primary entity, the user must include 2 lines.

- One line that adds the species/entity to ORCHESTRA. **But note** that ORCHESTRA does not know whether this is a primary entity or not based on this line. Therefore;
- A separate line must be included that defines this entity as 'primary_entity'.

The following sections describe how different species (elements, compounds, minerals and gases) are included as primary entity.

4.6.1 Set element as primary entity

The following lines describe how elements (H, N, O, S, Ca) are included as primary entity:

```
@entity(O, tot, 0) //add oxygen (O) as entity
@primary_entity(O, -9.0, tot, 1.0e-9) //set oxygen as primary entity
```

The @entity command adds an element as entity. This requires 3 input variables:

- The element name
- The phase to which it belongs (here: 'tot')
- A value (Hans? What is this value)

The @primary_entity command sets a species as 'primary'. This requires 4 input variables:

- The element name which will be set to 'primary'
- A value that ORCHESTRA uses as initial value to calculate equilibrium (always set to -9.0)
- The phase in which their quantity unit is expressed as input (here: 'tot'). This can also be the case if the entity itself is part of a different phase (for example: @entity(O, solution, 0)). Now, the input quantity is expressed in 'tot' (total in whole system). ORCHESTRA automatically converts this to the unit of its actual phase ('solution').
- Information on how much mol/L of the element is available (here 1.0e-9 mol/L).

4.6.2 Set chemical compound and ions as primary entity

Apart from elements, building blocks may also consist of chemical compounds (CO_3^- , NH_4^+) or ions (Ca^{+2} , H^+). For this, the syntax @species is used:

```
@species(CO3-2, -2) //add carbonate (CO3-2) as entity
@primary_entity(CO3-2, -9.0, tot, 1.0e-9) //set carbonate as primary entity
```

The @species command holds two arguments:

- The compound/ion name.
- The charge of the compound/ion

4.6.3 Set minerals as primary entity

Minerals are added using the @mineral command:

```
@mineral(Gypsum[s]) //add gypsum as entity
@primary_entity(Gypsum[s], -9.0, tot, 1.0e-9) //set gypsum as primary entity
```

Note, that ORCHESTRA itself does not contain information on the elemental composition of (e.g.) Gypsum. For this, either a database is required (see Chapter 4.3) or the method described in Section 4.9 must be applied.

4.6.4 Set gas as primary entity

Similar to minerals, gases can be added as primary_entity with the @gas syntax:

```
@gas(CH4[g]) //add gypsum as entity  
@primary_entity(CH4[g], -9.0, tot, 1.0e-9) //set gypsum as primary entity
```

4.6.5 Fixed logactivity for a primary entity

Let us consider the primary entity H^+ . Based on the previous chapters, this can be added with:

```
@species(H^+, 1) //add proton as entity  
@primary_entity(H^+, -9.0, tot, 1.0e-9) //set proton as primary entity
```

According to Chapter 4.6, the input quantity of H^+ (here: $H^+.tot = 1.0e^{-9} \frac{mol}{L}$) is not the actual amount of free H^+ in the system. In fact, it is the total amount of H^+ available in the system for all compounds that contain H^+ . This might introduce some problems for cases where the user wants to base equilibrium on a fixed pH; here, this requires the system to user the amount of free H^+ in the system as: $[H^+] = 10^{-pH}$. The question now is: *how do we set the amount of free H^+ as input, rather than the total amount of H^+ in the system?*

To do this, the user can relate the H^+ entity to a fixed log activity. In simple words: by doing this the user ‘tells’ ORCHESTRA what the amount of free H^+ in solution should be at equilibrium. Based on this log activity the concentrations of other components are determined.

For a given species “my_own_species+2”, this is included as follows:

```
@species(my_own_species+2, 2) //add proton as entity  
@primary_entity(my_own_species+2, 7.0) //set proton as primary entity
```

Here the @primary_entity syntax contains 2 arguments:

- The name of the entity/species
- The “fixed” log activity of the species

4.7 Equilibrium reactions

The chemical input file concludes with specifying the equilibrium reactions that ORCHESTRA should take into account. In ORCHESTRA, a “reaction” object is used to form new entities from existing entities. For example:

```
@species(HCO3-1, -1) //add bicarbonate as entity  
@reaction(HCO3-1, 3.455, 1, H+, 1, CO3-2) //set proton as primary entity
```

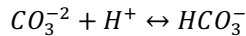
Here, 3.455 is the K-constant of the reaction

Alternatively, you can use the log K version of the reaction:

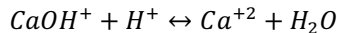
```
@species(HCO3-1, -1) //add bicarbonate as entity  
@logKreaction(HCO3-1, 3.7, 1, H+, 1, CO3-2) //set proton as primary entity
```

Both logKreactions and reactions can be mixed in a single input file.

The example above presents a very simple reaction, where:



But what if we have a more complex reaction, for example:



Here, the new species ($CaOH^+$) is formed, along with an already defined entity (H^+). The following syntax is used:

```
@species(CaOH+, 1) //add calcium hydroxide as entity  
@logKreaction(CaOH+, -12.679, 1, Ca+2, 1, H2O, -1, H+) //set proton as primary entity
```

Where:

- -12.679 is the log K constant of the reaction (this is listed in the minteq database)
- “1”, “1”, “-1” are the stoichiometry coefficients of Ca^{+2} , H_2O and H^+ , respectively.

4.8 Special case: mass-action and mass-balance

In the examples above, the coefficients indicate their share in the mass balance for the given reaction: “1, Ca+2” implies that 1 $CaOH^+$ contains 1 Ca^{+2} . This is called the *mass-balance coefficient*.

ORCHESTRA also uses information on the *mass-action coefficient* for a given species. By separating mass-action and mass-balance coefficients, we can use different coefficients for the reaction balance calculation and the calculation of the masses of the species involved.

This is further illustrated with a the syntax of a logKreaction for the adsorption of NH_4^+ to a body surface following the Freundlich equation:

$$\log(q_{NH_4^+}) = K_d + n \cdot \log(a_{NH_4^+})$$

Where $q_{NH_4^+}$ is the concentration of NH_4^+ adsorbed to the body surface, K_d is the Freundlich constant, n is a coefficient and $a_{NH_4^+}$ is the molar activity of NH_4^+ in solution.

n describes the shape of the curve, where a linear relationship is found for $n = 1$. For $n = 1$, the reaction is defined in ORCHESTRA below. Here it is assumed that the ‘ads’ phase and the NH_4^+ entity are defined earlier in the text file (see Chapter 4.5 & 4.6):

```
@species(NH4_ads, ads, 1) //add species to file and relate the species to phase 'ads'  
@logKreaction(NH4_ads, [Kd], 1, NH4+) //relate new species to NH4+ in solution
```

As $n = 1$, both the mass-action and mass-balance coefficients are 1; $NH_{4,ads}^+$ counts for 1 in the mass-balance of NH_4^+ . However, if a non-linear relation is found between NH_4^+ and $NH_{4,ads}^+$, a different mass-action coefficient can be used. For example, adopting $n = 0.8$ leads to the following input.

```
@species(NH4_ads, ads, 1) //add species to file and relate the species to phase 'ads'  
@logKreaction(NH4_ads, [Kd], "0.8, 1", NH4+) //relate new species to NH4+ in solution
```

Here, the “1” is replaced with “0.8, 1”, where 0.8 is the mass-action and 1 is the mass-balance coefficient.

4.9 Special case: custom primary entity

In the previous chapter ‘NH4_ads’ is a user defined entity where its composition is based on the logKreaction. In other words, ‘NH4_ads’ is an entity that is based on primary entities. However, the same method cannot be applied to defining custom primary entities; primary entities cannot be based on other primary entities following a logKreaction. Let us consider a system where our main building blocks (primary entities) are CO_3 , Ca^{+2} and NH_4^+ . Following section 4.6, these are included following:

```
@species(CO3-2, -2)
@primary_entity(CO3-2, -9.0, tot, 1e-9)
@species(Ca+2, 2)
@primary_entity(Ca+2, -9.0, tot, 1e-9)
@species(NH4+, 1)
@primary_entity(NH4+, -9.0, tot, 1e-9)
```

We also want to include a custom compound called ‘tutorial_compound’ with a composition $Ca(CO_3)_2NH_4$ as a primary entity:

```
@entity(tutorial_compound, tot, 1) //add new mineral as entity
@primary_entity(tutorial_compound, -9.0, tot, 1e-9) // set as primary entity
```

While we have successfully added the compound as a primary entity, ORCHESTRA does not know the composition of the compound (as we have not specified this anywhere!). The following setup, however, allows us to specify its composition in a separate line:

1. Open a new text file.
2. Add the following lines:

```
@class: composition(name, c1, n1){
    @link(<name>, <n1>, 0, <c1>)
}

@class: composition(name, c1, n1, c2, n2){
    @link(<name>, <n1>, 0, <c1>)
    @link(<name>, <n2>, 0, <c2>)
}

@class: composition(name, c1, n1, c2, n2, c3, n3){
    @link(<name>, <n1>, 0, <c1>)
    @link(<name>, <n2>, 0, <c2>)
    @link(<name>, <n3>, 0, <c3>)
}

@class: composition(name, c1, n1, c2, n2, c3, n3, c4, n4){
    @link(<name>, <n1>, 0, <c1>)
    @link(<name>, <n2>, 0, <c2>)
    @link(<name>, <n3>, 0, <c3>)
    @link(<name>, <n4>, 0, <c4>)
}
```

3. Save the file in the ORCHESTRA directory and give it an appropriate name (here: ‘kinetics_db.txt’).
4. Include the file with the ‘@scan command as described in Section 4.3.

```
***** extra text 0 *****
@class: extra_text_0(){
    @stop:
    @scan: objects2022.txt
    @scan: kinetics_db.txt
}
@extra_text_0()
***** end of extra text 0 *****
```

With the previous steps, a function called ‘@composition’ is formulated that allows the user to define a composition for a given entity. The ‘@composition’ command is used in the extra text section below the primary entity section:

```
//***** Extra text 2a *****
@class: extra_text_2a(){
    @composition(tutorial_compound, 1.0, Ca+2, 2.0, CO3-2, 1.0, NH4+)
}
@extra_text_2a()
```

As we have provided 'tutorial_compound' with a composition, we can use it in logKreactions similarly to other primary entities.

5 Examples

5.1 The $\text{Ca}^{+2} - \text{CO}_3^{-2}$ system

The first example is a simple case of the $\text{Ca}^{+2} - \text{CO}_3^{-2}$ system. The example calculates chemical speciation at equilibrium at different pH levels, given a fixed bulk composition of Ca^{+2} and CO_3^{-2} . The example represents a batch experiment of a closed system where the pH is fully controlled. **Important:** We assume that the system has infinite time to equilibrate. By doing so, no rate dependencies on mineral growth are introduced.

5.1.1 Setting up the chemistry input file

Before calculating chemical equilibrium, the user is required to construct a chemistry input file. This input file contains all the chemical information needed for ORCHESTRA to build a calculator object. The chemistry input file is constructed using the ORCHESTRA GUI. The GUI comes with the gitlab repository. Opening the GUI leads to the following screen.



On the right (or top when working on a windows machine), there are various tabs available. In general, only the 'chemistry' tab is needed.

Step 1: specify primary components

The ORCHESTRA chemical input file should contain information on what the primary species/master species for the given calculation are. Primary species can be described as the elements describing the *bulk composition*. These can either be elements (H, N, O, C, etc.) or chemical components and ions (CO_3^{-2} , NH_3 , SO_4^{-2} , H^+). In this example, we will calculate chemical equilibrium using chemical components and ions. In this case, the main components (or *building blocks*) are Ca^{+2} , CO_3^{-2} and H^+ . Do the following:

1. Navigate to 'chemistry' → 'Primary entities/Master species'.
2. Add Ca^{+2} , CO_3^{-2} & H^+ for the 'diss' tab.
3. Lastly, we will add water to the system. Go to the 'liter' tab and select H_2O .

Step 2: fix log activities if necessary

In most-simple words, ORCHESTRA works by iteratively converging to a solution where equilibrium is met. To do so, the program searches for the log activities at equilibrium of the different species. Now, the user has 2 options: (1) either **fix** the log activity of a master species, or (2) allow the log activity to **change** during the search for chemical equilibrium. For example, in this example we want to compare chemical speciation at different pH levels. Therefore, the pH must stay at a fixed level within every individual calculation; if we want to calculate chemical equilibrium at a pH of (e.g.) 7, we don't want

the system to allow a change in log activity of the H^+ . Therefore, the user must specify that the pH is fixed.

In this example the log activities are fixed for both H^+ and H_2O . To do so:

1. For the H_2O species, select 'fix log activity' and set the value to -0.0.
2. Do the same for H^+ : select 'fix log activity'.

If done correctly, the following is achieved:

Primary entity	Input variable	Fix log acti...	Log activity	Concentrat...	Phase	Expression
CO3-2		<input checked="" type="checkbox"/>		1.0E-9	tot	
Ca+2		<input checked="" type="checkbox"/>		1.0E-9	tot	
H+	pH	<input checked="" type="checkbox"/>	-7.0			H+.logact = -pH
H2O		<input checked="" type="checkbox"/>	-8.0			

Don't change the values in the column 'concentrations'. You can, but this does not matter as this will be done later in Python as well.

Step 3: select reaction network

The next step is the selection of the reaction network (in the Phases & Reactions tab). This is an important step that requires the user to critically think about the problem at hand. If a reaction is selected, ORCHESTRA takes this reaction into account when calculating chemical equilibrium. In this example, we assumed that the system calculates equilibrium at $t = \infty$. Therefore, all reactions need to be considered.

1. Navigate to the Phases & Reactions tab.
2. Check all reactions.

Include	Name	Log K (25C)	Phase	Coefficient	Reactant	Coefficient	Reactant	Coefficient	Reactant	Coefficient	Reactant
<input checked="" type="checkbox"/>	Alkalinity	0.0	tot	1.0	CO3-2						
<input checked="" type="checkbox"/>	Aragonite[s]	8.300000	min	1.0	CO3-2	1.0	Ca+2				
<input checked="" type="checkbox"/>	C	0.0	tot	1.0	CO3-2						
<input checked="" type="checkbox"/>	CO2[g]	18.14700	gas	1.0	CO3-2	2.0	H+	-1.0	H2O		
<input checked="" type="checkbox"/>	C[+4]	0.0	tot	1.0	CO3-2						
<input checked="" type="checkbox"/>	Ca	0.0	tot	1.0	Ca+2						
<input checked="" type="checkbox"/>	CaCO3	3.200000	diss	1.0	CO3-2	1.0	Ca+2				
<input checked="" type="checkbox"/>	CaHCO3+	11.59900	diss	1.0	CO3-2	1.0	Ca+2	1.0	H+		
<input checked="" type="checkbox"/>	CaOH+	-12.69700	diss	1.0	Ca+2	-1.0	H+	1.0	H2O		
<input checked="" type="checkbox"/>	Calcite[s]	8.480000	min	1.0	CO3-2	1.0	Ca+2				
<input checked="" type="checkbox"/>	H	0.0	tot	1.0	H[+1]						
<input checked="" type="checkbox"/>	H2CO3	16.68100	diss	1.0	CO3-2	2.0	H+				
<input checked="" type="checkbox"/>	HC03-	10.32900	diss	1.0	CO3-2	1.0	H+				
<input checked="" type="checkbox"/>	H[+1]	0.0	tot	1.0	H+						
<input checked="" type="checkbox"/>	Lime[s]	-32.69930	min	1.0	Ca+2	-2.0	H+	1.0	H2O		
<input checked="" type="checkbox"/>	O	0.0	tot	1.0	O[-2]						
<input checked="" type="checkbox"/>	OH-	-13.99700	diss	-1.0	H+	1.0	H2O				
<input checked="" type="checkbox"/>	O[-2]	0.0	tot	1.0	H2O						
<input checked="" type="checkbox"/>	Portlandite[s]	-22.80400	min	1.0	Ca+2	-2.0	H+	2.0	H2O		

Step 4: export chemistry text file

1. The chemistry setup is finalized! Export the chemistry file by selecting 'Export' at the top.
2. A text file called 'chemistry1.inp' is created in the ORCHESTRA folder.

5.1.2 Calculating chemistry with Python.

For this example, we will examine what the effects of pH are on the system composition at equilibrium. In Python, the pH is changed iteratively. For every pH, a new equilibrium composition is calculated using ORCHESTRA. In turn, the results are plotted using Python.

Step 1: create .py file and import modules.

1. Open a new python file and call it 'carbonate_species.py'

- Start the file by importing the required submodules:

```
import numpy as np
import matplotlib.pyplot as plt
import PyORCHESTRA # here, the ORCHESTRA submodule is imported
```

Step 2: get the ORCHESTRA function class ‘p’.

```
p = PyORCHESTRA.ORCHESTRA()
```

Step 3: Initialise the ORCHESTRA calculator.

Now, the user must define the boundary conditions of the system for which chemical equilibrium will be calculated.

- Name the chemistry text file. InputFile = ‘chemistry1.inp’
- Specify the number of cells. Here we will consider a 0-D system.
- Specify the variables that will be used as input. Here, this includes the bulk composition (total Ca^{+2} and CO_3^{-2} in the system) and pH. In addition to this, ORCHESTRA comes with pre-available parameters such as porosity and saturation.
- Specify the variables that the user wants as output. Here, this includes the concentration of several important species (e.g. CaCO_3 and CO_3^{-2}).
- Call the function ‘initialise’ to initialize the ORCHESTRA calculator object.

```
InputFile = 'chemistry1.inp'
NoCells = 1 #only 1 cell to have a 0-D system
InVars = np.array(['Ca+2.tot', 'CO3-2.tot', 'pH', 'porosity', 'saturation'])
OutVars = np.array(['CaCO3.con', 'CO3-2.con', 'HC03-.con', 'H2CO3.con', 'Ca+2.con',
                    'Calcite[s].min'])

p.initialise(InputFile, NoCells, InVars, OutVars)
```

Step 4: Set the initial conditions.

The ‘p’-object now contains an initialized system that is ready to be used. By specifying values for the given input parameters (in InVar), an equilibrium will be calculated.

- First, we create the variable matrix ‘IN’ containing arrays of the same length as InVars (1 value for every parameter must be given).
- Using the `np.where` function, we can change the value in IN at the position corresponding to that parameter.
- We will assume that the system is fully saturated, with a porosity of 1. The bulk composition is set to $0.5 \frac{\text{mol}}{\text{L}} \text{Ca}^{+2}$ and $0.5 \frac{\text{mol}}{\text{L}} \text{CO}_3^{-2}$.

```
IN = np.array([np.ones_like(InVars)]).astype(float)

IN[0][np.where(InVars == 'porosity')] = 1
IN[0][np.where(InVars == 'saturation')] = 1
IN[0][np.where(InVars == 'Ca+2.tot')] = 0.5
IN[0][np.where(InVars == 'CO3-2.tot')] = 0.5
```

Step 5: change pH and get equilibrium

The pH is increased from 2 to 12 with a stepsize of 0.001. For every new ‘configuration’, system equilibrium is calculated using ‘set_and_calculate’. When ORCHESTRA calculates equilibrium, it returns a matrix with values for the parameters listed in OutVars.

- Define range for pH (here, using `np.arange`).
- Do a simple for loop, iterating over the different pH’s.
- Assign the new pH-value to the correct position in InVars.
- Calculate equilibrium with `p.set_and_calculate(IN)`
- Assign output values to the correct lists.

```
pH_list = np.arange(2,12,0.001) # range of pH

# define output lists
CaCO3, CO3, HC03, H2CO3, Ca, calcite = [], [], [], [], [], []
```

```

# loop over every pH
for pH in pH_list:

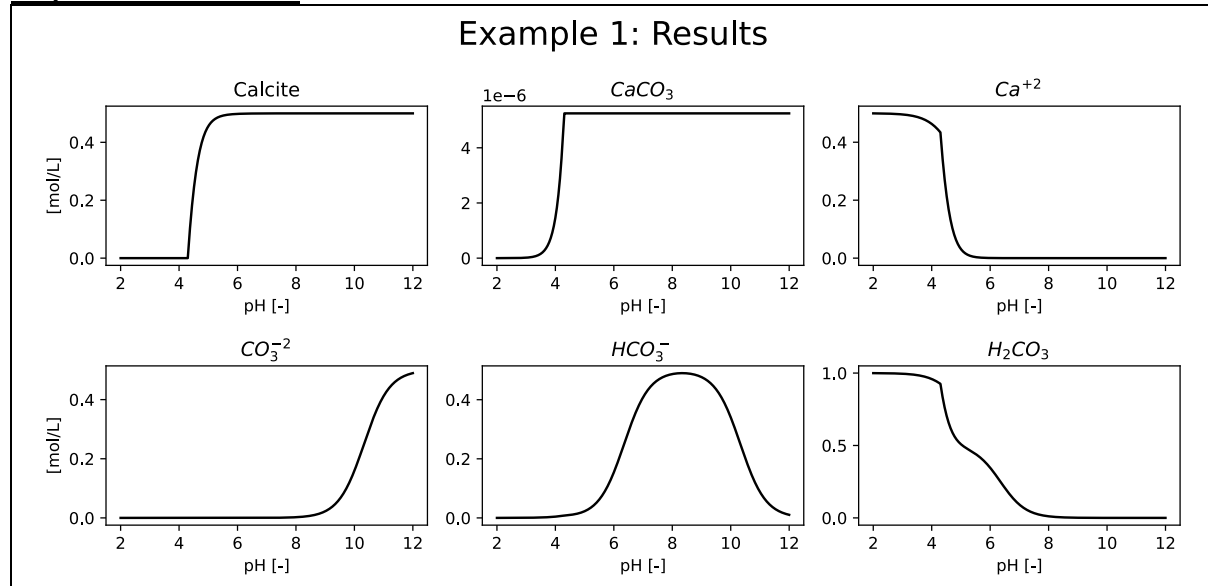
    # change pH
    IN[0][np.where(OutVars == 'pH')] = pH

    # run ORCHESTRA
    OUT = p.set_and_calculate(IN)

    # get output
    CaCO3.append(OUT[0][np.where(OutVars == 'CaCO3.con')])
    CO3.append(OUT[0][np.where(OutVars == 'CO3-2.con')])
    HCO3.append(OUT[0][np.where(OutVars == 'HCO3-.con')])
    H2CO3.append(OUT[0][np.where(OutVars == 'H2CO3.con')])
    Ca.append(OUT[0][np.where(OutVars == 'Ca+2.con')])
    calcite.append(OUT[0][np.where(OutVars == 'Calcite[s].min')])

```

Step 6: Plot the results



5.2 Calcite dissolution

In the previous example, ORCHESTRA calculated the calcite concentration based on a given composition of Ca^{+2} , CO_3^{-2} and H^+ . Now, we will do the opposite: “what would happen to the pH and carbonate concentrations if we dissolve calcite in the solution?”. For this, we will start with an initial concentration of calcite (0.5 mol/L). We dissolve calcite by iteratively decreasing the calcite mass (in Python), which will release Ca^{+2} and CO_3^{-2} in the solution, thus affecting the pH and concentrations. **It is assumed that no CO_3^{-2} and Ca^{+2} is initially present in the liquid!** To calculate the pH, ORCHESTRA is used. The following primary species (*‘building blocks’*) are used:

- $\text{CO}_3^{-2}.tot$
- $\text{Ca}^{+2}.tot$
- $\text{H}^+.tot$
- $\text{calcite_mineral}.tot$

$\text{calcite_mineral}.tot$ is the total amount of calcite ($\text{CaCO}_3[s]$) in the system.

To calculate chemical equilibrium with ORCHESTRA, a bookkeeping “trick” is used that allows ORCHESTRA to know how much CO_3^{-2} and Ca^{+2} is available in the liquid based on the amount of calcite present. This trick is based around understanding the following equations:

$$\begin{aligned}\text{CO}_3^{-2}.tot_{liquid} &= \text{CO}_3^{-2}.tot - \text{CO}_3^{-2}.tot_{calcite} \\ \text{Ca}^{+2}.tot_{liquid} &= \text{Ca}^{+2}.tot - \text{Ca}^{+2}.tot_{calcite}\end{aligned}$$

Let us, for example consider the case where (1) no calcite has been dissolved yet. As we assume that no free CO_3^{-2} and Ca^{+2} is initially present in the liquid, the following totals are applicable:

- $\text{calcite_mineral}.tot = 0.5 \text{ mol/L}$
- $\text{CO}_3^{-2}.tot = 0.5 \text{ mol/L}$
- $\text{Ca}^{+2}.tot = 0.5 \text{ mol/L}$

By defining the system this way, ORCHESTRA sees that all CO_3^{-2} and Ca^{+2} is present in calcite and therefore none is available for the other species in the liquid ($[\text{CO}_3^{-2}]$, $[\text{HCO}_3^-]$, $[\text{H}_2\text{CO}_3]$ & $[\text{Ca}^{+2}]$ are all 0).

Now, we take the case where 0.1 mol of calcite has been dissolved:

- $\text{calcite_mineral}.tot = 0.4 \text{ mol/L}$
- $\text{CO}_3^{-2}.tot = 0.5 \text{ mol/L}$
- $\text{Ca}^{+2}.tot = 0.5 \text{ mol/L}$

As you can see, the total amount of CO_3^{-2} and Ca^{+2} remain the same, but the total amount of calcite in the system changes. As the total amount of CO_3^{-2} and Ca^{+2} exceed those of calcite_mineral , ORCHESTRA knows that there must be 0.1 mol/L CO_3^{-2} and Ca^{+2} available to calculate equilibrium in the liquid (as 0.4 mol/L is part of calcite_mineral).

Now follows a step-by-step walkthrough on how to define this system using ORCHESTRA.

5.2.1 Setting up the chemistry input file

Step 1: specify primary components

The ORCHESTRA chemical input file should contain information on what the primary species/master species for the given calculation are. Primary species can be described as the elements describing the *bulk composition*. These can either be elements (H, N, O, C, etc.) or chemical components and ions (CO_3^- , NH_3 , SO_4^{-2} , H^+). In this example, we will calculate chemical equilibrium using chemical components and ions. In this case, the main components (or *building blocks*) are Ca^{+2} , CO_3^{-2} and H^+ . Do the following:

1. Navigate to ‘chemistry’ → ‘Primary entities/Master species’.
2. Add Ca^{+2} , CO_3^{-2} & H^+ for the ‘diss’ tab.
3. Lastly, we will add water to the system. Go to the ‘liter’ tab and select H_2O .

Step 2: set logactivities

In the previous example, the pH was an **input** parameter where we needed to set the logactivity to a fixed value (constant in equilibrium calculation). However, for this case, we want to relate the pH to the dissolution of calcite. For this, we need the pH to be the **output**. Therefore, set only H_2O to a fixed logactivity of -0.0:

The screenshot shows the software interface for setting primary entities. The top bar includes tabs for 'chemistry1.inp' (active), 'Import', and other options like 'Primary entities / Master Species', 'Phases & Reactions', 'Variables', and 'Adsorb'. Below this is a tree view under 'Selectable Primary Entities / Master Species in Database' with nodes for 'e-', 'w', 'z', and 'e'. A toolbar below the tree has buttons for 'tot', 'diss', 'min', 'gas', and 'solid'. The main area displays a table titled 'Selected Primary Entities / Master Species'.

Include	Primary entity	Input variable	Fix log acti...	Log activity	Concentrat...	Phase	Expression
<input checked="" type="checkbox"/>	C03-2		<input type="checkbox"/>		0.5	tot	
<input checked="" type="checkbox"/>	Ca+2		<input type="checkbox"/>		0.5	tot	
<input checked="" type="checkbox"/>	H+	pH	<input type="checkbox"/>		1.0E-9	tot	H+.logact = -pH
<input checked="" type="checkbox"/>	H2O		<input checked="" type="checkbox"/>	-0.0			

Step 3: add calcite_mineral as a primary entity

To do so, navigate to 'GUI view' and to the section "the primary entities". Add here calcite_mineral as a primary entity following the steps described in section 4.9. Here, we put calcite_mineral in the **solid** phase:

```
//***** The primary entities *****
@species(CO3-2, -2)
@primary_entity(CO3-2, -9.0, tot, 0.5)
@species(Ca+2, 2)
@primary_entity(Ca+2, -9.0, tot, 0.5)
@Global: pH
@Calc(1, "H+.logact = -pH")
@species(H+, 1)
@primary_entity(H+, pH, 7.0, lin, 0.1, tot, 1.0E-9)
@entity(H2O, liter, 55.6 )
@primary_entity(H2O, -0.0)
@entity(calcite_mineral, solid, 1) //add here calcite_mineral as species
@primary_entity(calcite_mineral, -9.0, tot, 0) //set species to primary entity
//*****
//*****
```

To check, navigate back to 'text view' → 'Primary entities/Master Species'. Here, calcite_mineral is now visible as an additional primary entity.

The screenshot shows the software interface for setting primary entities. The top bar includes tabs for 'chemistry1.inp' (active), 'Import', and other options like 'Primary entities / Master Species', 'Phases & Reactions', 'Variables', and 'Adsorb'. Below this is a tree view under 'Selectable Primary Entities / Master Species in Database' with nodes for 'e-', 'w', 'z', and 'e'. A toolbar below the tree has buttons for 'tot', 'diss', 'min', and 'gas'. The main area displays a table titled 'Selected Primary Entities / Master Species'.

Include	Primary entity	Input variable	Fix log acti...	Log activity	Concentrat...	Phase	Expression
<input checked="" type="checkbox"/>	C03-2		<input type="checkbox"/>		0.5	tot	
<input checked="" type="checkbox"/>	Ca+2		<input type="checkbox"/>		0.5	tot	
<input checked="" type="checkbox"/>	H+	pH	<input type="checkbox"/>		1.0E-9	tot	H+.logact = -pH
<input checked="" type="checkbox"/>	H2O		<input checked="" type="checkbox"/>	-0.0			
<input checked="" type="checkbox"/>	calcite_min...		<input type="checkbox"/>		0.0	tot	

Step 4: give composition to calcite mineral

As described in section 4.9, the composition of calcite_mineral is given in the extra_text segment below the definition of the primary entities. **Be sure to add the kinetics_db.txt file as indicated in section 4.9.** Add here the composition of CaCO_3 . This leads to the following:

```

//***** The primary entities *****
@species(CO3-2, -2)
@primary_entity(CO3-2, -9.0, tot, 0.5)
@species(Ca+2, 2)
@primary_entity(Ca+2, -9.0, tot, 0.5)
@Global: pH
@Calc(1, "H+Jogact = -pH")
@species(H+, 1)
@primary_entity(H+, pH, 7.0, lin, 0.1, tot, 1.0E-9)
@entity(H2O, liter, 55.6 )
@primary_entity(H2O, -0.0)
@entity(calcite_mineral, solid, 1 )
@primary_entity(calcite_mineral, -9.0, tot, 0.0)
//*****
//***** Extra text 2a *****

@class: extra_text_2a()
@composition(calcite_mineral, 1, CO3-2, 1, Ca+2)
// Here is some space for extra code that will be used in the calculations but will not be changed by the GUI.
}
@extra_text_2a()

```

Step 5: set reaction network

As we consider dissolution of minerals to be described kinetically, we must exclude those from the equilibrium calculation. Navigate to “phases & reactions” and uncheck all minerals:

Formation reactions in phase: <input type="checkbox"/> all <input checked="" type="checkbox"/> , depending on primary entity: <input type="checkbox"/> all <input checked="" type="checkbox"/> Show selected c								
Include	Name	Log K (25C)	Phase	Coefficient	Reactant	Coefficient	Reactant	Coefficient
<input checked="" type="checkbox"/>	Alkalinity	0.0	tot	1.0	CO3-2	1.0	Ca+2	
<input type="checkbox"/>	Aragonite[s]	8.300000	min	1.0	CO3-2	1.0		
<input checked="" type="checkbox"/>	C	0.0	tot	1.0	CO3-2			
<input checked="" type="checkbox"/>	CO2[g]	18.14700	gas	1.0	CO3-2	2.0	H+	-1.0
<input checked="" type="checkbox"/>	C[+4]	0.0	tot	1.0	CO3-2			
<input checked="" type="checkbox"/>	Ca	0.0	tot	1.0	Ca+2			
<input checked="" type="checkbox"/>	CaCO3	3.200000	diss	1.0	CO3-2	1.0	Ca+2	
<input checked="" type="checkbox"/>	CaHC03+	11.59900	diss	1.0	CO3-2	1.0	Ca+2	1.0
<input checked="" type="checkbox"/>	CaOH+	-12.69700	diss	1.0	Ca+2	-1.0	H+	1.0
<input type="checkbox"/>	Calcite[s]	8.480000	min	1.0	CO3-2	1.0	Ca+2	
<input checked="" type="checkbox"/>	H	0.0	tot	1.0	H[+1]			
<input checked="" type="checkbox"/>	H2CO3	16.68100	diss	1.0	CO3-2	2.0	H+	
<input checked="" type="checkbox"/>	HC03-	10.32900	diss	1.0	CO3-2	1.0	H+	
<input checked="" type="checkbox"/>	H[+1]	0.0	tot	1.0	H+			
<input type="checkbox"/>	Lime[s]	-32.69930	min	1.0	Ca+2	-2.0	H+	1.0
<input checked="" type="checkbox"/>	O	0.0	tot	1.0	O[-2]			
<input checked="" type="checkbox"/>	OH-	-13.99700	diss	-1.0	H+	1.0	H2O	
<input checked="" type="checkbox"/>	O[-2]	0.0	tot	1.0	H2O			
<input type="checkbox"/>	Portlandite[s]	-22.80400	min	1.0	Ca+2	-2.0	H+	2.0
								H2O

Note that Calcite[s] is still present in the list. This is because we have defined our own mineral called “calcite_mineral” with our own defined composition. Therefore, Calcite[s] has no actual relation to calcite_mineral and can still be treated as a separate species.

Step 6: export file

Press “Export”.

5.2.2 Calculating chemistry with Python.

For this example, we will examine what the effects of calcite dissolution are on the system composition at equilibrium. In Python, the amount of calcite is changed iteratively. For every calcite total, a new equilibrium composition is calculated using ORCHESTRA. In turn, the results are plotted using Python.

Step 1: create .py file and import modules.

3. Open a new python file and call it ‘calcite_dissolution.py’
4. Start the file by importing the required submodules:

```

import numpy as np
import matplotlib.pyplot as plt

```

```
import PyORCHESTRA # here, the ORCHESTRA submodule is imported
```

Step 2: get the ORCHESTRA function class 'p'.

```
p = PyORCHESTRA.ORCHESTRA()
```

Step 3: Initialise the ORCHESTRA calculator.

Now, the user must define the boundary conditions of the system for which chemical equilibrium will be calculated.

1. Name the chemistry text file. InputFile = 'chemistry1.inp'
2. Specify the number of cells. Here we will consider a 0-D system.
3. Specify the variables that will be used as input. Here, this includes the bulk composition (total calcite_mineral , Ca^{+2} , H^+ and CO_3^{-2} in the system). **Do not include the pH here as this is an output parameter.** In addition to this, ORCHESTRA comes with pre-available parameters such as porosity and saturation.
4. Specify the variables that the user wants as output. Here, this includes the pH.
5. Call the function 'initialise' to initialize the ORCHESTRA calculator object.

```
InputFile = 'chemistry1.inp'
NoCells = 1 #only 1 cell to have a 0-D system
InVars = np.array(['calcite_mineral.tot', 'Ca+2.tot', 'CO3-2.tot', 'H+.tot', 'porosity',
'saturation'])
OutVars = np.array(['pH'])

p.initialise(InputFile, NoCells, InVars, OutVars)
```

Step 4: Set the initial conditions.

The 'p'-object now contains an initialized system that is ready to be used. By specifying values for the given input parameters (in InVar), an equilibrium will be calculated.

1. First, we create the variable matrix 'IN' containing arrays of the same length as InVars (1 value for every parameter must be given).
2. Using the `np.where` function, we can change the value in IN at the position corresponding to that parameter.
3. We will assume that the system is fully saturated, with a porosity of 1. The bulk composition is set to $0.5 \frac{\text{mol}}{\text{L}} \text{Ca}^{+2}$ and $0.5 \frac{\text{mol}}{\text{L}} \text{CO}_3^{-2}$. Also include H^+ , give it a total of $0.1 \frac{\text{mol}}{\text{L}}$.

```
IN = np.array([np.ones_like(InVars)]).astype(float)

IN[0][np.where(InVars == 'porosity')] = 1
IN[0][np.where(InVars == 'saturation')] = 1
IN[0][np.where(InVars == 'Ca+2.tot')] = 0.5
IN[0][np.where(InVars == 'CO3-2.tot')] = 0.5
IN[0][np.where(InVars == 'H+.tot')] = 0.9
```

Step 5: change calcite mineral and get equilibrium

The total amount of calcite_mineral is iteratively lowered from 0.5 to 0.0 mol/L with a stepsize of 0.001. For every new 'configuration', system equilibrium is calculated using 'set_and_calculate'. When ORCHESTRA calculates equilibrium, it returns a matrix with values for the parameters listed in OutVars.

1. Define range for calcite_mineral (here, using `np.arange`).
2. Do a simple for loop, iterating over the different amounts of calcite_mineral.
3. Assign the new calcite_mineral-value to the correct position in InVars.
4. Calculate equilibrium with `p.set_and_calculate(IN)`
5. Assign output values to the correct lists.

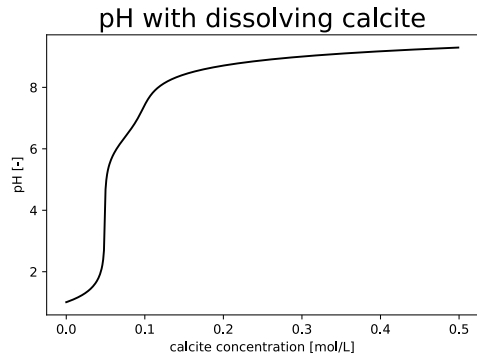
```
#define output lists
pH = []

#loop over different amounts of calcite
for calcite in calcite_list:
    #change amount of calcite
```

```
IN[0][np.where(InVars == 'calcite_mineral.tot')] = calcite  
  
#run ORCHESTRA  
OUT = p.set_and_calculate(IN)  
  
#get output  
pH.append(OUT[0])
```

Step 6: plot the results

As the figure indicates, the pH increases as calcite dissolves!



Bibliography

- Aguiar, C. M., A. R. Rufino, S. D. M. Hasan, and S. L. Lucena (2019). "Effects of pH and Temperature on the Enzymatic Hydrolysis of Crop Residues by Fungal Cellulases". In: *International Journal of Scientific and Engineering Research* 10 (11).
- Akindele, A. A. and M. Sartaj (2018). "The toxicity effects of ammonia on anaerobic digestion of organic fraction of municipal solid waste". In: *Waste management* 71, pp. 757–766.
- Aldin, S., G. Nakhla, and M. B. Ray (2011). "Modeling the Influence of Particulate Protein Size on Hydrolysis in Anaerobic Digestion". In: *Industrial & Engineering Chemistry Research* 50, pp. 10843–10849.
- Altree-Williams, A., J. Brugger, A. Pring, and P. Bedrikovetsky (2019). "Coupled reactive flow and dissolution with changing reactive surface and porosity". In: *Chemical Engineering Science* 206, pp. 289–304.
- Alvarado, A., S. West, G. Abbt-Braun, and H. Horn (2021). "Hydrolysis of particulate organic matter from municipal wastewater under aerobic treatment". In: *Chemosphere* 263.
- Amodeo, C., S. Masi, S. van Hulle, P. Zirpoli, I. Macnini, and D. Caniani (2019). "Methane oxidation in a biofilter (Part 2): A lab-scale experiment for model calibration". In: *Journal of Environmental Science and Health, Part A* 30, pp. 1404–1409.
- Anderson, P. R. and T. H. Christensen (1988). "Distribution coefficients of Cd, Co, Ni, and Zn in soils". In: *Journal of soil science* 39.1, pp. 15–22.
- Ariunbaatar, J., E. S. Di Perta, A. Panico, L. Frunzo, G. Esposito, P. N. L. Lens, and F. Pirozzi (2015). "Effect of ammoniacal nitrogen on one-stage and two-stage anaerobic digestion of food waste". In: *Waste management* 38, pp. 388–398.
- AWWA (2002). "U.S. Environmental Protection Agency Office of Ground Water and Drinking Water Standards and Risk Management Division". In.
- Barrow, N. J., G. W. Brümmer, and R. Strauss (1993). "Effects of surface heterogeneity on ion adsorption by metal oxides and by soils". In: *Langmuir* 9.10, pp. 2606–2611.
- Barrow, N. J., A. Debnath, and A. Sen (2022). "Effect of phosphate sorption on soil pH". In: *European Journal of Soil Science* 73.1, e13172.
- Batstone, D. J., J. Keller, I. Angelidaki, S. V. Kalyuzhnyi, S. G. Pavlostathis, A. Rozzi, W. T. M. Sanders, H. A. Siegrist, and V. A. Vavilin (2002). "The IWA anaerobic digestion model no 1 (ADM1)". In: *Water Science and technology* 45.10, pp. 65–73.
- Berge, N. D., D. R. Reinhart, and T. G. Townsend (2005). "The Fate of Nitrogen in Bioreactor Landfills". In: *Critical Reviews in Environmental Science and Technology* 35, pp. 365–399.
- Berge, N. D., D. R. Reinhart, J. Dietz, and T. Townsend (2006). "In situ ammonia removal in bioreactor landfill leachate". In: *Waste Management* 26.4, pp. 334–343.
- Blume, H., G. W. Brümmer, H. Fleige, R. Horn, E. Kandeler, I. Köger-Knabner, R. Kretzschmar, K. Stahr, and B. Wilke (2016). *Soil Science*. Springer, New York.
- Brand, E., T. C. M. de Nijs, J. J. Dijkstra, and R. N. J. Comans (2016). "A novel approach in calculating site-specific aftercare completion criteria for landfills in The Netherlands: Policy developments". In: *Waste Management* 56, pp. 255–261.
- Buchter, B., B. Davidoff, M. C. Amacher, C. Hinz, I. K. Iskandar, and H. M. Selim (1989). "Correlation of Freundlich Kd and n retention parameters with soils and elements". In: *Soil Sci* 148.5, pp. 370–379.
- Carrera, J., I. Jubany, L. Carvallo, R. Chamy, and J. Lafuente (2004). "Kinetic models for nitrification inhibition by ammonium and nitrite in a suspended and an immobilised biomass systems". In: *Process Biochemistry* 39.9, pp. 1159–1165.
- Chanem, O., J. Fellner, and M. Zairi (2020). "Ammonia inhibition of waste degradation in landfills – A possible consequence of leachate recirculation in arid climates". In: *Waste Management and Research* 10, pp. 1078–1086.
- Chefetz, B., P. G. Hatcher, Y. Hadar, and Y. Chen (1996). *Chemical and biological characterization of organic matter during composting of municipal solid waste*. Tech. rep. Wiley Online Library.

- Chen, D. M., B. L. Bodirsky, T. Krueger, A. Mishra, and A. Popp (2020a). "The world's growing municipal solid waste: trends and impacts". In: *Environmental Research Letters* 15.7, p. 074021.
- Chen, Y. M., W. J. Xu, D. S. Ling, L. T. Zhan, and W. Gao (2020b). "A degradation-consolidation model for the stabilization behavior of landfilled municipal solid waste". In: *Computers and Geotechnics* 118, p. 103341.
- Chiou, Y., L. Lee, C. Chang, and A. Chao (2007). "Control of carbon and ammonium ratio for simultaneous nitrification and denitrification in a sequencing batch bioreactor". In: *International biodeterioration & biodegradation* 59.1, pp. 1–7.
- Cho, K. H., J. Kim, S. Kang, H. Park, S. Kim, and Y. M. Kim (2014). "Achieving enhanced nitrification in communities of nitrifying bacteria in full-scale wastewater treatment plants via optimal temperature and pH". In: *Separation and Purification Technology* 132, pp. 697–703.
- Corsino, S. F., M. Capodici, C. Morici, M. Torregrossa, and G. Viviani (2016). "Simultaneous nitritation-denitrification for the treatment of high-strength nitrogen in hypersaline wastewater by aerobic granular sludge". In: *Water research* 88, pp. 329–336.
- Daniel, R. M., M. J. Danson, R. Eisenthal, C. K. Lee, and M. E. Peterson (2008). "The effect of temperature on enzyme activity: new insights and their implications". In: *Extremophiles* 12.1, pp. 51–59.
- Deng, W., L. Wang, L. Cheng, W. Yang, and D. Gao (2022). "Nitrogen Removal from Mature Landfill Leachate via Anammox Based Processes: A Review". In: *Sustainability* 14, p. 995.
- Dijkstra, J. J., A. van Zomeren, E. Brand, and R. N. J. Comans (2018). "Site-specific aftercare completion criteria for sustainable landfilling in the Netherlands: Geochemical modelling and sensitivity analysis". In: *Waste Management* 75, pp. 407–414.
- Dimock, R. and E. Morgenroth (2006). "The influence of particle size on microbial hydrolysis of protein particles in activated sludge". In: *Waste Research* 40, pp. 2064–2074.
- Dincer, A. R. and F. Kargi (2000). "Kinetics of sequential nitrification and denitrification processes". In: *Enzyme and microbial technology* 27.1-2, pp. 37–42.
- Drake, H. L. (2012). *Acetogenesis*. Springer Science & Business Media.
- Droge, S. and K. Goss (2012). "Effect of sodium and calcium cations on the ion-exchange affinity of organic cations for soil organic matter". In: *Environmental science & technology* 46.11, pp. 5894–5901.
- Droge, S. T. J. and K. Goss (2013). "Development and evaluation of a new sorption model for organic cations in soil: contributions from organic matter and clay minerals". In: *Environmental science & technology* 47.24, pp. 14233–14241.
- Ekinci, K., I. Tosun, B B., B. S. Kumbul, S., and K. Sülik (2019). "Effects of initial C/N ratio on organic matter degradation of composting of rose oil processing solid wastes". In: *International Journal of Environmental Science and Technology* 16.9, pp. 5131–5140.
- Erses, A. S., T. T. Onay, and O. Yenigun (2008). "Comparison of aerobic and anaerobic degradation of municipal solid waste in bioreactor landfills". In: *Bioresource technology* 99.13, pp. 5418–5426.
- Farmer, W. R. and J. C. Liao (1997). "Reduction of aerobic acetate production by *Escherichia coli*". In: *Applied and environmental microbiology* 63.8, pp. 3205–3210.
- Feng, J., S. Chen Zheng, T. H., F. Ma, S. C. Shao, S. F. Yang, and L. Zhang (2015). "Characterization of the anaerobic denitrification bacterium *Acinetobacter* sp. SZ28 and its application for groundwater treatment". In: *Bioresource technology* 192, pp. 654–659.
- Fidel, R. B., D. A. Laird, and K. A. Spokas (2018). "Sorption of ammonium and nitrate to biochars is electrostatic and pH-dependent". In: *Scientific reports* 8.1, pp. 1–10.
- Fytanidis, D. K. and E. A. Voudrias (2014). "Numerical simulation of landfill aeration using computational fluid dynamics". In: *Waste management* 34.4, pp. 804–816.
- Gerba, C. P., A. H. Tamimi, C. Pettigrew, A. V. Weisbrod, and V. Rajagopalan (2011). "Sources of microbial pathogens in municipal solid waste landfills in the United States of America". In: *Waste Management & Research* 29.8, pp. 781–790.
- Ghasemzadeh, K., E. Jalilnejad, and A. Basile (2017). "Production of bioalcohol and biomethane". In: *Bioenergy Systems for the Future*. Elsevier, pp. 61–86.
- Gholamifard, S., R. Eymard, and C. Duquennoi (2008). "Modeling anaerobic bioreactor landfills in methanogenic phase: Long term and short term behaviors". In: *water research* 42.20, pp. 5061–5071.
- Grady, C. P., G. T. Daigger, and H. C. Lim (1999). "Submerged Attached Growth Bioreactors". In: *Biological Wastewater Treatment. 2nd Ed.*, Marcel Dekker, Inc., New York.
- Groenenberg, J. E., G. F. Koopmans, and R. N. J. Comans (2010). "Uncertainty analysis of the nonideal competitive adsorption-donnan model: effects of dissolved organic matter variability on predicted metal speciation in soil solution". In: *Environmental science & technology* 44.4, pp. 1340–1346.
- Gupta, A. B. (1997). "Thiosphaera pantotropha: a sulphur bacterium capable of simultaneous heterotrophic nitrification and aerobic denitrification". In: *Enzyme and Microbial Technology* 21.8, pp. 589–595.

- Haarstrick, A., D. C. Hempel, L. Ostermann, H. Ahrens, and D. Dinkler (2001). "Modelling of the biodegradation of organic matter in municipal landfills". In: *Waste management & research* 19.4, pp. 320–331.
- Halim, A. A., H. A. Aziz, M. A. M. Johari, and K. S. Ariffin (2010). "Comparison study of ammonia and COD adsorption on zeolite, activated carbon and composite materials in landfill leachate treatment". In: *Desalination* 262.1-3, pp. 31–35.
- He, P. J., F. Lü, L. M. Shao, X. J. Pan, and D. J. Lee (2007). "Kinetics of enzymatic hydrolysis of polysaccharide-rich particulates". In: *Journal of the Chinese Institute of Chemical Engineers* 38, pp. 21–27.
- Hedström, A. (2001). "Ion exchange of ammonium in zeolites: a literature review". In: *Journal of environmental engineering* 127.8, pp. 673–681.
- Heijnen, J. J. and R. Kleerebezem (1999). "Bioenergetics of microbial growth". In: *Encyclopedia of bioprocess technology: Fermentation, biocatalysis, and bioseparation* 1, pp. 267–291.
- Heinen, M. (2006). "Simplified denitrification models: overview and properties". In: *Geoderma* 133.3-4, pp. 444–463.
- Hendry, M. J., L. I. Wassenaar, and T. Kotzer (2000). "Chloride and chlorine isotopes (^{36}Cl and $\delta^{37}\text{Cl}$) as tracers of solute migration in a thick, clay-rich aquitard system". In: *Water Resources Research* 36.1, pp. 285–296.
- Henze, M., P. Harremoes, J. Jansen, and E. Arvin (1995). *Wastewater Treatment-Biological and Chemical Processes*. Springer.
- Hills, D. J. and K. Nakano (1984). "Effects of Particle Size on Anaerobic Digestion of Tomato Solid Waste". In: *Agricultural Waste* 10, pp. 285–295.
- Isaka, K., S. Yoshie, T. Sumino, Y. Inamori, and S. Tsuneda (2007). "Nitrification of landfill leachate using immobilized nitrifying bacteria at low temperatures". In: *Biochemical Engineering Journal* 37.1, pp. 49–55.
- Jeppu, G. P. and T. P. Clement (2012). "A modified Langmuir-Freundlich isotherm model for simulating pH-dependent adsorption effects". In: *Journal of contaminant hydrology* 129, pp. 46–53.
- Jorgensen, S. E., O. Libor, K. Lea Graber, and K. Barkacs (1976). "Ammonia removal by use of clinoptilolite". In: *Water Research* 10.3, pp. 213–224.
- Kattenberg, W. and T. Heimovaara (2011). "Policy Process of Allowing Research Pilots for Sustainable Emission Reduction at Landfills in the Netherlands". In: *Thirteenth International Waste Management and Landfill Symposium, Sardinia*.
- Khalil, M. J., R. Gupta, and K. Sharma (2014). "Microbiological Degradation of Municipal Solid Waste in Landfills for LFG Generation". In: *International Journal of Engineering and Technical Research, Special Issue*.
- Kleerebezem, R. and M. C. M. Van Loosdrecht (2010). "A generalized method for thermodynamic state analysis of environmental systems". In: *Critical Reviews in Environmental Science and Technology* 40.1, pp. 1–54.
- Komilis, D., A. Evangelou, G. Giannakis, and C. Lympiris (2012). "Revisiting the elemental composition and the calorific value of the organic fraction of municipal solid wastes". In: *Waste management* 32.3, pp. 372–381.
- Lefebvre, X., S. Lanini, and D. Houï (2000). "The role of aerobic activity on refuse temperature rise, I. Landfill experimental study". In: *Waste management & research* 18.5, pp. 444–452.
- Leupold, K. E. S. (2018). "Thermodynamic and stoichiometric constraint-based inference of metabolic phenotypes". PhD thesis. University of Groningen.
- Li, J., B. Wu, Q. Li, Y. Zou, Z. Cheng, X. Sun, and B. Xi (2019). "Ex situ simultaneous nitrification-denitrification and in situ denitrification process for the treatment of landfill leachates". In: *Waste Management* 88, pp. 301–308.
- Lieten, S., H. (2018). "Landfill Management in the Netherlands". In: *A study commissioned by Rijkswaterstaat WVL*.
- Lin, C. and R. Chang (1999). "Hydrogen production during the anaerobic acidogenic conversion of glucose". In: *Journal of Chemical Technology & Biotechnology: International Research in Process, Environmental & Clean Technology* 74.6, pp. 498–500.
- Lozecznik, S., R. Sparling, S. P. Clark, J. F. VanGulck, and J. A. Oleszkiewicz (2012). "Acetate and propionate impact on the methanogenesis of landfill leachate and the reduction of clogging components". In: *Bioresource Technology* 104, pp. 37–43.
- Lu, S. and S. Feng (2020). "Comprehensive overview of numerical modeling of coupled landfill processes". In: *Waste Management* 118, pp. 161–179.
- Lu, S., J. Xiong, F. Feng, H. Chen, Z. Bai, W. Fu, and F. Lü (2019). "A finite-volume numerical model for bio-hydro-mechanical behaviors of municipal solid waste in landfills". In: *Computers and Geotechnics* 109, pp. 204–219.
- Lu, S., S. Feng, Q. Zheng, and Z. Bai (2021). "A multi-phase, multi-component model for coupled processes in anaerobic landfills: theory, implementation and validation". In: *Géotechnique* 71, pp. 826–842.
- Lu, Z. and J. A. Imlay (2021). "When anaerobes encounter oxygen: mechanisms of oxygen toxicity, tolerance and defence". In: *Nature reviews microbiology* 19.12, pp. 774–785.
- Luong, J. H. T. (1987). "Generalization of Monod kinetics for analysis of growth data with substrate inhibition". In: *Biotechnology and Bioengineering* 29.2, pp. 242–248.

- Lyu, Z., N. Shao, T. Akinyemi, and W. B. Whitman (2018). "Methanogenesis". In: *Current Biology* 28.13, R727–R732.
- Majdinasab, A., Z. Zhang, and Q. Yuan (2017). "Modelling of landfill gas generation: a review". In: *Reviews in Environmental Science and Bio/Technology* 16, pp. 361–380.
- Mannina, G., G. A. Ekama, M. Capodici, A. Cosenza, D. Di Trapani, and H. Ødegaard (2017). "Moving bed membrane bioreactors for carbon and nutrient removal: The effect of C/N variation". In: *Biochemical Engineering Journal* 125, pp. 31–40.
- Meeussen, J. and L. C. (2003). "ORCHESTRA: An Object-Oriented Framework for Implementing Chemical Equilibrium Models". In: *Environmental Science and Technology* 16, pp. 1175–1182.
- Meima, J. A., N. M. Naranjo, and A. Haarstrick (2008). "Sensitivity analysis and literature review of parameters controlling local biodegradation processes in municipal solid waste landfills". In: *Waste management* 28.5, pp. 904–918.
- Metcalf, L., H. P. Eddy, and G. Tchobanoglous (1991). *Wastewater engineering: treatment, disposal, and reuse*. Vol. 4. McGraw-Hill New York.
- Milne, C. K., D. G. Kinniburgh, W. H. Van Riemsdijk, and E. Tipping (2003). "Generic NICA- Donnan model parameters for metal-ion binding by humic substances". In: *Environmental Science & Technology* 37.5, pp. 958–971.
- Morgenroth, E., R. Kommedal, and P. Harremoës (2002). "Processes and modeling of hydrolysis of particulate organic matter in aerobic wastewater treatment—a review". In: *Water Science and Technology* 45.6, pp. 25–40.
- Mormile, M. R., K. R. Gurijala, J. A. Robinson, M. J. McInerney, and J. M. Suflita (1996). "The importance of hydrogen in landfill fermentations". In: *Applied and Environmental Microbiology* 62.5, pp. 1583–1588.
- Muhammad, M. H., A. L. Idris, X. Fan, Y. Guo, Y. Yu, X. Jin, J. Qiu, X. Guan, and T. Huang (2020). "Beyond risk: bacterial biofilms and their regulating approaches". In: *Frontiers in microbiology* 11, p. 928.
- Munawar, E. (2014). "Modeling the degradable organic carbon in municipal solid waste landfills". PhD thesis.
- Neill, C. and J. Gignoux (2006). "Soil organic matter decomposition driven by microbial growth: a simple model for a complex network of interactions". In: *Soil Biology and Biochemistry* 38.4, pp. 803–811.
- Nielsen, P. H. (1996). "Adsorption of ammonium to activated sludge". In: *Water research* 30.3, pp. 762–764.
- O'Flaherty, V., G. Collins, and T. Mahony (2010). "Anaerobic Digestion of Agricultural Residues". In: *in: Environmental Microbiology, second edition. Mitchell, R. and Gu. J. D.*
- Onay, T. T. and F. G. Pohlund (2001). "Nitrogen and sulfate attenuation in simulated landfill bioreactors". In: *Water Science and Technology* 44.2-3, pp. 367–372.
- Oosterhuis, M., D. Ringoot, A. Hendriks, and P. Roeleveld (2014). "Thermal hydrolysis of waste activated sludge at Hengelo wastewater treatment plant, The Netherlands". In: *Water science and technology* 70.1, pp. 1–7.
- Petruzzelli, G., G. Guidi, and L. Lubrano (1985). "Ionic strength effect on heavy metal adsorption by soil". In: *Communications in Soil Science and Plant Analysis* 16.9, pp. 971–986.
- Price, G. A., M. A. Barlaz, and G. R. Hater (2003). "Nitrogen management in bioreactor landfills". In: *Waste Management* 23.7, pp. 675–688.
- Prommer, H., D. A. Barry, and G. B. Davis (2002). "Modelling of physical and reactive processes during biodegradation of a hydrocarbon plume under transient groundwater flow conditions". In: *Journal of Contaminant Hydrology* 59.1-2, pp. 113–131.
- Puyuelo, B., S. Ponsá, T. Gea, and A. Sánchez (2011). "Determining C/N ratios for typical organic wastes using biodegradable fractions". In: *Chemosphere* 85.4, pp. 653–659.
- Reichel, T., L. K. Ivanova, R. P. Beaven, and A. Haarstrick (2007). "Modeling decomposition of MSW in a consolidating anaerobic reactor". In: *Environmental Engineering Science* 24.8, pp. 1072–1083.
- Renou, S., J. G. Givaudan, S. Poulaïn, F. Dirassouyan, and P. Moulin (2008). "Landfill leachate treatment: Review and opportunity". In: *Journal of Hazardous Materials*.
- Ritzkowski, M. and R. Stegmann (2012). "Landfill aeration worldwide: Concepts, indications and findings". In: *Waste Management* 32, pp. 1411–1419.
- Roels, J. A. (1980). "Application of macroscopic principles to microbial metabolism". In: *Biotechnology and bioengineering* 22.12, pp. 2457–2514.
- Rowe, R. K. and H. P. Sangam (2002). "Durability of HDPE geomembranes". In: *Geotextiles and Geomembranes* 20, pp. 77–95.
- Roychowdhury, S., D. Cox, and M. Levandowsky (1988). "Production of hydrogen by microbial fermentation". In: *International Journal of Hydrogen Energy* 13.7, pp. 407–410.
- Sanci, R. and H. O. Panarello (2012). "CO₂ and CH₄ Flux Measurements from Landfills—A Case Study: Gualeguaychú Municipal Landfill, Entre Ríos Province, Argentina". In: *Greenhouse Gases- Emission, Measurement and Management*, pp. 953–978.
- Sanders, W. T. M. (2001). "Anaerobic hydrolysis during digestion of complex substrates". In: *Dissertation at Wageningen University*.

- Sanders, W. T. M., M. Geerink, G. Zeeman, and G. Lettings (2000). "Anaerobic hydrolysis kinetics of particle substrates". In: *Water Science and Technology* 41, pp. 17–24.
- Scharff, H. (2014). "Landfill reduction experience in The Netherlands". In: *Waste Management* 34, pp. 2218–2224.
- Schmidt, I., O. Sliekers, M. Schmid, E. Bock, J. Fuerst, J. G. Kuenen, M. S. M. Jetten, and M. Strous (2003). "New concepts of microbial treatment processes for the nitrogen removal in wastewater". In: *FEMS microbiology reviews* 27.4, pp. 481–492.
- Sekhohola-Dlamini, L. and T. Memory (2019). "Microbiology of municipal solid waste landfills: a review of microbial dynamics and ecological influences in waste bioprocessing". In: *Biodegradation*.
- Shampine, L. F. and M. W. Reichelt (1997). "The matlab ode suite". In: *SIAM journal on scientific computing* 18.1, pp. 1–22.
- Sieber, J. R., M. J. McInerney, and R. P. Gunsalus (2012). "Genomic insights into syntrophy: the paradigm for anaerobic metabolic cooperation". In: *Annual review of microbiology* 66, pp. 429–452.
- Šimek, M. and J. E. Cooper (2002). "The influence of soil pH on denitrification: progress towards the understanding of this interaction over the last 50 years". In: *European Journal of Soil Science* 53.3, pp. 345–354.
- Sposito, G. (1982). "On the use of the Langmuir equation in the interpretation of "adsorption" phenomena: II. The "two-surface" Langmuir equation". In: *Soil Science Society of America Journal* 46.6, pp. 1147–1152.
- Staszewska, E. and M. Pawłowska (2011). "Characteristics of emissions from municipal waste landfills". In: *Environment Protection Engineering* 37.4, pp. 119–130.
- Strock, J. S. (2008). "Ammonification". In: *Encyclopedia of ecology, five-volume set*. Elsevier Inc., pp. 162–165.
- Tang, Y. J., A. L. Meadows, and J. D. Keasling (2007). "A kinetic model describing Shewanella oneidensis MR-1 growth, substrate consumption, and product secretion". In: *Biotechnology and bioengineering* 96.1, pp. 125–133.
- Turnhout, A. G. van, C. Brandstätter, C. Kleerebezem, J. Fellner, and T. J. Heimovaara (2018). "Theoretical analysis of municipal solid waste treatment by leachate recirculation under anaerobic and aerobic conditions". In: *Waste Management* 71, pp. 246–254.
- Turnhout, A. G. van, H. Oonk, H. Scharff, and T. J. Heimovaara (2020). "Optimizing landfill aeration strategy with a 3-D multiphase model". In: *Waste Management* 102, pp. 499–509.
- Valencia, R., W. van der Zon, H. Woelders, H. J. Lubberding, and H. J. Gijzen (2011). "Anammox: an option for ammonium removal in bioreactor landfills". In: *Waste management* 31.11, pp. 2287–2293.
- Valentini, A., G. Garuti, A. Rozzi, and A. Tilche (1997). "Anaerobic Degradation Kinetics of Particulate Organic Matter: a New Approach". In: *Water Science Technology* 36, pp. 239–246.
- Vaverková, M. D. (2020). "Landfill Impacts on the Environment – Review". In: *Geosciences* 9 (431).
- Vavilin, V. A., B. Fernandez, J. Palatsi, and X. Flotats (2007). "Hydrolysis kinetics in anaerobic degradation of particulate organic material: An overview". In: *Waste Management* 28, pp. 939–951.
- (2008). "Hydrolysis kinetics in anaerobic degradation of particulate organic material: an overview". In: *Waste management* 28.6, pp. 939–951.
- Veeken, A. and B. Hamelers (1999). "Effect of temperature on hydrolysis rates of selected biowaste components". In: *Bioresource Technology* 69, pp. 249–254.
- Veeken, A., S. Kalyuzhnyi, H. Scharff, and B. Hamelers (2000). "effect of pH and VFA on hydrolysis of organic solid waste". In: *Journal of Environmental Engineering* 126, pp. 1076–1081.
- Vogelaar, J. C. T., B. Klapwijk, H. Temmink, and J. B. van Lier (2003). "Kinetic comparisons of mesophilic and thermophilic aerobic biomass". In: *Journal of Industrial Microbiology and Biotechnology* 30.2, pp. 81–88.
- Walsh, R. (2018). "Comparing enzyme activity modifier equations through the development of global data fitting templates in Excel". In: *PeerJ* 6, e6082.
- Warith, M., X. Li, and H. Jin (2005). "Bioreactor landfills: state-of-the-art review". In: *Emirates Journal for Engineering Research* 10.1, pp. 1–14.
- Warith, M. A. and R. Sharma (1998). "Technical review of methods to enhance biological degradation in sanitary landfills". In: *Water Quality Research Journal* 33.3, pp. 417–438.
- Wiszniewski, J., D. Robert, J. Surmacz-Gorska, K. Miksch, and J. V. Weber (2006). "Landfill leachate treatment methods: A review". In: *Environmental Chemistry Letters* 4, pp. 51–61.
- WorldBank (2021). *Urban Population*. URL: <https://data.worldbank.org/indicator/SP.URB.TOTL>.
- Xiao, D., Y. Chen, W. Xu, and L. Zhan (2021). "An Anaerobic Degradation Model for Landfilled Municipal Solid Waste". In: *Applied Sciences* 11 (7557).
- Yao, J., Q. Kong, H. Zhu, Z. Zhang, Y. Long, and D. Shen (2015). "Adsorption of ammonia on municipal solid waste incinerator bottom ash under the landfill circumstance". In: *Korean Chemical Engineering Research* 53.4, pp. 503–508.
- Yen, H. and D. E. Brune (2007). "Anaerobic co-digestion of algal sludge and waste paper to produce methane". In: *Bioresource technology* 98.1, pp. 130–134.
- Youcai, Z., C. Zhugen, S. Qingwen, and H. Renhua (2001). "Monitoring and long-term prediction of refuse compositions and settlement in large-scale landfill". In: *Waste Management & Research* 19.2, pp. 160–168.

- Zamri, M. F. M. A., S. Hasmady, A. Akhiar, F. Ideris, A. H. Shamsuddin, M. Mofijur, I. M. R. Fattah, and T. M. I. Mahlia (2021). "A comprehensive review on anaerobic digestion of organic fraction of municipal solid waste". In: *Renewable and Sustainable Energy Reviews* 137 (110637).
- Zhang, L., T. Tsui, K. Loh, Y. Dai, and Y. W. Tong (2022). "Acidogenic fermentation of organic wastes for production of volatile fatty acids". In: *Biomass, Biofuels, Biochemicals*. Elsevier, pp. 343–366.